MECHANICAL AND METABOLIC STRESSES CONTRIBUTE TO HIGH FORCE CONTRACTION SIGNALING

A Dissertation
Presented to
The Academic Faculty

by

Jill Anne Rahnert

In Partial Fulfillment
of the Requirements for the Degree
Doctor of Philosophy in the
School of Applied Physiology

Georgia Institute of Technology

May 2012

MECHANICAL AND METABOLIC STRESSES CONTRIBUTE TO HIGH FORCE CONTRACTION SIGNALING

Approved by:

Dr. Thomas Burkholder, Advisor
School of Applied Physiology
Georgia Institute of Technology

Dr. Alan Sokoloff
School of Medicine
Emory University

Dr. Edward Balog
School of Applied Physiology
Georgia Institute of Technology

Dr. Rudolph Gleason
School of Mechanical Engineering
Georgia Institute of Technology

Dr. Gordon Warren
School of Nursing and Health Professions
Georgia State University
School of Applied Physiology
Georgia Institute of Technology

Date Approved: March 14, 2012

To my family

ACKNOWLEDGEMENTS

I would like to thank my advisor Dr. Tom Burkholder for your guidance and encouragement. Thank you for always having time to discuss or answer questions, for imposing deadlines, for making constructive comments, for your patience and mostly for having a real interest in helping me succeed. I have learned more than I could have imagined and that exceeds the containment of the lab. I truly appreciate your time and effort in helping with this project and everything along the way. I could not have asked for a better advisor or a better learning opportunity. I would like to thank my committee members: Gordon Warren, Rudy Gleason, Ed Balog and Alan Sokoloff. Particularly, I would like to thank, Alan for funding this work and supporting me the past few years. Thank you, Ed for all your help, your efforts along the way and for contributing to the great learning experience I have had here. Thank you, Gordon and Rudy for your time, input and interest in my project. I appreciate you all and thank you.

I would like to thank my labmate, George for the many and wide-ranging discussions we have had. Thank you to Rono Srimani and Mike Mallow for your help in the lab running the many gels needed. It has been great having you in the lab.

Thank you to my family. To my parents for supporting whatever chose to do. I would like to especially thank my sister, Nikki, and my husband, Matt for their endless support and encouragement. To neither can I express enough gratitude. Thank you Nikki for always being there and doing whatever you can to help, which is more than could be known. Thank you to Matt for supporting me, for putting up with me and for being patient with me. Thank you for everything that cannot possibly be listed, I love you.

TABLE OF CONTENTS

LIST OF TABLES

Page

LIST OF FIGURES

LIST OF ABBREVIATIONS

ATP	Adenosine triphosphate
DNA	Deoxyribonucleic acid
EDL	*Extensor digitorum*
FO	Functional overload
HFC	High force contraction
HFES	High frequency electrical stimulation
I_o	Optimal current
L_o	Optimal length
LFES	Low frequency electrical stimulation
MAPK	Mitogen-activated protein kinase
MHC	Myosin heavy chain
P_i	Inorganic phosphate
P_t	Twitch force
RNA	Ribonucleic acid
TA	*Tibialis anterior*

SUMMARY

Force production by a muscle is critical to maintaining proper function and overall health of a human or animal. Muscle adapts to increased loading with hypertrophy by activating a number of intracellular signaling cascades that regulate protein synthesis. The overall hypothesis is that force-dependent processes acutely activate growth-related signaling during active force generation. This project took two approaches. The first employed a general survey of muscles in which age-dependent changes in muscle activity differed. No conclusive activity-dependent signaling emerged however coordinated signaling among kinases broke down with age. The second approach utilized an *in situ* muscle preparation in which force production or metabolic costs were specifically controlled. Similar sub-maximal force levels generated by different methods found that force, *per se*, is not a primary modulator of growth-related signaling but that ERK phosphorylation is dependent on fiber-activation. Prolonging the duration of electrical stimulation applied to the nerve or increasing the frequency at which stimulations are applied was expected to increase the metabolic stress associated with contraction. Several growth-related kinases correlated with markers of metabolic stress, i.e. increased AMPK activity and decreased glycogen content, which were decoupled from force decline. This suggests energy depletion, specific to stimulation pattern, strongly influences the immediate response to high force contraction signaling. The overall conclusion is that signaling molecules previously implicated in force-dependent signaling lie much too downstream to relay strict force-dependent signaling.

CHAPTER 1

INTRODUCTION

Overview

Skeletal muscle is the most abundant tissue type in the body comprising 40-50% of the body mass. Muscle is a major site for glucose storage, a reservoir for protein and amino acids and muscle protein turnover contributes to up to 50% of one's resting metabolic rate thus, muscle mass contributes to the well-being of the whole system. Mass begins to decline by 0.5-2% per year starting at the age of 40 (Baumgartner et al., 1998) and decreased quality of muscle has critical long-term health implications as it is linked to the development of a number of diseases such as diabetes, obesity, and cardiovascular disease (Karagounis and Hawley, 2010; Nair, 2005; Phillips, 2007). Sarcopenia, the muscle loss related to age is a growing health concern as the elderly population rises and sedentary lifestyles become more prevalent. Decreased muscle mass is coupled with reduced muscle strength making normal, everyday activities more challenging. Muscle wasting is linked to gait and balance problems increasing the risk for falling and injury by 35% and is a predictor of disability and institutionalization due to loss of functional independence (Baumgartner et al., 2004; Janssen et al., 2004a; Janssen et al., 2004b). Maintaining or engaging in physical activity, particularly resistance exercise is encouraged to help preserve muscle mass and function.

Skeletal muscle, like most systems, has the ability to adapt to demands imposed by the outside environment. Short duration, high force contractions (HFC) are an anabolic signal leading to increased protein synthesis and skeletal muscle hypertrophy. Molecular biology approaches have contributed to our understanding by identifying processes or pathways important in muscle growth. For example, increases in the rate of

protein synthesis occur prior to changes in gene transcription (Chesley et al., 1992; Laurent et al., 1978; Wong and Booth, 1990; Wong and FW, 1990) and post-translational modifications that affect the activity or availability of a number of proteins have been identified in the regulation of protein synthesis and cell size (Baar and Esser, 1999; Mayhew et al., 2011; Ohanna et al., 2005) The most prominent aspect of HFC is the high force and this force has been linked to activation of important growth related signaling cascades (Hornberger and Chien, 2005; Hornberger et al., 2004; Spangenburg et al., 2008). However, the mechanism by which mechanical signals are transduced into biochemical signals is unclear.

Mechanical forces are important in determining muscle structure and morphology as well as biochemical and molecular phenotypes of fibers comprising muscle. Central to the motivation for this project is the concept that muscle growth occurs in response to increased force requirements and that this adaptation maintains some intrinsic state of the muscle. However, muscle contraction is a complex, energy-consuming event. Metabolic stresses associated with maintaining energy balance often co-varies with force production and may also activate common growth-related signaling cascades. Thus, a specific gap in our understanding of hypertrophy induced by high-force contractions is how force and metabolic stress interact with respect to activation of growth-related signaling cascades. This project is designed under the hypothesis that force, specifically peak force, is the important anabolic signal and aims to assess the effects of muscle activity on intracellular signaling and to isolate general mechanical and metabolic contributions to intracellular signaling associated with force production. Improving our understanding of the contraction-induced signals to which the muscle responds to and how they contribute to growth-related signaling is of key importance and will facilitate the design of therapeutic or rehabilitation strategies to minimize strength loss or muscle wasting. The goal of this dissertation is to provide a better understanding of the growth-related signaling events induced by decoupling components of muscle activity and high force contractions.

Muscle Force

Muscle contractions generate force and produce movements of the bones to which they originate and insert. The functional requirements of muscle force are met through modulation of neural and mechanical processes. This section will discuss development of force production and its modulation by intrinsic properties and the energy cost associated with force production.

Force Production

Neural Control of Force Production

The process of muscle activation and force generation involves a sequence of events collectively called excitation-contraction coupling (E-C coupling). In skeletal muscle, motorneuron activity elicits action potentials by releasing acetylcholine from the nerve terminal resulting in sodium influx through ionotropic receptors on the muscle fiber membrane. Local depolarizations propagate across the cell membrane via activation of voltage-gated sodium channels and triggers calcium release from intracellular stores. This calcium binds to and activates the contractile apparatus to produce force. Muscle relaxation begins when excitation ceases. The membrane repolarizes and calcium is actively removed from the cytoplasm. Although action potentials produce an all-or-none response in the muscle fiber, the actual force produced by the whole muscle can be controlled in multiple ways related to different aspects of E-C coupling. Below, developments of key pieces of information relating to force generation and features associated with modulation of force production are highlighted.

Up until the mid-1600's the brain was thought to send out animal spirits that travel down nerves to produce muscle contraction (Cobb, 2002). This 'animal spirits' theory, constructed by early Greek physicians, was challenged and disproven with Swammerdam's development of the muscle-nerve preparation, still in use today, by

observing muscle contraction following 'irritation' of a cut nerve (Cobb, 2002; Swammerdam and Flloyd, 1978). Some 100 years later, similar experiments led to the discovery that an external electrical current could travel by self-propagating depolarizations ('action potential') to elicit a muscle contraction and that contraction strength could be modulated by stimulus intensity (Barbara and Clarac, 2011; Cobb, 2002; Martonosi, 2000). It eventually became clear that nerves and muscle fibers acted as a functional unit, a motor unit. A motor unit (MU) is the motorneuron (MN) and all the fibers it innervates and the intensity of the stimulus applied is the nervous systems mechanism by which it controls force generation.

The intensity of the stimulus applied by the nervous system to the nerve determines the both the number of MU recruited and the frequency at which the MU fires. During voluntary contractions motor units are recruited following the size principle (Henneman, 1957; Henneman and Olson, 1965), which says that MU recruitment is a function of MN axon size. That is, progressive increase of the stimulus intensity recruits progressively larger motoneurons and motor units (Henneman, 1957). MN axon size, like the MU, is related to physiological characteristics of the fibers innervated, as a single MN innervates a single type of fiber (Burke et al., 1973; Henneman and Olson, 1965). Experimentally, modulation of force production by an artificial stimulus can be achieved by altering the current applied to the nerve or by altering the duration of the stimulus (pulse width) applied by electrical stimulation, either of which affect whether the nerve depolarizes, or by altering the frequency of stimulation.

MU activation depends on both the current amplitude and stimulation duration. The excitability of a nerve can be described by features of this stimulus strength-duration curve (Figure 1.1), termed rheobase and chronaxie. Rheobase is the minimum stimulus strength (voltage or current) required to elicit a response (i.e. an action potential) while chronaxie is the time required for a current of twice the rheobase to elicit an action potential. Figure 1.1 illustrates this relationship and indicates large, and faster, MU are

more excitable than small, slower MU. Physiologically, the stimulus strength required to activate a particular fiber depends on the capacitance and input resistance of the cell. Capacitance is related to cell size such that cells with greater surface area have a greater capacitance but lower input resistance. Thus, although larger fibers are more excitable, they require more charge to actually depolarize the cell. The experimental design in aim II will utilize this relationship to alter the number of MU activated. Applying a maximal current and pulse width to a nerve insures activation of all MUs, thus all fibers, and generates maximum force. Reducing either the current or pulse width de-recruits smaller MU and therefore decreases force produced by the whole muscle (Figure 1.1). By contrast, altering the frequency of electrical stimulation to the nerve affects the force produced by individual fibers.

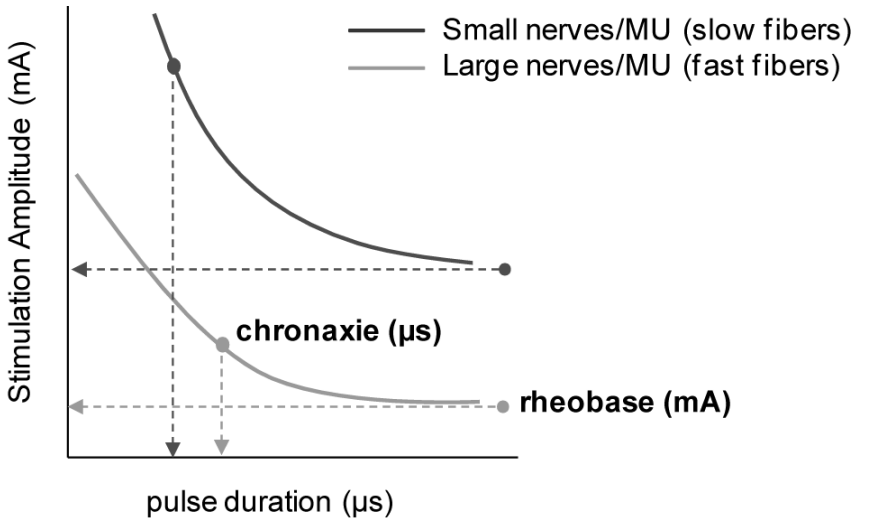

Figure 1.1 Stimulus-duration curve.

Experimentally modulating the frequency of the applied electrical stimulation less than the that producing maximum force, produces sub-maximal force levels and varies both the level of calcium in the cell and level of force produced by the muscle. Physiologically, motorneuron firing frequency determines the degree of fiber activation within a motor unit. That is, the faster or the higher the rate action potentials are

generated within the fiber, the greater the force the fiber is able to produce. The time course for the force produced by a single action potential, a twitch, is related to the kinetics of regulating calcium concentrations (Ashley and Ridgway, 1969). Calcium (Ca^{2+}) is the main regulatory ion and is required for muscle contraction and the cytoplasmic free Ca^{2+} concentration is tightly regulated from approximately 0.05mM at rest to <1mM during contraction (Ashley and Ridgway, 1969; Weber, 1959). The proteins involved in calcium handling define many aspects of contraction (e.g. speed and duration) as the calcium transient is related to force production. The force-frequency relationship in muscle results from incomplete calcium removal thus higher cytoplasmic calcium concentrations and at high frequency produces a tetanic contraction.

In summary, activation of the muscle is under neural control and the nervous system has multiple ways in which the force produced by the muscle can be precisely controlled. Aim 2 of this project will utilize pulse width manipulation to alter the level of muscle activation. At the muscle level, properties intrinsic to the muscle allow for further modulation of force production.

Mechanical Factors Affecting Force Production

Functional Properties

The current model for force production by striated muscle represents a convergence of separate mechanical, morphological and biochemical observations, formally unified by Andrew Huxley in the 1950s. Early experimental observations of muscle contraction indicated that changes in muscle length or changes in shortening velocity affected the force a muscle was able to generate. For example, in cardiac muscle, it was observed that the more the heart fills with blood, the more forceful the contraction (Patterson et al., 1914). In skeletal muscle, the amount of active force produced by a fully activated muscle contracting isometrically depended on the muscle

length (Blix, 1893; Ramsey and Street, 1940). In both cardiac and skeletal muscle, active force decreases when the muscle is either shortened below or lengthened beyond resting length. However, total force produced by the muscle increases when the muscle activated at longer lengths resulting in ever increasing force. This is due to passive force, the force seen without activating the muscle, and implies the muscle has some resistance to lengthening beyond a certain length.

Another early phenomenon of contracting muscle, observed by Fenn, was that heat production increased during shortening contractions above that produced by maximal isometric contractions. This increased energy consumption was nearly proportional to work done by the muscle (Fenn, 1923; Fenn, 1924). The amount of force a shortening muscle can produce also depends on the speed or velocity at which it shortens (Gasser and Hill, 1924). Hill (1938) and Katz (1939) later provided details for this relationship between tension, speed of shortening and heat production (Hill, 1938; Katz, 1939). Essentially, the faster a muscle is allowed to shorten, the less force it is able to produce but the greater the amount of energy is consumed. It can also be said that the load imposed on the muscle determines how fast the muscle is able to shorten. In concentric activations, in which the muscle shortens, force will always be less than the maximum but heat production and energy consumption is greater. By contrast, eccentric activations that allow the muscle to lengthen while activated actually produces dramatically greater force and less energy released (Fenn, 1924).

Biochemical and Structural Properties

Biochemical and structural studies proceeded rather independently but key discoveries laid the foundation for the basic understanding of muscle contraction. Myosin was the first protein to be identified in muscle and known to be one of the principle components of (Banga et al., 1947; Kuhne, 1864; Szent-Gyorgyi, 1945). One key discovery was that myosin is an ATPase. Myosin has the ability to split high-energy

phosphate and that the chemical energy stored in these bonds was converted into mechanical energy used for contraction. Adenosine triphosphate, or ATP, would later be identified as the likely source of energy for contraction (Engelhardt and Ljubimowa, 1939). Further studies discovered that "myosin" actually consisted of two proteins, one that was unaffected (myosin, the ATPase) and one whose viscosity was reduced (actin) by exposure to ATP (Needham, 1942; Szent-Gyorgyi, 2004). Interaction of ATP with actinomyosin was the basic contractile event however at this time there was no attempt to relate these findings to the striated appearance of muscle.

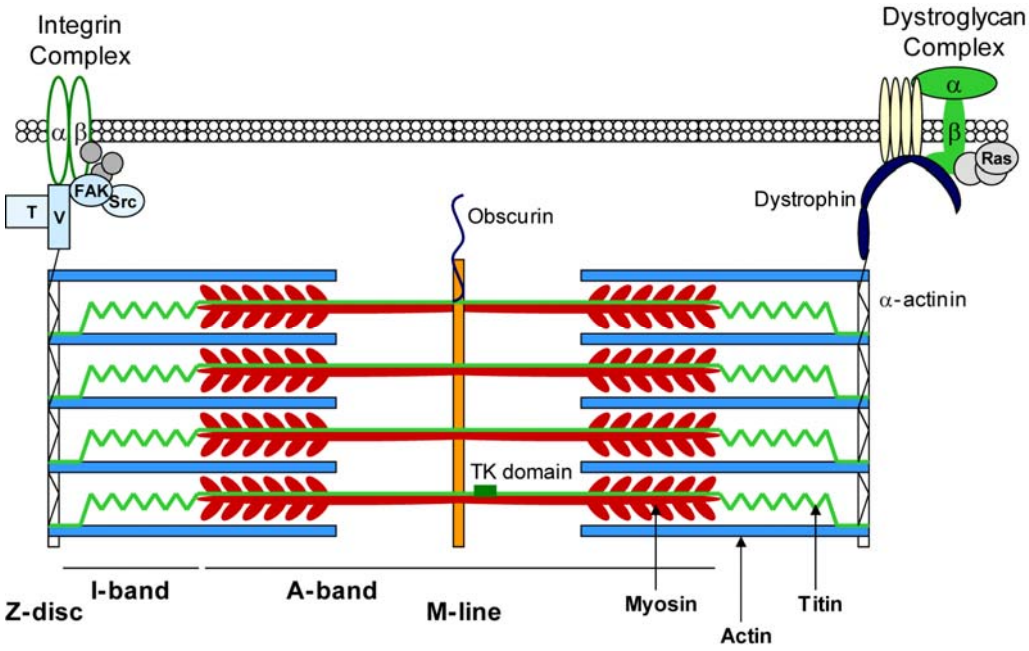

Figure 1.2 Structure of the sarcomere.

Structurally, the striated appearance of myofibrils have long been recognized and described as repeating sarcomeres, the most basic functional unit of muscle (See Figure 1.2). Dark bands were presumed to be myosin however how it functions with respect to contraction was unclear. In 1954 the landmark studies by two independent groups observed the striated pattern of contracted fibers compared to resting fibers under

microscopes. Together their interpretation of these images led to the sliding filament theory (Huxley and Niedergerke, 1954; Huxley, 1957b; Krause, 1869). Both groups demonstrated that the width of the dark A-band remains constant at different sarcomere lengths or during contraction and changes in sarcomere length results from changes in the light I-band alone. The A-band is myosin thick filaments and the I-band included the thin filament, actin. Both groups hypothesized that muscle shortens by relative sliding of actin past myosin and towards the middle of the sarcomere. It was further proposed and later observed that links or "bridges" exist between the actin and myosin filaments and that ATP (hydrolysis) powers the formation of these bridges and aids in the sliding of filaments (Huxley and Taylor, 1958).

Mechanisms of Contraction- Cross-bridge Model

Development of the cross-bridge theory arose from integration of muscle biochemistry with muscle structure by AF Huxley. The goal was to account for the structural and physical changes that occur with contraction (Huxley, 1957a; Huxley and Simmons, 1971). The cross-bridge theory provides a mechanism for filament sliding in that there is a physical attachment of myosin to actin. The 1957 model proposed a two-state process in which cross-bridges were attached and producing force or not attached and not producing force. Transitions between the two states were described by attachment and detachment rate constants in which detachment requires ATP hydrolysis. In order to relate the model to previous observations of the relationship of force to muscle length or shortening velocity, the model relied on a few assumptions including: the force generated by the muscle is proportional to the number of cross-bridges formed and attachment and detachment rates are proportional to the stretch of the cross-bridges. Visualization of cross-bridge formations and anatomical measures of actin and myosin allowed for integration of sarcomere structure with the cross-bridge model and described how the number of cross-bridges formed explains why filament overlap is proportional to

force (Gordon et al., 1966; Huxley and Taylor, 1958). Huxley would further refine this model and propose a swinging cross-bridge model that accounts for much of the observed characteristics of muscle contraction (Huxley and Simmons, 1971). Incorporation of ATP hydrolysis (Lymn and Taylor, 1971) into proposed mechanism of contractions (stages of cross-bridge attachment) formed the basic principle of cross-bridge cycling that drives muscle contraction. Force production, beginning in a state of rigor, depends on binding of ATP to myosin releasing the actin-myosin interaction, followed by 're-priming' of the myosin head and ATP hydrolysis into adenosine diphosphate and inorganic phosphate (ADP-Pi). Myosin-ADP-Pi is then able to bind actin in a weakly bound state. Release of Pi is associated with the transition from weakly bound state to a strongly bound state of myosin-ADP. The 'powerstroke' continues with the release of ADP and the myosin head moves, pulling the actin filament towards the myosin.

The dependence of force on length or velocity has different consequences for ATP turnover because of the mechanics of cross-bridge formation associated with each. For example, increased shortening velocity increases ATPase activity whereas isometric activation at short length has little change in ATPase activity (see Figure 1.3; (Hilber et al., 2001; Potma et al., 1994)). During maximum isometric contractions, the dominant cross-bridge state is likely the strongly bound, high force state, cross-bridge turnover is relatively slow, and force production is dominated by steric factors. If filament overlap is not optimal, for example, sarcomere length falls on the descending limb of the force-length curve, fewer cross-bridges form and less active force is produced. If sarcomere length fall on the ascending limb where there is substantial filament overlap, or double overlap, cross-bridges cycle but a lower percentage of properly forming cross-bridges are cycling, thus force production decreases more than energy costs (Fenn and Latchford, 1933; Stephenson et al., 1989).

By contrast, with increasing shortening velocity, cross-bridges spend less time in the strongly bound state as cross-bridge cycling rate is increased. ADP release, or

detachment from the force-producing state, is the slowest event in cross-bridge cycling (Potma and Stienen, 1996; Potma et al., 1994). Increasing the shortening velocity is associated with increases in the rate of actinomyosin detachment (Potma et al., 1994). The increased energy costs observed with shortening contractions compared to isometric contractions has been attributed to this difference in cross-bridge mechanics (Potma and Stienen, 1996; Potma et al., 1994). So, although force production requires energy expenditure, comparing force produced by varied velocity and varied length decouples force from energy costs.

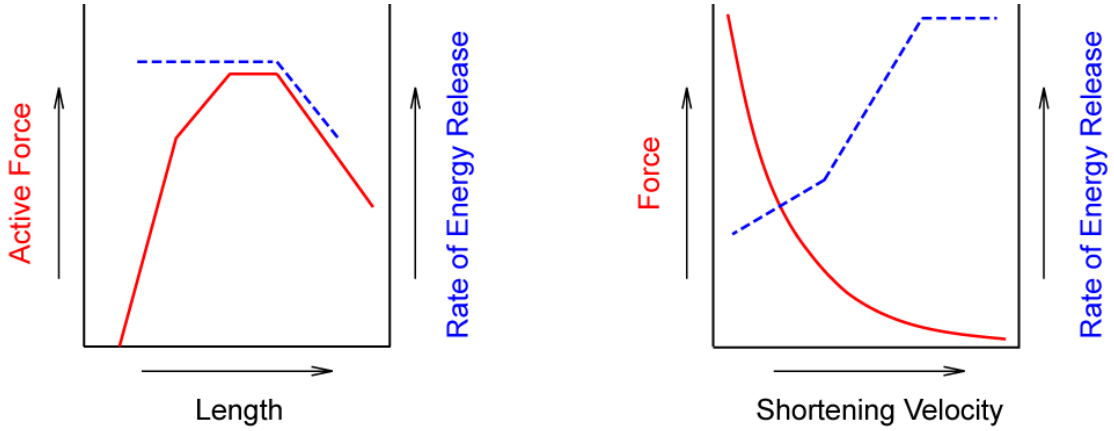

Figure 1.3. Force-length and force-velocity curves and associated energy costs.

Energetic Costs

Overview

The primary consumers of energy during contraction include the ATPase activity of myosin, required for myosin to bind to actin and force to be produced, of SERCA, the calcium pump in the sarcoplasmic reticulum (SR) membrane required for pumping calcium back into the SR and muscle relaxation, and of the Na^+-K^+ pump in the sarcolemma, required for restoring the electrochemical gradients and membrane potential (Homsher and Kean, 1978; Walsh et al., 2006). The rate of ATP hydrolysis can be

measured by heat production chemical analyses and typically about 30% or up to 40% of ATP consumed during contraction can be attributed to pump activity, as ions are transported up their concentration gradients (Barclay et al., 2008). This means the majority of ATP consumed is for the interaction between actin and myosin, thus force production. During intense contractile activity the rate of ATP consumption can increase by ~100-fold (Sahlin et al., 1998). The rate of ATP turnover or energy consumption depends on level of fiber activation, cross-bridge cycling and ion pumps. The rate of cross-bridge cycling depends on the mechanical conditions of force production. It may be possible that local concentrations of ATP deplete, however, in general, whole cell ATP concentration remain relatively constant and highly protected (Sahlin et al., 1998).

Mechanisms to Restore ATP

ATP concentration is maintained by aerobic or anaerobic processes that, under resting and moderate activity, can match the ATP demand of the muscle. Oxidative (aerobic) metabolism includes transfer of oxidized substrates through the tricarboxylic acid (TCA) cycle and NADH molecules through the electron transport chain (ETC) and ATP production through oxidative phosphorylation. ATP generated in the mitochondria matrix by oxidative metabolism is the primary source of ATP under resting conditions as this generates the greatest ATP yield and can sustain prolonged increases in ATP demand. Carbohydrates and fats are the major source of metabolic fuel for ATP production however protein oxidation may contribute. Glucose uptake in response to feeding is stored in the muscle as glycogen serving as a local reservoir for glucose. Glucose metabolism via glycolysis results in the production of pyruvate, which can be oxidized into acetyl CoA. Fats are also stored in the muscle as well as in adipose tissue. Fatty acid metabolism via β-oxidation results in the production of acetyl CoA. Under aerobic conditions production of acetyl CoA is fed into the TCA cycle, which generates ATP and NADH. NADH molecules are further utilized in the electron transport chain

where the majority of ATP is generated. Here, electrons are systematically and sequentially transferred to oxygen, and in the process creates a proton gradient across the mitochondrial membrane and ATP synthase generates ATP as protons are pumped back across the gradient.

In the face of dramatic and rapid increases in energy demand (e.g. for powerful bursts of energy), oxidative metabolism is not sufficient and induces a major energetic challenge. Phosphocreatine (PCr) breakdown ($PCr + ADP + H^+ \rightarrow ATP + Cr$) and glucose breakdown via glycolysis occur under anaerobic conditions to rapidly (re-) generate ATP within the cytoplasm. In response to maximal activation, PCr is able to resynthesize approximately 3 times the resting ATP thereby matching ATP demand, but only for a short time (~10s in humans) as stores are rapidly depleted (Hargreaves and Spriet, 2006; Sahlin et al., 1998). During a rest or recovery period, the PCr store is also able to rapidly regenerate as ATP production continues and creatine kinase transfers phosphates back to creatine. In humans, this may take about 4 min (Sahlin et al., 1998) but in rodents this is much quicker with near recovery by 60-90s (Challiss et al., 1989). Glycolysis, which is capable of producing about 12 times the resting ATP, is activated at the same time however contribution to ATP production by glycolysis is slightly delayed from PCr as more steps are involved (Hargreaves and Spriet, 2006). Under anaerobic conditions, pyruvate, the byproduct of glycolysis, is converted into lactate. Lactate may accumulate within the cell, where under aerobic conditions may be oxidized and enter the TCA cycle, or be transported out of the cell in to the bloodstream or utilized by other cells (Hargreaves and Spriet, 2006).

Adequate cellular ATP concentrations inhibit these bioenergetic processes. Because of the large differences in concentration maintained of each adenylate molecule, with ATP having the greatest concentration, small decreases ATP result in large increases in AMP (Hardie and Hawley, 2001). ATP allosterically inhibits enzyme kinetics associated with glycolysis as well as inhibits oxidative phosphorylation (Hargreaves and

Spriet, 2006). These metabolic processes are regulated primarily by feedback mechanisms that affect enzyme activity and mass action. That is, progression of a pathway depends on the concentration of both the reactants and the products where accumulation of either the product or the reactants controls the direction of the reaction. During exercise, Ca^{2+} activation of the contractile apparatus results in a drop in ATP levels and accumulation of AMP, ADP and Pi triggers enzyme activity and metabolic processed to restore ATP. The resulting increase in substrate availability (i.e. ADP, pyruvate) drives processes of oxidative metabolism forward in the presence of oxygen. In addition, exercise promotes oxidation of NADH, thus increases NAD^{+} availability, and along with acetyl CoA accumulation, increases flux through the TCA cycle producing more NADH required for the electron transport chain. However, ADP and Pi are the limiting factors of oxidative phosphorylation.

Myosin Heavy Chain

The intensity of metabolic stress depends on the muscles molecular and metabolic compositions that determine its capacity to respond to that stress. Most muscles are comprised of a mixture of fibers that vary in contractions speed, oxidative and glycolytic capacity and the capacity for energy production influences the perception of metabolic load. Experimentally it was determined that there is an intimate relationship between fiber type and mechanical performance of the fiber that derive from specific metabolic enzymes and calcium handling proteins, which coincide with specific myosin heavy chain isoforms (MHC). That is, muscles with high vascularity tend to have plentiful mitochondria, a high capacity for oxidative metabolism and myosin heavy chain with relatively low ATPase activity. Thus, the adaptation to persistent activation appears to minimize processes of ATP consumption and maximize processes for ATP generation. MHC isoforms are the main determinant of calcium-activated ATPase activity although multiple myosin light chain (MLC) isoforms exist with fiber type dependence (Schiaffino

and Reggiani, 2011). The rate of ATP consumption varies in fibers with different MHC expression and is related to different shortening velocities observed (Han et al., 2003; Sweeney et al., 1986).

In adult mammals, there are 4 main MHC isoform expressed: MHC-I for slow, type I fibers, MHC-IIa, MHC-IIx and MHC-IIb for fast, type II fibers. Most fibers appear to express only a single isoform of MHC, although co-expression of multiple isoforms is seen in up to 15% of unperturbed fibers (Caiozzo et al., 2003). The myosin ATPase, required for cross-bridge formation, is responsible for about 70% of the ATP hydrolysis. ATP consumption is about 3-fold greater in fast than in slow muscles (Barany, 1967; Crow and Kushmerick, 1982). During isometric contraction, the rate of ATP hydrolysis can vary greatly and increases from MHC-I → IIa → IIx → IIb (Bottinelli et al., 1994). The release of ADP is the rate-limiting step of the cross-bridge cycle (Weiss et al., 2001) and MHC isoforms determine the rate of cross-bridge detachment due to differing affinities for ADP. Thus, MHC isoform is a major determinant of the rate of ATP consumption (Weiss et al., 2001).

In general, although fiber type differences among the fast fibers exist, the rates of all aspects of force production are faster in fast fibers compared to slow fibers. For instance, the amplitude of the calcium transient from a single action potential is greater and shorter, thus force develops and declines much more quickly in fast fibers compared to slow (Baylor and Hollingworth, 2003). The greater number of calcium release channels (ryanodine receptors, RyR) contributes to the greater Ca^{2+} release in fast fibers. In addition, the greater density and fiber type specificity of Ca^{2+}-ATPase pumps (SERCA1) and Ca^{2+} buffers along with the larger volume of sarcoplasmic reticulum (SR) in fast fibers accounts for most of this diversity between Ca^{2+} transients (Schiaffino and Reggiani, 2011).

Muscle must have the ability to meet the energy demands and match ATP production. Fast fibers consume more energy (ATP) but are active only for a short time

and are therefore supported by metabolic processes that rapidly replenish ATP. Phosphocreatine levels are 15-20% greater in fast fibers (Soderlund and Hultman, 1991) and glycogen content about 16-31% greater at rest in fast (Schiaffino and Reggiani, 2011). In addition, enzymes of glycolysis, such as phosphofructokinase, the rate – limiting enzyme in glycolysis and lactate dehydrogenase, which converts pyruvate to lactate are both expressed at higher levels and possess higher activity in fast fibers (Schiaffino and Reggiani, 2011). Thus, PCr and glycolysis are relied on more heavily in fast fibers but inevitably these processes limit the fibers contractile activity. On the other hand, slow fibers consume less ATP during contraction and can pretty well match ATP demands with regeneration supported by oxidative metabolism. Slow fibers have more mitochondria, and correspondingly more mitochondrial enzymes, and have greater vascularization providing increased substrate supply and metabolic waste removal (Schiaffino and Reggiani, 2011). Greater fatty acid metabolism as well as pyruvate oxidation from glycolysis provides two sources of acetyl CoA as substrate for the TCA cycle. Together, slow fibers are more suitable to perform chronic, low force activities.

Skeletal Muscle Hypertrophy

Resistance exercises have long been employed as a means of increasing muscle mass and strength for athletic performances or rehabilitation strategies. The mechanisms involved in this adaptation can be better understood by studying how the muscle responds to different workloads. This section will provide a historical perspective of the progressive overload strategy, provide an overview of different models used to study muscle hypertrophy and discuss the concept of homeostasis, which may drive adaptation.

Concept of Progressive Overload

From the earliest times, cultures around the world have recognized the relationship between physical activity and overall health (MacAuley, 1994). Gymnastic

programs were developed and taught in Eastern cultures (e.g. Cong Fu, Yoga) and Western cultures (e.g. traditional gymnastics) as ways to strengthen the body and mind together and remain prepared for war/battle. With the Greeks desire for physical perfectionism, this practice eventually gained a competitive aspect. In the 6th century B.C. legend has it that Milo of Croton, who carried a full-grown bull twice around the Olympic stadium, 'trained' his muscles by carrying that growing calf every day since its birth (Gardiner, 2002). While this may be an exaggeration emphasizing Milo's great ability, the idea of progressive overload was perhaps unknowingly conceived. In the late 19th century, scientific studies led to theories that tissues may respond to their mechanical environment. For example, it was observed that bone remodels in response to altered loads resulting in a stronger bone (Wolff, 1892). Similarly, an 1897 study in which dogs were trained to run on running wheels at different workloads is commonly cited as one of the first observations of work-induced hypertrophy. Specifically it was determined that fiber size increased without an increase in number (Morpurgo, 1897).

Following the World Wars, DeLorme (1940's) observed responses to military rehabilitation strategies. In short, he noticed patients recovered more quickly when performing low repetition at high force versus high repetition at low force and that there were specific adaptation with each (i.e. strength vs. endurance). From his observations, he introduced 10-repetition maximum (10-RM) and that after so long, weight should be added to progressively overload the muscle as strength increased. Many studies on training followed that contributed to understanding of stimulating growth by overloading the muscle (Berger, 1962; Hather et al., 1991; Jones et al., 1989). From these studies, complied by the American College of Sports and Medicine (ACSM), emerges a picture of training and states that for muscle growth in healthy individuals, a small number of contractions (2-6 repetitions per set) at greater than 70% 1RM performed 2-3 times per week results in fiber hypertrophy (2009). The phenotypic result is a shift in MHC

isoforms from IIx → IIa, and larger fiber/muscle cross-sectional area primarily of type II fibers (Campos et al., 2002; Hortobagyi et al., 1996).

The hypertrophic process in humans is rather slow (>3mo) as size increases about 0.1-0.2% per day. However, a single bout of resistance exercise (RE) increases protein synthesis by ~30% within 2-3 hours and is maintained for 24-48 hrs (Biolo et al., 1995; Chesley et al., 1992). Chesley (1992) found that this increase in myofibrillar protein synthesis (MPS) came without any changes in RNA capacity. It was suggested that the increase in RNA activity might occur by increases in the rate of protein translation. MAP kinase and Akt-mTORC1 are intracellular signaling cascades involved in regulating protein synthesis. In humans, MAP kinase phosphorylation is immediately increased upon muscle contraction (Aronson et al., 1997; Williamson et al., 2003) and inhibition of mTORC1 with the drug rapamycin prevents contraction-induced increase in MPS (Drummond et al., 2009).

Non-Human Models of Muscle Growth

Animal models of exercise have been developed to manipulate load and have contributed to the molecular understanding of how muscle responds to different signals. Various models used to produce high force contractions (HFC) support the notion that the amount of tension is critical to initiating compensatory growth (Booth and Thomason, 1991; Goldspink and Howells, 1974; Timson, 1990; Wong and Booth, 1990; Wong and FW, 1990). An important finding from across all models, which agrees with human studies, is that the primary response of muscle to HFC is an increase in protein synthesis (Baar and Esser, 1999; Chesley et al., 1992; Wong and Booth, 1990; Wong and FW, 1990). This section will present an overview of exercise models focusing on those that contribute to the understanding of muscle growth.

Compensatory/Functional overload model

Three versions of functional overload (FO) were developed beginning in the 1960's aimed to drastically increase the amount of force a muscle was asked to produce. The concept of FO is to disrupt function of the majority of a group of synergist muscles, leaving a small muscle as the sole force producer of that group. The most commonly used group is the rodent triceps surae, which includes the large force producing gastrocnemius muscle, the smaller plantaris and the small, postural soleus muscle. Tenotomy was the first developed in which the Achilles tendon is severed leaving only the plantaris able to produce force (Goldberg et al., 1975; Goldberg, 1967). Denervation is fundamentally similar in that the gastrocnemius and soleus, with their nerve branch severed, receives no neural input thus does not contribute to force production. Although there are rapid increases in mass (~20-40%), spontaneous reattachment of tendon or re-growth of the nerve confounds interpretation. More common now, synergist ablation is the complete removal of the synergist muscles and ensures prolonged overload of the remaining muscle. All three versions are associated with an initial inflammatory response during the first week of recovery from surgery, however, the synergist ablation method result in substantial (~50-100%) muscle and fiber hypertrophy (Armstrong et al., 1979).

FO is a chronic, high-force contraction model that induces rapid hypertrophy to an extent not achieved in humans or by other models. Although FO is clearly a non-physiological model and unlike resistance training, this model allows the study of the upper limits of the adaptive process. Following an initial period of awkward gait, this model imposes this chronic increased load. Muscle recruitment, measured by EMG activity, doubles but remains sub-optimal (Gardiner et al., 1986). Still, the muscle enlarges at rate of 0.86-4% per day, which is high compared to humans where the muscle is exposed to high forces approximately 0.1% of the week and enlarges 0.1-0.2% per day (Booth and Thomason, 1991). FO results in increased protein synthesis and RNA, but in contrast to human resistance exercise (RE) and other models of HFC, FO commonly

results in increased DNA, which is suggested to be due to infiltration of inflammatory cells and activation of satellite cells. Hypertrophy, in general, can occur in the absence of satellite cell addition (Blaauw et al., 2009; McCarthy et al., 2011), but whether the massive and rapid growth in response to FO requires activation of satellite cells is unclear, at least in the short term adaptation (Adams et al., 2002; Adams and Haddad, 1996; Adams et al., 1999; McCarthy et al., 2011). In response to the altered neural patterns imposed by this model, MHC isoforms transition from type II and type I fibers, rather than a shift within type II fiber seen in humans, and reflects the need for a more oxidative phenotype for continuous activations (Chalmers et al., 1992; Olha et al., 1988).

This process of increasing protein synthesis is clouded by the inflammation and repair/regeneration processes, however, it activates the same growth-related signaling cascades as human resistance training and other models of HFC. Most investigators allow a recovery period 5-7 day before analyses therefore, the time course of signaling is more difficult to compare to other models. The initial response of intracellular signaling cascades appears similar in that MAPK are activated, although the temporal patterns between molecules are different (Carlson et al., 2001). Further, rapamycin prevents the compensatory overload-induced increase in hypertrophy (Bodine et al., 2001) as well as prevents the increase in human MPS following resistance exercise (Drummond et al., 2009). Satellite cell depleted muscle FO results similar initial intracellular signaling through mTORC1 (Adams et al., 2002). This suggests the muscle may undergo two phases of changes: the first, hypertrophic signaling induced by high forces in response to the increase in load and the second, changes that includes activation of satellite cells and fiber type conversions.

Resistance exercise-like models

In an effort to mimic human resistance training, some investigators have trained various animals to lift weights (Lowe and Alway, 2002). This generally entails adding

weight to the animal's limbs and with operant conditioning, forcing them to climb or perform squat-like movements in order to obtain food (Bolster et al., 2003; Goldspink and Howells, 1974; Klitgaard, 1988; Kubica et al., 2005). For example, Klitgaard developed an apparatus in which animals must enter a vertical tube and with a weight attached to a neck harness, must push the weight up to reach food. After 36 weeks, hind limb mass (soleus and plantaris) increased by about 30% and maximum force production increased by about 40-70%. Weight lifting in animals results in an increase in protein synthesis following an acute bout (Kubica et al., 2005) and a modest increase (~10-30%) in muscle and fiber size following training. In general this model results in a similar rate (0.7% per day) of muscle enlargement as seen in humans (Booth and Thomason, 1991).

Weight lifting in animals is most similar to human resistance training in that there can be progressive overload of muscles with physiological recruitment of motor units since these are voluntary contractions. In contrast to FO, the rate of protein synthesis and protein accretion in RE-like models occurs much more slowly but more closely mimics human resistance training. The primary drawbacks to this model include the length of time required for hypertrophic response, the required training period and the potentially stressful environment of that training, therefore these studies are more limited. Still, Jefferson and Kimball's group used operant training and found immediate activation of mTORC1 effectors and rapamycin treatment inhibits this signaling and the increase in protein synthesis (Bolster et al., 2003). MAP kinases were not analyzed at the immediately time point.

<u>High frequency electrical stimulation model</u>

High frequency electrical stimulation (HFES) has become an increasingly useful model. The method was used by Wong and Booth (1990) whereby field-stimulation was used to invoke a series of maximally contraction in the hind limb muscles and results in plantar flexion of the ankle with the TA and EDL being slightly lengthened while

activated. Importantly, muscles that were stimulated to contract against a load hypertrophied 15-30% over a 10-week training period. Baar and Esser (1999) modified this method by removing the external load and implanting a cuff electrode onto the sciatic nerve allowing repetitive training via nerve activation. The stimulation parameters aimed to mimic resistance training by eliciting activation in the form of sets and repetitions (i.e. 10 sets of 6 reps). Here, the load imposed on the TA is that from resisting the concentric activity of the gastrocnemius-plantaris-soleus complex and hypertrophy, ~14% increase in TA mass, was evident after 6 weeks of training. Two important concepts were further confirmed in these studies: 1) loading a muscle is the primary stimulus and results in muscle growth and 2) loading triggers an increase in protein synthesis prior to changes in DNA or RNA content (Baar and Esser, 1999; Wong and Booth, 1990; Wong and FW, 1990). In addition, Baar and Esser's study indicated loading specifically alters the rate of protein translation initiation and many have since used this model to study the underlying mechanisms regulating protein synthesis.

HFES maximally activates all motor units within the muscle ensuring simultaneous activation of all fibers throughout the stimulation. The major benefit is that it provides consistency between activations and control over contraction parameters. The disadvantage is that these types of contractions are non-physiological. Motor unit recruitment order is not followed and simultaneous activation of all fibers does not occur. Animals and humans are generally unable to voluntarily maximally contact a muscle. Nevertheless, that the investigator is ultimately able to precisely control the stimulus and pattern of stimulus the muscle receives is of great importance for experimental design. Other variations of high frequency electrical stimulation include *ex vivo* and *in situ* muscle preparations. The *in situ* muscle preparation used in this dissertation allows the muscle to remain in a near physiological environment, with blood supply and tissue connections intact. The major advantage to the *in situ* set-up versus *in vivo* is specific conditions or mechanics of a single muscle can be accurately measured or controlled.

The demands imposed by HFES are similar to RE in either humans or animals in that the time the muscle spends performing high force contractions is relatively low. However, exact stimulation conditions vary. Generally, studies that aim to represent RE, elicit stimulations in sets with repetition (Baar and Esser, 1999; Garma et al., 2007; Nader and Esser, 2001; Thomson et al., 2008). HFES results in similar range of hypertrophy, about 15-30% depending on the length of study and muscle analyzed (Baar and Esser, 1999; Garma et al., 2007; Wong and FW, 1990) but is achieved more quickly than with RE (3-6 weeks vs. 12-16 weeks). Wong and Booth (1990) report an increase in protein synthesis of ~50-60% in the TA and a 28% increase in protein content. Similar to humans, increases in RNA and DNA follow these increases in protein synthesis. The change in mass as a result of HFES has been correlated with signaling downstream of mTORC1 and inhibition by rapamycin prevents this signaling and subsequent change in protein synthesis and muscle mass. Other studies utilize short, rapid activations, generally for less than 10 minutes to analyze immediate response to muscle activation (Martineau and Gardiner, 2001; Russ and Lovering, 2006; Ryder et al., 2000; Wretman et al., 2001). Similar to FO and RE, HFES results in rapid activation of MAP kinases although the exact conditions resulting in activation may differ.

Homeostasis

The experimental models support the idea that muscles adapt to increased loads by increasing fiber cross sectional area and muscle mass thus allowing maximal force production to increase. The function of the adaptation in response to a specific perturbation is to minimize similar cellular disturbances in the future. As a result, the muscle is able to perform more effectively and do work longer.

Homeostasis represents a physiological balance and acts to maintain an internal state. It is this homeostatic process that initiates an adaptation such that the deviation caused by a perturbation is relieved and returns to its homeostatic state. Homeostatic

states are intrinsic properties of muscle, such as mechanical stress, that can be sensed and interpreted by cellular processes within the muscle. These states are derived from extrinsic properties that are beyond direct, cellular measurement, such as force or mass, but it is these extrinsic properties that determine functional efficacy and can be manipulated by an intervention or altered as an adaptation. Homeostatic states are a ratio between two extrinsic properties. For the case of muscle hypertrophy, it appears that the extrinsic adaptation in muscle size to the extrinsic perturbation of mechanical demand results in maintenance of an intrinsic state. Because overloading is a prominent stimulus for hypertrophy, it can be hypothesized that peak force per cross sectional area (F/CSA) is the intrinsic property maintained. That is, the homeostasis process triggers an increase in CSA so that the increased loading imposed by HFC is dispersed across the adaptive increase in CSA thus, F/CSA is maintained. This implies a mechanical behavior is transduced into the cell for it to respond.

Regulation of Protein Synthesis

In response to mechanical forces, muscle responds with an increase in protein synthesis, which is tightly regulated by post-translational mechanisms. However, various other stimuli can create an anabolic environment for the muscle, which can also influence the rate of protein synthesis by similar post-translational mechanisms. This section will provide an overview of protein synthesis and identify sites of regulation.

Process of Protein Synthesis

The rate of cell growth, as measured by protein accretion or cell number, is subject to regulation by a number of stimuli, which includes mechanical simulation, external growth factors and nutrient availability. One of the major controls of protein accretion is the rate at which messenger RNA (mRNA) is translated into protein by ribosomes. The process of protein translation involves three stages: initiation, where a

ribosome is recruited to an mRNA; elongation, where the ribosome progressively lengthens the amino acid chain; and termination, where the fully translated protein and ribosome are released from the mRNA. Each stage has specific translation factors that are subject to regulation.

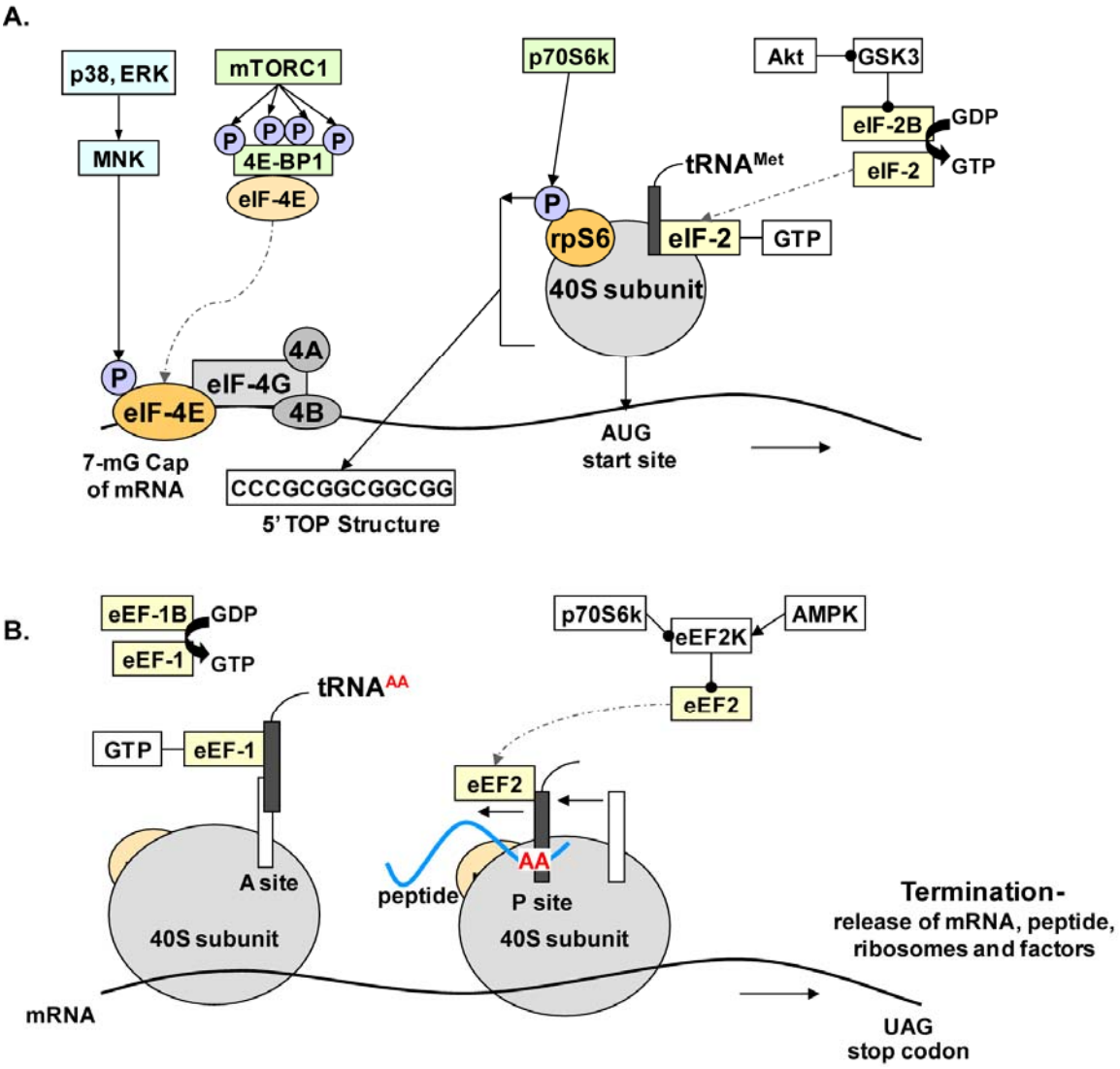

Figure 1.4 Process of protein synthesis. A) Initiation stage. Assembly of the 4F complex, which includes eIF-4E, 4G, 4A and 4B, to the mRNA is followed by recruitment of a Met-tRNA bound 40S subunit complex to the mRNA. Regulation of key components are depicted. B) Elongation and termination stage. Recruitment of subsequent aminoacyl-tRNA involves GTP-bound eEF-1and progression of the peptide through the ribosome requires eEF-2. Progression along the mRNA continues until the ribosome reaches the stop codon and release causes the complex to break-up.

Initiation includes assembly of the eIF-4F complex to the 5' end of mRNA, recruitment of the Met-tRNA to the 40S ribosomal subunit by GTP-bound eukaryotic Initiation Factor (eIF)-2 followed by recruitment of the ribosomal complex to the mRNA (Figure 1.4A). During initiation, the eIF4 complex binds to the 7-methylguanosine (7-mG) cap present on all mRNAs, and denatures the structure of the 5'UTR (untranslated regions), which facilitates annealing of the 40S ribosomal subunit. Regulation of initiation is dependent on the availability of eIF-4E, which is required for formation of the eIF-4F complex. Formation of the 4F complex can be enhanced directly through phosphorylation of eIF-4E or reduced by competitive binding of eIF-4E to its binding protein, 4E-BP1 (Proud, 2007). Only 40S subunits associated with Met-tRNA/eIF-2 complexes are capable of initial annealing, and initiation depends strongly on the abundance of eIF-2B. eIF-2B is the guanine nucleotide exchange factor (GEF) for eIF-2. The catalytic subunit of eIF-2B, eIF-2Bε, is required for the GDP-GTP recycling on eIF-2 and regulates the availability of competent eIF-2 and competent 40S. Activity of eIF-2B can be inhibited by phosphorylation of eIF-2Bε or enhanced by increased translation of eIF-2 Bε (Mayhew et al., 2011; Proud, 2007). Phosphorylation of the ribosomal protein S6 (rpS6), a component of the 40S ribosomal subunit increases its affinity for specific mRNAs, based on the presence of TOP structure (a tract of oligonucleotides rich in pyrimidines) in the 5'UTR. mRNAs that contain a 5'-TOP structure encode much of the translational apparatus (e.g. ribosomal proteins and translation factors) including eIF-2Bε. It is thought that phosphorylation of the rpS6 by p70S6 kinase promotes specific translation of 5'-TOP mRNAs, as both these events are sensitive to the drug rapamycin. Genetic p70S6k knockout models identified some redundancy as serum induced translation still occurred (Pende et al., 2004) although it is possible that regulation by p70S6k may arise under conditions of stress (Mayhew et al., 2011). Nevertheless, p70S6k KO animals have smaller myoblasts and overall reduced body size emphasizing the role of p70S6k in regulating growth and cell size (Ohanna et al., 2005; Pende et al.,

2004; Shima et al., 1998). Analysis of polysome profiles following high force contractions show a shift to heavier polysomes, indicating more ribosomes associated with mRNA, and suggest changes in protein synthesis results from stimulation of translation initiation (Baar and Esser, 1999). Accordingly, initiation is thought to be the rate-limiting step as multiple steps are under tight control.

Elongation includes recruitment of appropriate aminoacyl tRNAs, and progression along the mRNA and requires two elongation factors, eEF-1 and eEF-2 (Figure 1.4B)(Proud, 2007). With a similar regulation of activity as eIF-2 (initiation) undergoes, eEF-1B is the GEF for eEF1A. GTP bound eEF-1A recruits the aminoacyl tRNA to the A-site of the ribosome based on the codon currently in the A-site. eEF-2 promotes translocation of the forming peptide within the ribosome. eEF2 can be phosphorylation on its T56 residue by eEF2 kinase, which results in inhibition of eEF2 preventing interacting with the ribosome (Redpath et al., 1993). eEF2K is regulated negatively or positively by phosphorylation. p70S6k is thought to phosphorylate and inhibit eEF2K, thereby enhancing elongation, and, AMPK can phosphorylate and activate eEF2K, thereby reducing the progression of elongation (Horman et al., 2002; Wang et al., 2001). Termination occurs with recognition of the stop codon and release of the translated protein.

Sites of regulation

Initiation depends strongly on the availability of eIF-4E, the abundance of eIF-2B and activity of p70S6k. These proteins are subject to post-translational modifications under the control of upstream signaling cascades, particularly cascades involving mTOR (Proud, 2007). The mammalian target of rapamycin complex (mTORC1) directly phosphorylates p70S6k at threonine 389 (T389), the residue most closely associated with kinase activity (Hornberger et al., 2007), and indirectly controls eIF-4E availability by controlling the interaction between eIF-4E and its inhibitory binding protein (4E-BP1).

Hyperphosphorylation of 4E-BP1 by mTORC1 releases inhibition thus increases availability of eIF-4E to form the 4F initiation complex with mRNAs. Inhibition of mTORC1 by the drug rapamycin abolishes phosphorylation p70S6k and 4E-BP1 and reduces protein synthesis (Bodine et al., 2001; Drummond et al., 2009).

The mammalian target of rapamycin can form 2 complexes, mTORC1 and mTORC2. The major difference being the regulatory protein associated with mTOR (i.e. In mTORC1, Raptor, the regulatory associated protein of mTOR is associated with mTORC1 while Rictor, rapamycin-insensitive companion of mTOR is associated with mTORC2). Importantly, mTORC1 is the complex sensitive to rapamycin and widely implicated in the regulation of protein synthesis (Hornberger et al., 2004) and direct activation of mTORC1 signaling in muscle cells is sufficient to induce hypertrophy (Goodman et al., 2010).

Protein translation is also regulated by several MAPK signaling, independent of mTOR, although the exact circumstances behind this signaling are not clear. For example, both p38 and ERK MAP kinases can contribute indirectly to the phosphorylation of unbound eIF-4E and this is thought to increase the affinity of eIF-4E to the 7-mG cap structure of mRNA (Gautsch et al., 1998; Pyronnet, 2000). However phosphorylation of eIF-4E may not be required for translation to proceed (McKendrick et al., 2001). Full activation of p70S6k is regulated by sequential phosphorylation (Pullen and Thomas, 1997; Weng et al., 1998) and p38 and ERK have both been implicated in phosphorylation of the auto-inhibitory site (T421/S424), which occurs prior to phosphorylation of T389. In p70S6k KO animals, p90S6 kinase, under the control of ERK MAPK, appeared to be responsible for rpS6 phosphorylation observed (Pende et al., 2004). In most cases it seems MAPK signaling can encourage translation but mTOR activity is still primarily required.

Signals that influence protein translation

Cell growth is strongly influenced by external growth factors, nutrient availability, mechanical signals and cellular energy status. In muscle, infusion or over-expression of IGF-I increases protein synthesis and muscle hypertrophy (Adams and Haddad, 1996; Adams and McCue, 1998). The best-described mTORC1 pathway is initiated by growth factor and insulin stimulation. Canonically, upon generation of PIP_3 (via PI3 kinase activation) Akt is recruited to the membrane and phosphorylated by PDK1 on T308 followed by phosphorylation by mTORC2 on S473 (Moore et al., 2011b). Akt is a serine/threonine kinase and is thought to target mTOR directly by phosphorylation on S2448 or indirectly by phosphorylation of TSC1/2 on multiple residues, S939, S981, and T1462 (Figure 1.5) (Miyazaki and Esser, 2009; Nave et al., 1999; Winter et al., 2011). Mitogen activation of ERK MAPK has also been reported to activate mTOR via phosphorylation of TSC1/2 and importantly, these sites are distinct from those phosphorylated by Akt (Winter et al., 2011). TSC1/2, the tuberous sclerosis complex, functions as a negative regulator of mTOR activity (Gao et al., 2002; Inoki et al., 2003). Thus, in this case, phosphorylation inhibits its negative regulation. TSC1/2 is a GAP (GTPase Activating protein), which acts on Rheb, a small G-protein also part of the mTOR complex. Inhibition of TSC1/2 allows accumulation of GTP-bound Rheb, which strongly activates mTOR.

Feeding induced amino acid availability can regulate mTOR activity and this appears to be different from feeding induced insulin signaling via Akt. By contrast, feeding has no effect on basal phosphorylation and does not alter exercise-induced phosphorylation of MAPK (Holm et al., 2010; Karlsson et al., 2004; Moore et al., 2011a). Amino acid regulation of protein translation is highly sensitive to changes in the level of the specific amino acid, leucine, through a process that does not involve TSC1/2. The exact mechanism of amino acid regulation is unclear but seems to involve the relocation of mTOR to its regulatory protein, Rheb. It appears amino acid sensitivity lies in the

interaction of mTOR with a small GTPase, Rag, which then can direct mTOR to Rheb (Ma and Blenis, 2009).

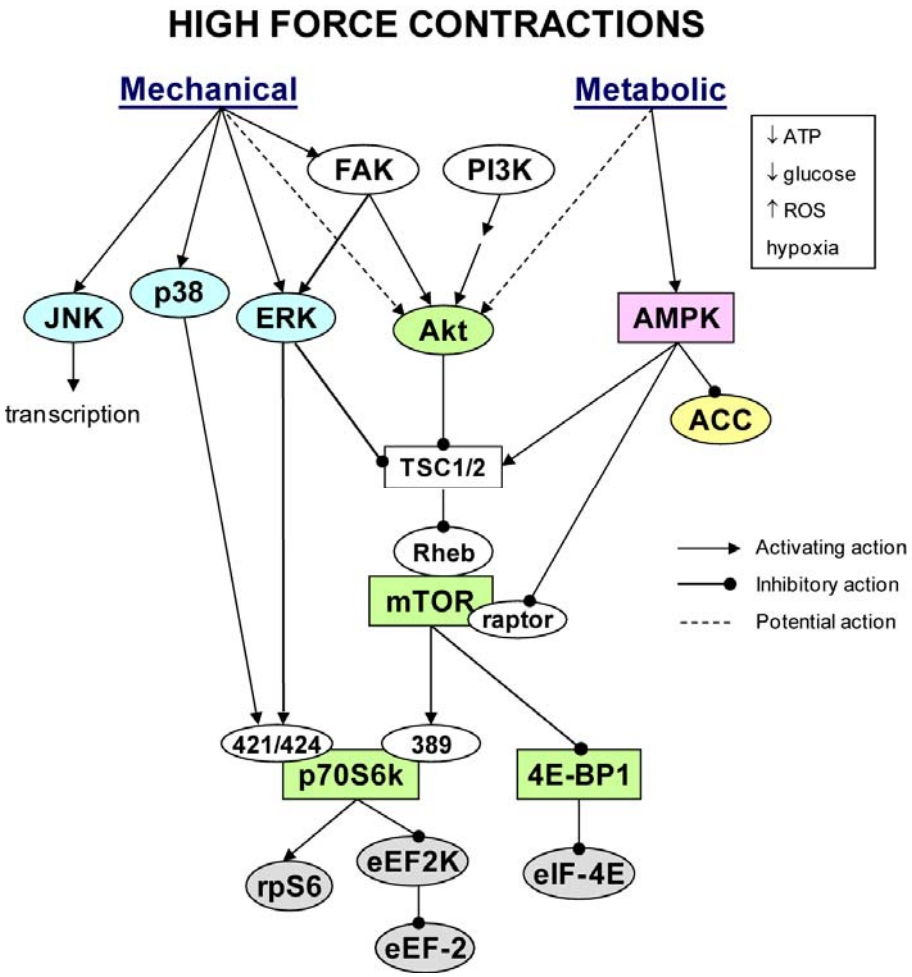

Figure 1.5 Signaling cascades.

Production of high forces has been linked to the induction of protein synthesis by the activation of important growth-related signaling cascades, primarily the Akt-mTOR-p70S6k and the mitogen-activated protein (MAP) kinase cascades. The degree of muscle hypertrophy in response to repeated high force contractions has been specifically correlated degree of phosphorylation of p70S6k, which lies downstream of both signaling cascades, and is, in general, used as a molecular marker of protein synthesis. Contraction induced signaling simultaneously imposes a mechanical and metabolic stress on the

muscle. The influence of mechanical signals and metabolic signals on intracellular signaling will be discussed independently.

Mechanotransduction

Basic physiological functions, from growth and development to cell shape and phenotype, are strongly influenced by mechanical forces. Many of these processes involve activation of intracellular signaling cascades. This section will discuss mechanisms in place in the membrane and sarcomere that may transduce mechanical signals.

Overview

Mechanotransduction is the process by which mechanical stimuli are converted into the biochemical signals required for cellular responses. Sensing mechanical information is a property of many cell types (e.g. muscle, bone, hair, skin, neurons) and organisms (e.g. bacteria, invertebrates). The conceptual idea is that architectural structure of the cell presents a general mechanism for coordinated changes in cell shape. This change can alter protein conformations or organization that may then activate cellular responses. Various potential mechanisms for force transmission are present within the sarcomere and the membrane structure with the primary candidates being titin kinase and FAK, respectively. Mechanically induced deformation of these proteins may alter their biochemical activity, effecting mechanotransduction.

Sarcomere Mechanisms

Internal forces arise from active and passive forces generated by the contractile apparatus. Actin and myosin are fixed at the Z-disc and M-line, which are connected by the uniquely positioned giant protein, titin (See Figure 1.2, page 8). The hexagonal array of myosin thick and actin thin filaments include a number of other proteins that form a scaffold that support this structure. Proteins associated with the Z-disc, including α-

actinin, anchor the thin filaments and provide a physical link between sarcomeres as well as to the non-sarcomeric cytoskeleton. The M-line plays a role in maintaining the myosin thick filament lattice at the center of the sarcomere and contains structural proteins such as myomesin and the giant protein obscurin. Active force generation imposes a mechanical stress on the various structures of the sarcomere. The architectural arrangement of Z-disc and M-line proteins provides structure and stability and helps to disperse the stress produced by contractile forces. Electron and atomic force microscopy found the mechanical properties of the Z-disc and the M-line are very different and may participate in different aspects of the response to mechanical stresses (Gautel, 2011; Horowits and Podolsky, 1987). The Z-disc perceives both passive and active forces and its structure (supported by interactions of actin, α-actinin and titin) provides resistance to deformation of the Z-disc, whereas the M-line deforms ('buckles") rapidly only during active force production due to shear forces of myosins (Goldstein et al., 1991; Horowits and Podolsky, 1987). Both structures contain proteins that may dislodge and translocate in response to mechanical stress. However, it is suggested that the M-line would be the optimal place for a mechanosensor as here it could detect the actual workload (Agarkova and Perriard, 2005).

Obscurin and titin are two of the giant sarcomeric proteins and both have active enzyme or kinase activity located at the M-line. Obscurin is situated around the periphery of myofibrils at the z-disc and M-line and integrated into the M-line so may be subjected to deformation with the sarcomere M-line (Kontrogianni-Konstantopoulos et al., 2003). Obscurin contains a RhoGEF domain implicated in hypertrophic growth (Borisov et al., 2003; Borisov et al., 2006; Ford-Speelman et al., 2009) and local protein unfolding induced by mechanical tension may activate enzymatic domains like GEFs. However, aside from myofibrillogenesis, it is not clear that the obscurin RhoGEF domain has a mechanosensory function.

Titin receives much of the attention for the potential of a sarcomeric mechanosensor. Two mechanically sensitive domains are potential mechanotransducers: the elastic region located in the I-band, the kinase domain located at the M-line. A number of signaling molecules associate with the elastic region and may responsive to mechanical stretch. For example, there is evidence that FHL1/2 and MARPs shuttle to and from the nucleus in response to stretch and FHL1/2 has been associated with MAP kinase signaling cascades (Kojic et al., 2004; Sheikh et al., 2008). The C-terminus of titin, containing the titin kinase (TK) domain, is integrated into the M-line structure that includes myomesin, obsucrin and myosin. It follows that if M-line deforms under active force that this would result in a conformational change in the nearby TK domain. TK is regulated by autoinhibitory domain that can be relieved by mechanical forces (Grater et al., 2005; Puchner et al., 2008). The mechanically-unfolded, active kinase domain is then able to interact with signaling complexes involved in protein turnover (Nbr-1, p62 and MURF) and gene expression (Lange et al., 2005). In addition, there is evidence for a FHL2 binding site in the M-line region of titin thus, another potential interaction between the active force sensing region and growth signaling through MAK kinases (Lange et al., 2002). Contractile forces generated from the sarcomere are linked to the cytoskeleton and extracellular matrix and may also act on membrane mechanisms.

Membrane Mechanisms

External stimuli acting on muscle may arise from attachment of the muscle to the bone, the fibers to the tendon or the fibers to other fibers. These forces increase the stress or tension on the cell membrane and are associated with membrane deformation allowing for transmission across the membrane. Various proteins in the cell membrane may sense forces applied externally to the muscle. The general mechanism commonly discussed is the force-induced membrane distortion resulting in conformational changes in transmembrane or membrane bound proteins resulting in modified protein function.

Conformational changes perhaps arise from changes in the energy state induced by tension, as protein conformations favor that with the lowest free energy. Deformation may also cause reorganization of proteins such that interactions are created or disrupted and may contribute to availability of active sites (Orr et al., 2006).

The surface area of skeletal muscle is actually much greater than the cell size. Excess membrane is maintained within folds along the surface and caveolae. Upon stretch or deformation, these caveolae open, potentially to prevent membrane damage. Caveolae structure is formed by the protein caveolin and may act as a scaffolding complex binding multiple signaling protein (Engelman et al., 1998).

Stretch-activated channels (SAC) are present in multiple cell types responsive to mechanical deformation. Increasing membrane tension has been shown to increase open probability of the channel. In this case, ion flux (Ca^{2+} or Na^{+}) into the cell may act as second messengers to activate intracellular signaling cascades. In skeletal muscle, SAC are likely not force transducers. They seem to play a role in damage induced by eccentric contractions or cell stretch but inhibition does not always attenuate hypertrophy signaling (Hornberger et al., 2005; Spangenburg and McBride, 2006; Yeung et al., 2005).

Focal adhesions (FA) attract a lot of attention as mechanotransducers within the cell membrane as associated proteins provide a physical link between the extracellular matrix (ECM) and the intracellular cytoskeleton and ability to activate intracellular signaling cascades. FA complexes are located at discrete places along the membrane and can immediately react to changes in tension (Pardo et al., 1983). Costameres specifically refer to FA positioned above the sarcomere Z-line and are thought to be important in the lateral transmission of force. FA includes both integrin-mediated complexes as well as the dystroglycan complexes (DGC, See Figure 1.2, page 8). In skeletal muscle, the $\alpha 7\beta 1$ integrin is most abundant heterodimer complex. Integrins directly bind laminin in the ECM and actin through various focal adhesion proteins such as vinculin, paxilin etc (Katsumi et al., 2004; Sawada and Sheetz, 2002). Similar to integrins, dystroglycan is an

α/β heterodimer spanning the membrane to bind laminin in the ECM. Intracellularly, dystroglycan is linked to sarcoglycans and to actin through the dystrophin protein (Rando, 2001). Both integrins and dystroglycan lack internal kinase or enzyme activity but are associated with various signaling molecules that are thought to convert the mechanical events into intracellular signals via PI3K and MAPK cascades (Gan et al., 2006; Klossner et al., 2009; Wang et al., 2001a). In general, force-dependent deformations of the cell membrane may alter the organization of proteins within the complex or alter the conformation of protein to expose new binding sites, which in turn can activate signaling cascades.

Of particular interest are the integrin complexes as formation is dynamic and assembly depends on mechanical interactions. Integrin ligation and ECM binding result in force-dependent changes that recruit focal adhesion proteins to the adhesion site (Katsumi et al., 2005; Sawada and Sheetz, 2002). Assembly of proteins (i.e. vinculin, talin, α-actinin) then links the ECM to the cytoskeleton and contractile apparatus. In the absence or inhibition of stress, these structures rapidly disassemble (Chicurel et al., 1998). Activation of focal adhesion kinase, FAK, has been widely implicated in mechanical and load induced signaling (Fluck et al., 1999; Gordon et al., 2001). FAK is a non-receptor tyrosine kinase that translocates to focal adhesions in response to force by activating intracellular signaling cascades (Mack et al., 2004). FAK is rapidly phosphorylated at T397 in the autoinhibitory domain and correlates with increased FAK activity (Calalb et al., 1995; Parsons, 2003). Upon activation of FAK, a number of downstream signaling cascades are activated. For example, cell adhesion-mediated activation of PI3-kinase and Akt is necessary for cell survival. Cell stretching induces activation of MAPK by FAK (Gan et al., 2006). Thus, FAK appears to have the ability to initiate cell signaling in response to mechanical load.

In summary, active force generation may induce deformation of sarcomere structure (i.e. M-line, titin), which may physically activate kinase domains of specific

proteins such as obscurin or titin. These can potentially interact with MAPK cascades however direct evidence is lacking. Force generation may induce deformation of membrane bound protein complexes such as SAC, dystroglycans and integrins. FAK is of interest as a mechanotransducer as it has been linked to MAPK and Akt activation. There is likely interaction between signaling induced by external or internally derived means as mechanotransduction signaling of external forces is interrupted if either contraction is inhibited or intracellular connections are broken (Chen, 2008; Cox et al., 1994; Hornberger and Esser, 2004).

Mechanical Stress Dependent Signaling

The various models of high force contractions impose very different force signals and elicit different responses among downstream signaling networks. As mentioned, FO adapts to chronic high loads induced by the weight of the animal. In this model load dependence is seen as the presence of increased load/activity versus normal loading. HFES, although more similar to RE with a discrete amount of time spent at high load, imposes intermittent maximum simultaneous activations. Evidence for load dependence is often derived from use of eccentric (EC) activations to induced greatest force. However, many unique features are associated with EC including cell damage and calcium leakage (McCully and Faulkner, 1985; Yeung et al., 2003) and may trigger qualitatively different responses than isometric and concentric activation. Nevertheless, common signaling themes have emerged in response to increased load (See Figure 1.5 page 30).

TOR and MAPK signaling after FO

Functional overload (FO) results in rapid and substantial muscle growth. At 7 days post-surgery, increased mass is associated with increased mTORC1 signaling. 4E-BP1 phosphorylation and eIF-4E/4G binding, indicating formation of the 4F complex, are

increased (Bodine et al., 2001; Thomson and Gordon, 2006) along with p70S6k^{T389} and downstream rpS6 phosphorylation (Adams et al., 2002; Spangenburg et al., 2008; Thomson and Gordon, 2006). These effectors of mTORC1 signaling appear to remain elevated for at least 2 weeks (Adams et al., 2002) suggesting continuously elevated protein synthesis. Prior treatment with rapamycin inhibits mTORC1 signaling and prevents hypertrophy (Bodine et al., 2001) indicating load-induced growth involves mTORC1. Cardiac muscle-specific ablation of raptor prevents mTORC1 formation, reduces p70S6k and 4EBP-1 phosphorylation and blocks adaptive hypertrophy in response to aortic pressure overload, further indicating a requirement for mTORC1 in hypertrophic growth (Shende et al., 2011). Upstream of mTOR, Akt phosphorylation robustly increases in response to FO and is subsequently down regulated when the overload stimulus is removed (Bodine et al., 2001). Over-expression of Akt is sufficient to induce muscle hypertrophy (Blaauw et al., 2009) and suggests Akt phosphorylation may be dependent on muscle loading (Blaauw et al., 2009; Bodine et al., 2001).

FO and other mechanical force cause a substantial increase in the synthesis and release of IGF-1 from muscle (Adams and Haddad, 1996; Goldspink et al., 1995; McKoy et al., 1999), and Akt is potently activated by growth factors such as IGF-I. Growth factors, IGF-I and muscle-derived IGF-I are released from active muscles (Clarke and Feeback, 1996; Goldspink et al., 1995) and increase protein synthesis (Adams and Haddad, 1996). Together, this drove the hypothesis that load-induced increase in GF, particularly IGF-I, may initiate growth-related signaling. Early studies hypothesized that IGF-I or systemic growth factors contribute to FO-induced growth however, hypophysectomized or diabetic animals responded to FO with similar growth as animals with systemic pituitary hormones and insulin available (Goldberg, 1967; Goldberg and Goodman, 1969).

MAPKs are activated within the first 24 hours following compensatory overload, which is prior to changes in IGF-I levels. Interestingly, ERK1/2 and JNK are transiently

activated while p38 phosphorylation remained elevated (Carlson et al., 2001) indicating the contraction-related trigger may be different. MAP kinases are capable of responding to a number of stimuli and can regulate a number of different cellular processes (Cargnello and Roux, 2011). p38 and JNK are also known as stress-activated protein kinases being activated by common environmental stressors such as ischemia, osmotic stress, oxidation, cytokines, etc. JNK is known to activate a number of transcription factors associated with the regulation of cell proliferation. p38 also has diverse downstream targets. Of particular interest here are its role in the metabolic adaptation and potential role in regulating protein synthesis. p38 is implicated in contractile activity induced activation of PGC-1α (peroxisome proliferator-activated receptor γ co-activator-α), which has a well-known role in mitochondria biogenesis and fiber type transformations (Yan et al., 2011). Within the protein synthesis cascade, p38 shares downstream targets with ERK (Figure 1.5, page 30) but which activation presumably arises from different stimuli. Growth factors are the best-known activators of ERK however, mechanical activity and force production result in rapid phosphorylation of ERK. ERK is involved in enhancing protein synthesis via mTOR-dependent and independent mechanisms (See Figure 1.5, page 30). Together, activation of MAPK in response to FO can result from a number of stimuli associated with this model.

TOR and MAPK signaling after HFES

Phosphorylation of p70S6k increases within 6 hours of a single bout of HFES and correlates closely with hypertrophy induced by repeated HFES (Baar and Esser, 1999). Subsequent studies from various labs find activation of p70S6k^{T389} is not always delayed, but may increase by 0.5-6-fold immediately following an HFES bout, and consistently indicate phosphorylation increases or is maintained for at least 6hrs (Nader and Esser, 2001; Thomson et al., 2008; Witkowski et al., 2010). HFES also produces decrease in the phosphorylation of eIF-2B and eEF2, molecules whose phosphorylation decreases

translation initiation and elongation (Atherton et al., 2005), suggesting enhancement of protein synthesis. A transient increase in Akt phosphorylation has been reported immediately following HFES in some (Atherton et al., 2005; Nader and Esser, 2001; Sakamoto et al., 2002; Thomson et al., 2008; Witkowski et al., 2010) but not all studies (Brozinick and Birnbaum, 1998; Parkington et al., 2003; Sherwood et al., 1999). In any case, this potentially transient increase is in contrast to the sustained activations seen in FO. Although the HFES may differ, for example in whether *in vivo*, *in situ* or *ex vivo* this does not seem to explain slightly different results. It is possible that rodent strain, muscle or potentially nutritional status may explain some discrepancies in Akt signaling.

HFES results in rapid, but transient, phosphorylation of both p38 and ERK in either isolated muscle or intact muscle although the extent may vary (Nader and Esser, 2001; Ryder et al., 2000; Wretman et al., 2001). Long duration activation, such as the 3s duration used in many of the above studies may provide a different signal than shorter, 0.05 or 0.17s duration activations used by others. Both ERK and p38 were less activated by long (10s) stimulations compared to short (0.2s) activations (Ryder et al., 2000). Atherton reports rapid activation of ERK but not p38 following 3s activations. HFES increased phosphorylation of p38 to a slightly greater degree than LFES or running suggesting a force-dependent mechanism (Nader and Esser, 2001). Martineau and Gardiner (2001) specifically manipulated force using concentric, isometric, and eccentric activations, and found that ERK phosphorylation correlated with the peak force, while phosphorylation of p38 was unchanged, suggesting that ERK phosphorylation was force-dependent. Similar experiments by Wretman et al (2001) found eccentric and concentric activations of phosphorylated ERK to a similar degree, while p38 phosphorylation was exaggerated in the higher-force eccentric activations.

TOR and MAPK signaling after RE

Intracellular signaling in response to RE in humans appears to depend on prior training history. Unaccustomed exercise induces MAPK and mTORC1 signaling and this is blunted when the exercise is familiar due to training (Coffey et al., 2006; Mayhew et al., 2011; Mayhew et al., 2009). As was seen in short-duration HFES, resistance exercise in humans results in a decrease in Akt phosphorylation immediately and 24 hrs post-activity (Deldicque et al., 2008). However, at least one study shows an increase (Burd et al., 2010). Also similar to HFES, MAPK are rapidly activated, with phosphorylation of ERK and its downstream target MNK increased immediately and for at least 2 hours. At least one study shows no increase in either JNK or p38 phosphorylation (Williamson et al., 2003).

From these models, it seems there is some evidence of force-dependent signaling up stream of mTORC1 signaling: Akt emerged from FO model and MAP kinases emerged from the HFES models. Reports of Akt activation was variable even across similar protocols and suggests that Akt phosphorylation may not due to the force produced by the muscle but by a signal related to contraction. The importance of Akt phosphorylation in load-induced signaling has also been questioned. Akt signaling was most prominent in FO, however, recent studies specifically demonstrate that a non-working IGF receptor does not affect hypertrophy after loading and Akt is activated to the same extent. In addition, genetic knockout of PTEN, a phosphatase regulating Akt phosphorylation, does not alter the response to FO despite the greater Akt phosphorylation. These data support a growth factor- and an Akt-independent mechanism triggered by mechanical overload (Goodman et al., 2010; Philp et al., 2011; Spangenburg et al., 2008).

Interpreting the force dependence of MAP kinases is primarily confounded by the use of eccentric activations to produce high force. In contrast to isometric or concentric activations, eccentric activations are associated with membrane damage, calcium influx

and unique signaling. Injury imposed by active lengthening includes loss of force production and disruption of cytoskeletal elements like desmin, which links z-disks and costameres (Friden and Lieber, 2001; McCully and Faulkner, 1985). Increased calcium influx may occur through membrane damage or through stretch-activated channels. The resulting increase in calcium concentration may contribute to intracellular signaling and/or activate proteases that induce damage and contribute to protein degradation (Balnave and Allen, 1995). Active lengthening of muscle and stretch of cultured myocytes rapidly activates p54 JNK MAPK and suggests stretch is a strong initiator of JNK (Boppart et al., 2001; Martineau and Gardiner, 2001; Russ and Lovering, 2006). Cell damage and JNK phosphorylation are velocity dependent suggesting JNK may reflect cell damage (Burkholder, 2003; Frey et al., 2009). In addition, eccentric activation uniquely induces expression of myogenin and ankyrin-related proteins, even at the same force level (Hentzen et al., 2006).

AMPK dependent signaling

Conditions that produce energetic stress promote formation of reactive oxygen species, reduced energy and energy stores (i.e. glycogen) and inhibit growth-related processes. AMP-activated protein kinase is well-known as the cellular energy sensor and is primarily activated by a decrease in cellular AMP:ATP levels. AMPK is phosphorylated on T172 by upstream kinases in response to ATP-consuming processes, such as exercise, and is also modulated by metabolic signals that limit or inhibit ATP synthesis, such as ischemia, or starvation (i.e. low glucose/glycogen levels). For example, glycogen availability may affect AMPK by inhibiting activity at normal levels via the glycogen binding domain (McBride and Hardie, 2009) but increase AMPK activity when glycogen levels are low, which would also result in an increased AMP:ATP ratio (Wojtaszewski et al., 2003). Because of extensive allosteric regulation, phosphorylation is not necessarily indicative of activity. AMPK receives inputs from

various stimuli and the resulting activation is reflected in phosphorylation of downstream targets. Phosphorylation of acetyl CoA carboxylase (ACC) is a primary physiological target of AMPK and is most often used as an *in* vivo marker of AMPK activity. Active, unphosphorylated ACC promotes fatty acid (FA) synthesis so phosphorylation and inhibition by AMPK increases net oxidation of FA and ATP synthesis. Chronic activation of AMPK also induces fiber type transitions to more oxidative phenotypes, which allows the cell to better cope with similar cellular disturbances in the future. Increased AMPK levels have been implicated in the blunted response of aged animals to overload as treatment with the AMPK inhibitor, compound-C restored hypertrophy in old animals to the level of young animals (Gordon et al., 2008).

Metabolic stress and AMPK negatively influence cell size and muscle mass. Genetic AMPK knockouts demonstrate increased protein synthesis in myotubes and hypertrophy in whole muscle (Lantier et al., 2010). Treatment with 5-aminoimidazole-4-carboxamide ribonucleotide (AICAR), which acts as an AMP mimetic, decreases protein synthesis and induces atrophy in myotubes and muscle (Bolster et al., 2002; Deshmukh et al., 2008; Thomson et al., 2008). AICAR has also been shown to inhibit DNA synthesis, S-phase and cell number indicating inhibition of growth and proliferation (Du et al., 2008). AICAR and AMPK activation impose its negative regulatory influence on protein synthesis by two mechanisms: inhibition of mTOR and it downstream effectors, and phosphorylation of eEF2 on T52. Phosphorylation, and inhibition, of eEF2 on T52 is likely due to activating effects of AMPK phosphorylation on eEF2K, rather than direct phosphorylation (Horman et al., 2002; Williamson et al., 2006). Thus, AMPK has a mechanism for inhibiting the elongation stage on protein translation. Phosphorylation of TSC1/2 by AMPK occurs on distinct residues from that of Akt and ERK and results inhibition of mTOR (Inoki et al., 2003; Winter et al., 2011). In addition, AMPK may act by binding and sequestering raptor. The inhibitory actions of AMPK, at least on mTOR, can override positive signals that also act on mTOR such as muscle loading and insulin

stimulation (Deshmukh et al., 2008; Goodman et al., 2011; Miranda et al., 2008; Thomson et al., 2008).

AMPK activation may affect Akt and MAPK signaling as well although this is less clear. AICAR stimulated rats showed decreased phosphorylation of Akt, mTOR and $p70S6^{T389}$ and reduced eIF-4E association with eIF-4G (Bolster et al., 2002). In cardiac fibroblasts serum activated ERK and partially inhibited AICAR induced AMPK phosphorylation. By contrast, activation of AMPK by AICAR inhibited serum induced ERK phosphorylation suggesting energy state is important (Du et al., 2008). AICAR had a different response in murine C2C12 cells in which ERK phosphorylation was increased following AICAR treatment. In this study, increased AMPK also corresponded to decreased translation initiation and transiently increased eEFF2 phosphorylation indicating decreased translation elongation (Williamson et al., 2006). Contractions in glycogen deplete muscle do not exhibit a contraction-induced increase in Akt phosphorylation, whereas ERK1/2 phosphorylation was unaffected, suggesting a strong influence of metabolic status on the Akt pathway.

However, AMPK activity occurs concurrent with HFC-induced signaling through mTORC1 (Dreyer et al., 2006; Thomson et al., 2008) suggesting that moderate levels of AMPK activity do not completely prevent the anabolic stimuli induced by HFC. HFES appears less likely than chronic LFES or running to increase AMPK activity. For example, *ex vivo* isometric stimulations did not alter AMPK phosphorylation and eEF2 phosphorylation was reduced (Atherton et al., 2005). Thomson (2008), using sciatic nerve stimulation of the same regimen also found no increase in AMPK phosphorylation but did find increased ACC phosphorylation indicating AMPK activity. Correspondingly, eEF2 phosphorylation, which suppresses translation elongation, was unaltered in response to HFES. Decreased eEF2 phosphorylation was observed at a later time point when ACC phosphorylation returned to baseline but mTORC1 signaling was still elevated. HFES (0.2s activations every 2s for 30 min) have resulted in AMPK and

ACC phosphorylation. Insulin stimulation prior to electrical stimulation was able to blunt contraction induced AMPK but was unable to prevent contraction-suppressed p70S6k (Miranda et al., 2008). It could be argued that in this study, the stimulation regimen without rest periods was more similar to chronic activation rather than intermittent activation. In humans, AMPK activity increased particularly during unaccustomed exercise (Coffey et al., 2006). AMPK phosphorylation is less consistent and becomes force-dependent. Tannerstedt (2009) report no change in AMPK following lengthening contractions of 50% 1RM however, higher intensity exercises (10 sets of 10 and 70% 1RM) did result in increased AMPK (Dreyer et al., 2006; Tannerstedt et al., 2009). Similarly, Holm (2010) found heavy load but not light load increased AMPK activity and eEF2 phosphorylation as well as ERK, p38 and p70S6k^{T389} phosphorylation. Together this suggests that intensity or load is an important stimulus to AMPK.

In summary, HFC involves mechanical stress and it is this stress that has been implicated in the activation of growth-related signaling. HFC concurrently involve various metabolic stresses, which may contribute to similar signaling pathways within the muscle. Whether mechanical and metabolic stimuli activate distinct cascades is not clear.

Specific Aims

Increased peak muscle load results in increased muscle mass and strength, whereas reduced peak muscle load, due to aging, inactivity or prolonged bed rest, results in significant loss of muscle mass and strength. Following an acute increase in load, the rate of protein translation increases prior to changes in gene transcription and coincident with post-translational mechanisms that strongly influence the rate of protein synthesis. These post-translational modifications can be induced by a number of cellular stresses that co-vary with force, but the central role of mechanical stress *per se* has been inferred from this covariance. This project is based on the overall hypothesis that growth-related signaling is acutely activated by force-dependent processes during active force

generation. Force appears to activate the extracellular-regulated protein kinase 2 (ERK2) while co-varying stresses appear to influence Akt/mTOR signaling. This dissertation will use observational and functional assessment of muscle force to delineate mechanical and metabolic markers influencing protein synthesis. The working model suggests that contractile force activates MAPK (ERK2) phosphorylation while metabolic stresses activate AMPK and Akt phosphorylation.

Specific Aim 1: Determine whether sustained muscle activity preserves muscle growth signaling in aged animals. Aging is associated with a decrease in overall activity, a loss of muscle mass and reduced protein synthesis and may results from systemic effects of aging or reduced muscular activity. Muscles of the head appear to retain mass with age and perform tasks whose activity level may not decline with aging. A detailed analysis of head, tongue and limb muscles will be used to compare the regulation of protein synthesis in young and old rats in order to determine whether growth-related signaling may be related to muscle activity or aging. This aim is based on the specific *hypothesis that activation of growth-promoting signals is preserved in aged muscles that retain force requirements.*

Specific Aim 2: Determine whether MAPK pathways are activated by force. High force contractions result in simultaneous stresses including metabolic, oxidative stress and mechanical stress. These stimuli may activate multiple cascades, therefore, it is possible that increased protein synthesis may result from combined stress signals. Force of the *tibialis anterior* will be altered by using intrinsic muscle properties: length-tension, force-velocity and force-stimulus intensity relationships to produce similar force levels with distinct metabolic and oxidative stress levels. The phosphorylation status of growth-related proteins will be measured and analyzed against measures of metabolic stresses. This aim is based on the specific *hypothesis that activation of MAPK signaling correlates with peak muscle tension independent of metabolic influences.*

Specific Aim 3: Determine whether MAPK pathways are enhanced by metabolic stress. Muscle contraction consumes energy and metabolic stress increase as ATP consumption exceeds ATP production and AMP level rise. The combination of high force contraction and metabolic stress may augment intracellular signaling leading to increased protein synthesis. Metabolic stress will be altered by increasing the duration of muscle stimulation and work-to-rest ratio (duty cycle) of the stimulation regimen. The phosphorylation status of growth-related proteins will be measured and analyzed against measures of metabolic and stress. This aim is based on the specific *hypothesis that metabolic stress associated with repetitive high force contractions contributes to MAPK phosphorylation.*

CHAPTER II

CHANGES IN GROWTH-RELATED KINASES IN HEAD, NECK AND LIMB MUSLCES WITH AGE

Abstract

Sarcopenia coincides with declines in several systemic processes that signal through the MAP kinase and Akt-mTOR-p70S6k cascades typically associated with muscle growth. Effects of aging on these pathways have primarily been examined in limb muscles, which experience substantial activity and neural changes in addition to systemic hormonal and metabolic changes. Head and neck muscles are reported to undergo reduced sarcopenia and disuse with age relative to limb muscles, suggesting muscle activity may contribute to maintaining mass with age. However many head and neck muscles derive from embryonic branchial arches, rather than the somites from which limb muscles originate, suggesting that developmental origin may be important. This study compares the expression and phosphorylation of MAP kinase and mTOR networks in head, neck, tongue, and limb muscles from 8- and 26-month old F344 rats to test the hypothesis that physical activity and developmental origin contribute to preservation of muscle mass with age. Phosphorylation of p38 was exaggerated in aged branchial arch muscles. Phosphorylation of ERK and p70S6k$^{T421/S424}$ declined with age only in the biceps brachii. Expression of p70S6k declined in all head and neck, tongue and limb muscles although no change in phosphorylation of p70S6k on T389 could be resolved. A systemic change that results in a loss of p70S6k protein expression may reduce the capacity to respond to acute hypertrophic stimuli, while the exaggerated p38 signaling in branchial arch muscles may reflect more active muscle remodeling.

Introduction

Normal aging is associated with a decline in muscle mass, which is correlated with a decline in circulating growth hormones, reduced activity and denervation (Giovannini et al., 2008; Lynch et al., 2007; Nair, 2005). Sarcopenia, the slow, progressive loss of muscle mass and function, reduces independence and quality of life in the elderly (Baumgartner et al., 2004; Janssen et al., 2004a). Beginning in the fourth decade, muscle mass declines about 0.5-2% per year (Baumgartner et al., 1998) thus, the extent of muscle loss is often only evident when compared over long periods of time.

The primary cause of sarcopenia is unclear, but systemic changes and reduced muscle activity have been identified as potential sources. Production of growth factors, such as IGF-I, GH and testosterone, and receptor sensitivity or number decline with age (Proctor et al., 1998; Szulc et al., 2004), suggesting that sarcopenia may reflect a systemic loss of anabolic drive. It seems unlikely that any single hormone acts as a master regulator of muscle size (Flueck and Goldspink, 2010), but a general decline in anabolic factors might lead to a general decline in muscle size. Physical activity is also a potent anabolic stimulus and declines with age in humans and animals (Caspersen et al., 2000; Holloszy et al., 1985). Resistance exercise can attenuate the effects of age on muscle as training studies demonstrate elderly can increase muscle strength, size and protein synthesis (Frontera et al., 1988; Trappe et al., 2002; Welle et al., 1995), however, strength training appears to be compensatory and not antagonistic to sarcopenia (Pearson et al., 2002). The decline in activity may reflect compromised neuromuscular function, and aged muscles show evidence of extensive denervation (Larsson and Ansved, 1995; Wang et al., 2005).

Growth signals and physical activity converge on similar biochemical signaling pathways, but the interaction among the stimuli and pathways is poorly understood. Two signaling networks have drawn special interest in integrating diverse stimuli to regulate muscle growth. The Akt-mTOR-p70s6k cascade is a critical pathway regulating protein

synthesis (Bodine et al., 2001), and activation of Akt is adequate to increase muscle mass (Blaauw et al., 2009; Bodine et al., 2001). The MAP kinase cascades, including $p42/44^{ERK}$, p38 and JNK cascades, are important in protein translation, gene transcription and satellite cell activation (Anjum and Blenis, 2008; Long et al., 2004; Widegren et al., 2001). IGF-I activates both Akt and MAP kinase cascades through receptor-mediated mechanisms (Shah et al., 2000; Sherwood et al., 1999). Mechanical stimuli also activate Akt and MAP kinase signaling, although the mechanism of this activation is uncertain (Goodyear et al., 1996; Hornberger et al., 2005; Nader and Esser, 2001; Sakamoto and Goodyear, 2002). AMP-activated protein kinase (AMPK) is activated in response to ATP depletion and inhibits mTOR signaling (Kimball, 2006). Recent studies show AMPK phosphorylation is increased in aged muscles, particularly fast twitch muscles (Thomson and Gordon, 2006).

Comparisons between muscles with differing changes in activity with age may show the influence of muscle activity on growth signaling. Voluntary locomotor activity, measured by wheel running distance or exploratory and home cage behaviors, declines continuously in rats after 10 months of age (Holloszy et al., 1985; Skalicky et al., 1996) and hind limb mass declines up to 30% in Fischer 344 (F344) rats (Daw et al., 1988). Muscles of the head, neck and tongue are involved in functions such as mastication, respiration and vision that decline less with age in rodents than locomotion. Peng and Kang (1984) reported that running wheel activity declined from 75 minutes/day to under 5 minutes per day in aged Long Evans rats, while feeding behavior changed by less than 30%, with some measures increasing and some decreasing, and similar results are seen in F344 and F344/BN (Zhang et al., 2008). Muscles of the jaw and tongue lose less than 15% of mass and fiber area (Connor et al., 2008; McLoon et al., 2004). Activity, strength and size of head, neck and tongue muscles may decline with age, but those changes are much less pronounced than limb muscles.

Muscles of the head and neck also differ from limb musculature in their innervation and developmental origin, which may contribute to differences in growth signaling. These muscles are innervated by cranial nerves, rather than by spinal motorneurons, and may not be subject to denervation observed in hind limb muscles (Larsson and Ansved, 1995; Sturrock, 1987). Further, most head and neck, but not tongue, muscles derive from branchial arches of somitomeres, rather than the somites (Noden and Francis-West, 2006; Yamane, 2005), and undergo a distinct myogenic program that may make them differently sensitive to growth stimuli, suggesting that their preservation with age may reflect their unique developmental origin. By contrast, tongue muscles, like limb muscles, derive from somites and represent a unique intersection of features from sarcopenia sensitive and sarcopenia spared muscle.

This study analyzes the phosphorylation state of kinases associated with growth-signaling networks in three classes of muscle to compare the influence of activity and developmental origins. This comparative design will test the hypothesis that physical activity and developmental origin contribute to growth signaling with age. The relative importance of cell lineage and general physical activity in the activation of these signaling networks and in the preservation of muscle mass may be revealed by comparison of head, tongue, and limb muscles from old and young rats. The key findings of the current study show exaggerated ERK and p70S6k$^{T421/S424}$ phosphorylation in young biceps brachii, exaggerated p38 phosphorylation in aged head and neck muscles, and a system wide decline in p70S6k expression. The systemic loss of p70S6k protein expression may reduce the capacity for muscle hypertrophy in response to periodic vigorous activity.

Materials and Methods

Animals and Tissue Preparation

Male Fischer 344 rats aged 8 months or 26 months (n = 8 per group) were obtained from the National Institute on Aging (NIA) colony. Average weight of animals was 403g ± 37 (young: 414g ± 19; old: 397g ± 45). The Fischer 344 strain is supplied by the NIA for use in aging studies. Mean survival age is 24 months with 25% survival to 26 months. Animals were sacrificed by CO_2 asphyxiation, and experimental muscles dissected and immediately frozen in liquid nitrogen. Procedures were reviewed and approved by Institutional Animal Care and Use Committee at Georgia Institute of Technology and performed in compliance with the *Guide for Care and Use of Laboratory Animals*.

Muscles

Seven muscles (Table 2.2) were chosen to represent different developmental origins and different general functions. Furthermore, muscles with opposing functions and different fiber type composition were included to mask phenotypic differences. The biceps brachii (BB) is an elbow flexor, innervated by the musculocutaneous nerve, with motor fibers derived from the embryonic somites. The pectoralis (P) is a flexor and adductor of the shoulder, innervated by the pectoral nerve, and of somitic origin. The styloglossus (SG) is an extrinsic retractor of the tongue, innervated by the hypoglossal or 12th cranial nerve, also of somitic origin. The geniohyoid (GH) is an elevator of the hyoid bone active in deglutition, also innervated by the hypoglossal nerve and of somitic origin. The masseter (M) is a jaw closer, innervated by the trigeminal or 5th cranial nerve, with fibers derived from the first branchial arch of the embryonic somitomere. The posterior digastric (PD) is a jaw opener, innervated by the facial or 7th cranial nerve, with fibers derived from the 2nd branchial arch. These muscles were grouped according

to functional role (locomotion or mastication) and by developmental origin (somitic or branchial arch), so muscles will belong to one of three classes or functional Origins: somitic+locomotion (BB), somitic+mastication (SG, GH), or branchial arch+mastication (M, PD). The superior rectus extraocular muscle (EOM) is an eye elevator, innervated by the occulomotor or 3rd cranial nerve, originating from the non-segmented paraxial mesoderm.

Western Blotting

Muscles were by homogenized in a low salt detergent buffer (50mM Tris, pH 7.5; 30mM NaCl; 5mM EDTA, 1% Triton X-100 plus NaF, $NaVO_3$ and protease inhibitors) to minimize myofilament extraction and pelleted at 15,000 x g. The protein concentration of the supernatant was measured by BCA (Pierce) according to manufacturer's protocol. The pellet, enriched in myofilaments, was resuspended in 0.1M PBS, pH 7.3 with 5% protease inhibitor for myosin heavy chain (MHC) separation. Soluble protein (15ug) was separated by SDS-PAGE, transferred to nitrocellulose membranes, and detected by Western blot. Primary antibody dilutions were: p-ERK$^{T202/T204}$ 1:3000; p-JNK 1:500; p-P38$^{T180/Y182}$ 1:2000; p-Akt^{S473} 1:2000; p-P70S6k$^{T421/S424}$ 1:2000; p-p70S6k^{T389} 1:2500; p-ACC 1:1000; total ERK2 1:2500; total p38 1:2000; total Akt 1:2000; pan p70 1:2000. All antibodies are purchased from Cell Signaling except JNK, from Santa Cruz. Bands were visualized by enhanced chemiluminescence and quantified by scanning densitometry.

Five muscles, the BB, SG, GH, M, and PD, were selected for multivariate analysis. Each young animal was arbitrarily paired with an old animal, and all ten of the paired muscles were loaded on a single gel. Data from each gel was normalized to the average of all young muscles to allow comparisons across muscles and across age groups. EOM and P were analyzed separately, which prevents direct comparison with the five core muscles, but does allow resolution of age-dependent signaling.

Myosin Separation Gels

The MHC isoform content was determined by SDS-PAGE separation on 8% polyacrylamide gels using a procedure derived from (Talmadge and Roy, 1993). Pellet containing myofilaments was resuspended in 0.1M PBS, pH 7.3 with 5% protease inhibitor, quantified (BCA), diluted in Laemmli buffer (62.5 mmol/L Tris, pH 6.8, 10% glycerol, 2.3% SDS, 5% β-mercaptoethanol, with antiproteolytic factors) and loaded 1ug protein/ per lane onto gel. Electrophoresis was carried out at 4°C for 22 hours at 140 V. Bands were visualized by Coomassie staining and MHC I, MHC IIa, MHC IIx and MHC IIb were quantified in Image J software (NIH) by reference to rat MG, soleus and tongue body samples run synchronously.

Real-time PCR

RNA was extracted from muscle by homogenization in 1ml of Trizol reagent (Invitrogen) according to manufacturer's protocol. Total RNA yield was determined by UV spectroscopy, and reverse transcription was performed with 1ug of total RNA using Multiscribe RT kit (Invitrogen) according to manufacturer's protocol using random primers. For amplification of myosin heavy chain isoforms, reactions contained 250nM forward and reverse primers in Platinum SYBR Green qPCR Supermix (Invitrogen). MHC standards and primer sets were used as previously described (Rahnert et al., 2010), and all primers and amplicon lengths are given in Table 2.1. The thermal protocol for all targets was 50°C for 2 min and 95°C for 10 min, followed by 40 cycles of 95°C for 15 s and 62°C for 1 min. Reaction products were validated at least once by size determination on agarose gel, and by terminal dissociation melting curve for every sample.

Table 2.1 Primers used for real time PCR and product size for myosin heavy-chains and calcium channels

Target	Forward Primer 5' → 3'	Reverse Primer 5' → 3'	Amplicon Size (bp)
B-actin	TTCAACACCCCAGCCATGT	GTAGATGGGCACAGTGTGGGT	120
MHC-2x	GTACCACAGGGAAACTGGCTT	CTTGGTCATCAATGCTGGG	222
MHC-2a	GTCTGCCAACTTCCAGAAGC	CAGCTTGTTCAAATTCTCTCTGAA	307
MHC-2b	AAAGGTGGCCATTTACAAGCT	CAGCAGAGTTCAGACTTGTCAG	146
MHC-I	AAGTCCTCCCTCAAGCTCATGGC	ATTTTCCCGGTGGAGAGC	135
$Ca_{V1.1}$	AGCTACCACCATGCTGATCC	CCCTCGCTTTCTGACTTTTG	333
RyR-1	CAAGACCTGAGCTGAGACCC	CCCAATCTCAATTTCTCGGA	242

Statistics

Data are expressed as means ± SD and are log transformed for presentation in figures to equalize visual elevations and reductions of phosphorylation or expression. Statistical analysis was by 2-way ANOVA (functional Origin x Age) with a significance threshold of $p < 0.05$, followed by post hoc t-tests using the Bonferroni/Dunn correction for multiple comparisons. Factor analysis was used to extract principal components of the data set either as a whole data set or split by age. Factor scores were Varimax transformed and the orthogonal solutions of the whole set were analyzed by 2-way ANOVA (Muscle x Age) with a significance threshold of $p < 0.05$.

Results

Independent factors associated with expression and signaling

Results of myosin separation and western blots are shown in Tables 2.3 and 2.4. To facilitate interpretation of this large data set, which included all muscles except EOM and P, we performed factor analysis, to extract statistically independent sets of correlated variables. Factor analysis revealed two factors that account for 43% of the population variance (Table 2.2), leaving the remaining 57% of variance distributed across 13 residual factors. The primary factor accounted for 27% of the population variance and

combines expression of MHC IIb (factor weight 0.959), MHC IIx (-0.885), and MHC IIa (-0.913) such that faster muscles had greater Factor 1 values. Thus, this factor may be best interpreted as "Fast". Two-way ANOVA revealed PD and SG were slower than the rest ($p<0.0001$), that young muscles were faster than old ($p=0.01$, Figure 2.1A), and that slowing with age was uniform across all muscles (age x muscle interaction, $p=0.86$). Expression of p70S6k (factor weight 0.502) and its phosphorylation on T389 (-0.456) were weaker components of Factor 1, which suggests fast muscles express more p70S6k and may have a greater capacity to respond to signals although, at rest p70S6k is less active. Factor 2 contained 16% of the population variance and included most of the kinase phosphorylation levels, particularly $p70S6k^{T421/S424}$ (0.828) and $ERK^{T202/T204}$ (0.745), as well as $p38^{T180/Y182}$, JNK T54 and Akt^{S473}. This factor is best interpreted as "Growth Signaling" and suggests the activity of all of these kinases is coordinated, but independent of fiber type. Two-way ANOVA revealed a muscle specific effect of age (muscle x age interaction, $p=0.02$) in which Factor 2 decreases in BB and increases in M and GH with age, while PD and SG are unchanged, and suggests age-related signaling is different in BB (Figure 2.1B). The residual factors individually represent 10% or less of the population variance.

Factor analysis was also performed separately on muscles from old and young animals to examine age-related changes in signaling patterns. The primary factor in both age groups was a combination of MHC isoforms (data not shown); however, p70S6k expression and phosphorylation (T389) were components of Factor 1 only in young animals (0.631 and –0.488, respectively), and not in old animals (0.268 and –0.335, respectively). Interestingly, there was no core "Growth Signaling" factor in old animals. The weighting of all phosphorylations was greater than 0.480 in Factor 2 of young muscles, but in old animals these components were spread across Factors 2, 3 and 4, suggesting that several signaling modules become more independent or discoordinated with age.

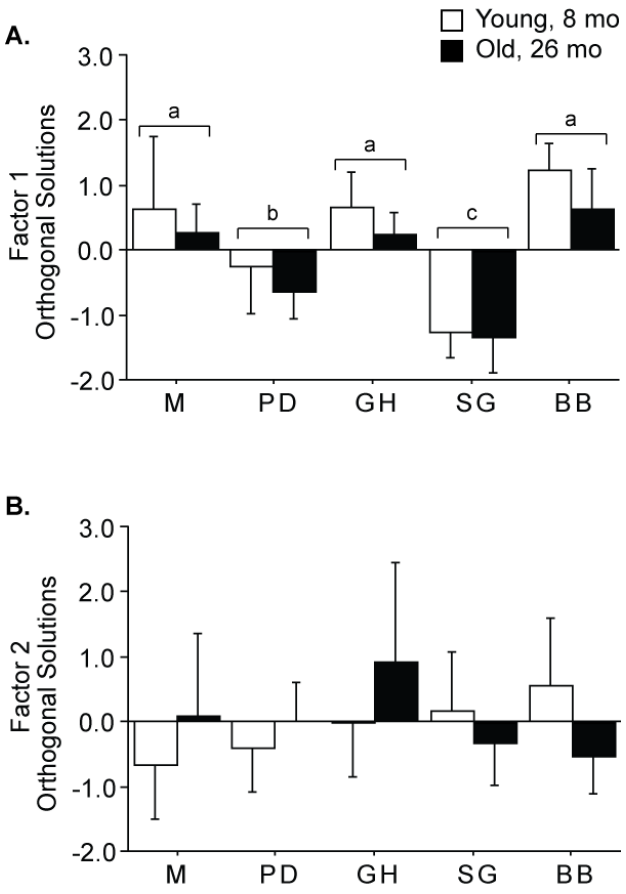

Figure 2.1 The major factors identified by factor analysis were analyzed by 2-way ANOVA. For Factor 1 (A), significant effects of age ($p=0.01$), and muscle ($p<0.0001$), but not age X muscle ($p=0.86$), were found. Muscles designated with the same letter were indistinguishable in post hoc T-tests. Factor 2 (B) had a significant interaction of age X origin ($p=0.02$), but no main effects (age $p=0.63$; origin $p=0.23$). The interaction effect indicates that the decrease with age in BB is different than the increase seen in M, GH. Mean ± S.D. of linear factor scores.

Table 2.2 Components of 2 orthogonal factors revealed by factor analysis of whole data set.

	Factor 1 (Fast)	**Factor 2** (Signaling)
p-ACC	0.402	0.113
p-Akt	0.113	0.513
p70$^{T421/S424}$	0.136	0.828
p70^{389}	-0.456	-0.060
p-ERK	0.405	0.745
p-p38	0.067	0.560
p-JNK 46	0.065	0.107
p-JNK 54	-0.078	0.650
Akt	0.021	-0.129
p70S6k	0.502	-0.084
ERK	-0.202	0.116
IIb	0.959	0.144
IIx	-0.885	-0.213
IIa	-0.913	-0.049
I	0.149	-0.018

Table 2.3. Protein and mRNA expression of conventional MHC isoforms in young (8 month) and old (26 month) muscles of F344 rats with different origins and functions. Extraocular (EOM); Masseter (M); Posterior digastric (PD); Geniohyoid (GH); Styloglossus (SG) and Biceps brachii (BB).

	BRANCHIAL ARCH				**SOMITIC**			
	Eye		**Mastication**		**Mastication**		**Locomotion**	
	EOM		**M**	**PD**	**GH**	**SG**	**BB**	**P**
Function	Vision		Jaw Closer	Jaw Opener	Hyoid Elevation	Tongue Retrusion	Stability/Locomotion	Stability/Locomotion
MHC composition by protein analysis								
	EOM		**M**	**PD**	**GH**	**SG**	**BB**	**P**
	Y	O	Y	O	Y	O	Y	O	Y	O	Y	O	Y	O
IIb	47±5%	56±7%	51±14%	48±9%	35±10%	33±5%	49±5%	50±7%	29±5%	25±6%	61±7%	53±12%	60±13%	62±11%
IIx	27±3%	27±6%	35±8%	37±5%	39±5%	41±3%	34±4%	34±5%	43±6%	43±4%	26±4%	31±7%	29±8%	24±6%
IIa	17±4%	12±3%	13±7%	14±5%	20±6%	23±3%	15±2%	16±3%	27±4%	32±2%	10±4%	13±5%	9±5%	10±5%
I	9±5%	6±4%	1±1%	1±1%	6±3%	3±2%	2±2%	0±1%	1±2%	1±1%	3±1%	3±1%	2±2%	3±2%
"Fast" Factor Score			0.63	0.26	-0.26	-0.65	0.67	0.23	-1.27	-1.36	1.22	0.62		
			0.457		-0.466		0.448		-1.309		0.922			
MHC composition by mRNA analysis														
	EOM		**M**		**PD**		**GH**		**SG**		**BB**			
	Y (n=1)	O (n=1)	Y	O	Y	O	Y	O	Y	O	Y	O		
IIb	46%	59%	59±16%	62±6%	36±6%	26±9%	69±12%	63±6%	33±10%	44±12%	71±9%	68±24%		
IIx	30%	21%	39±14%	37±7%	46±6%	42±9%	24±10%	27±14%	52±10%	42±9%	21±5%	28±19%		
IIa	12%	5%	2±2%	1±1%	11±5%	13±4%	8±2%	8±2%	14±2%	13±2%	5±3%	3±3%		
I	12%	15%	0±0%	0±1%	7±3%	20±13%	0±0%	2±1%	2±2%	2±2%	3±2%	2±2%		

Table 2.4 Summary of protein expression and phosphorylation in muscles of young (8 month) and old (26 month) F344 rats.

	Branchial Arch- Mastication				**Somitic- Mastication**				**Somitic- Locomotion**	
	M		PD		GH		SG		BB	
	Y	O	Y	O	Y	O	Y	O	Y	O
p-ACC	1.12±0.3	0.99±0.3	0.84±0.3	0.89±0.5	1.23±0.5	1.04±0.4	0.71±0.2	0.84±0.4	0.99±0.2	0.97±0.4
Akt	1.66±0.2	1.81±0.5	0.89±0.2	1.06±0.4	0.69±0.3	0.85±0.2	0.93±0.2	1.02±0.2	0.86±0.2	0.65±0.3
p-Akt	1.10±0.6	1.56±1.3	1.05±0.4	0.90±0.5	0.83±0.2	0.88±0.6	1.02±0.5	0.65±0.4	1.05±0.3	0.49±0.2
Rel Akt	0.67±0.4	0.93±0.8	1.23±0.5	0.86±0.4	1.66±1.6	1.03±0.6	1.20±0.7	0.62±0.3	1.23±0.4	0.73±0.5
p70	1.02±0.2	0.84±0.2	1.08±0.4	0.83±0.3	1.21±0.4	0.73±0.2	0.54±0.1	0.35±0.1	1.18±0.4	0.51±0.2
$p70^{T421/S424}$	0.72±0.5	1.10±1.0	0.81±0.5	1.10±0.8	1.00±0.6	2.01±1.6	0.98±0.6	0.49±0.2	1.57±0.9	0.52±0.3
Rel T421	0.66±0.3	1.35±1.1	0.85±0.6	1.50±1.1	1.09±1.2	3.26±3.2	1.72±0.9	1.73±1.1	1.32±0.7	1.16±0.7
$p70^{T389}$	1.08±0.5	0.71±0.3	1.13±0.2	0.99±0.4	0.78±0.3	0.76±0.2	1.23±0.3	1.14±0.4	0.89±0.3	0.73±0.3
Rel T389	1.00±0.6	0.72±0.2	1.01±0.4	1.33±0.6	0.73±0.4	1.86±1.4	2.20±0.2	5.44±1.6	1.23±0.8	2.55±0.8
ERK2	1.04±0.3	0.88±0.3	1.07±0.2	1.17±0.4	0.82±0.2	1.08±0.5	1.10±0.3	1.01±0.3	1.03±0.4	0.76±0.2
p-ERK	1.02±0.7	0.84±0.6	0.68±0.5	0.78±0.4	1.03±0.5	1.20±0.9	0.68±0.3	0.69±0.6	1.68±0.6	0.78±0.3
Rel ERK	0.95±0.5	1.00±0.7	0.67±0.5	0.52±0.2	1.50±1.1	1.09±0.7	0.72±0.5	0.66±0.5	1.84±0.8	1.06±0.4
p-p38	0.79±0.5	2.05±1.1	0.94±0.3	1.51±0.5	1.05±0.3	1.46±0.7	0.96±0.5	0.69±0.3	1.32±0.6	0.95±0.4
p-JNK 46	1.11±0.5	1.13±0.7	0.92±0.3	0.98±0.6	1.00±0.2	0.81±0.2	0.87±0.4	0.74±0.4	1.07±0.2	1.03±0.3
p-JNK 54	0.83±0.2	1.33±0.5	0.82±0.4	0.90±0.3	1.16±0.4	1.24±0.4	1.06±0.3	1.09±0.7	1.03±0.3	0.84±0.3

Table 2.5. mRNA expression of L-type calcium channel (Ca_V) and ryanodine receptor (RyR) isoforms in muscles of young (8 month) and old (26 month) F344 rats.

Calcium channel mRNA expression (fold β-actin)										
	Branchial Arch - Mastication				**Somitic - Mastication**				**Somitic - Locomotion**	
	M		**PD**		**GH**		**SG**		**BB**	
	Y	O	Y	O	Y	O	Y	O	Y	O
$Ca_{V1.1}$	0.7±0.2	1.3±1.1	1.8±1.4	1.5±0.6	2.3±1.4	2.3±1.3	1.5±1.0	1.4±0.4	2.2±1.0	1.2±0.6
RyR-1	1.6±1.3	1.1±1.3	1.1±0.7	1.0±0.7	1.3±1.0	1.3±1.2	0.9±0.9	1.2±1.3	1.0±0.6	0.9±1.1

MHC and calcium channel expression does not differ with age

Although factor analysis was able to distinguish an age-related change in MHC profile, no individual MHC isoform had a significant change in expression by mRNA or protein with age in these animals (Table 2.3). The significant decrease in the "Fast" factor with age ($p=0.01$) was resolvable because the correlations between MHC IIb, IIx, and IIa were able to overcome the inter-sample variability. Expression of the L-type calcium channel ($Ca_{V1.1}$) and the calcium release channel, ryanodine receptor (RyR-1) may shift or down-regulate prior to changes in MHC isoforms, however, neither the calcium channel expression nor the ratio of $Ca_{V1.1}$ to RyR-1 differ with age in any muscle (Table 2.5). This is consistent with similar transcript data from mice (Zheng et al., 2001), although there may be a decrease in $Ca_{V1.1}$ protein (Renganathan et al., 1998).

Aging does not increase ACC phosphorylation

Acetyl coenzyme A carboxylase (ACC) is a primary physiological target of AMPK and its phosphorylation was used as an index of *in vivo* AMPK activity. ACC phosphorylation was extremely uniform (Table 2.4), and no effect of age ($p=0.74$) or muscle origin ($p=0.99$) could be resolved. This suggests that the resting metabolic requirements of these muscles are similarly satisfied and that persistent metabolic stress is not a likely contributor to sarcopenia.

Akt-p70 signaling cascade

The effect of age was more apparent on p70S6k than on Akt. There was no effect of age on Akt expression ($p=0.84$) or phosphorylation ($p=0.16$) (Table 2.4), but expression was exaggerated in the branchial arch (BA) muscles ($p<0.0001$), and there was a trend ($p=0.060$) for increased phosphorylation in BA muscles. By contrast, significant effects of age ($p<0.0001$) and origin ($p=0.03$) were found for expression of p70S6k, with lower expression in aged muscle (Figure 2.2B) and lower expression in the

tongue than in branchial arch muscles (Figure 2.2B). Phosphorylation of p70S6k on T389 is closely correlated with activity, and this tended (p=0.07) to decrease with age, independent of muscle origin (origin effect, p=0.27, interaction effect p=0.66, Figure 2.2D). Neither age (p=0.54) nor origin (p=0.62) had an effect on p70S6k$^{T421/S424}$ phosphorylation. There was a significant interaction (Origin x Age p=0.03, Figure 2.2C) within the five core muscles, indicating reduced phosphorylation specifically in aged BB, however, this effect could not confirmed in P (Table 2.6), so this reduction seems unique to BB.

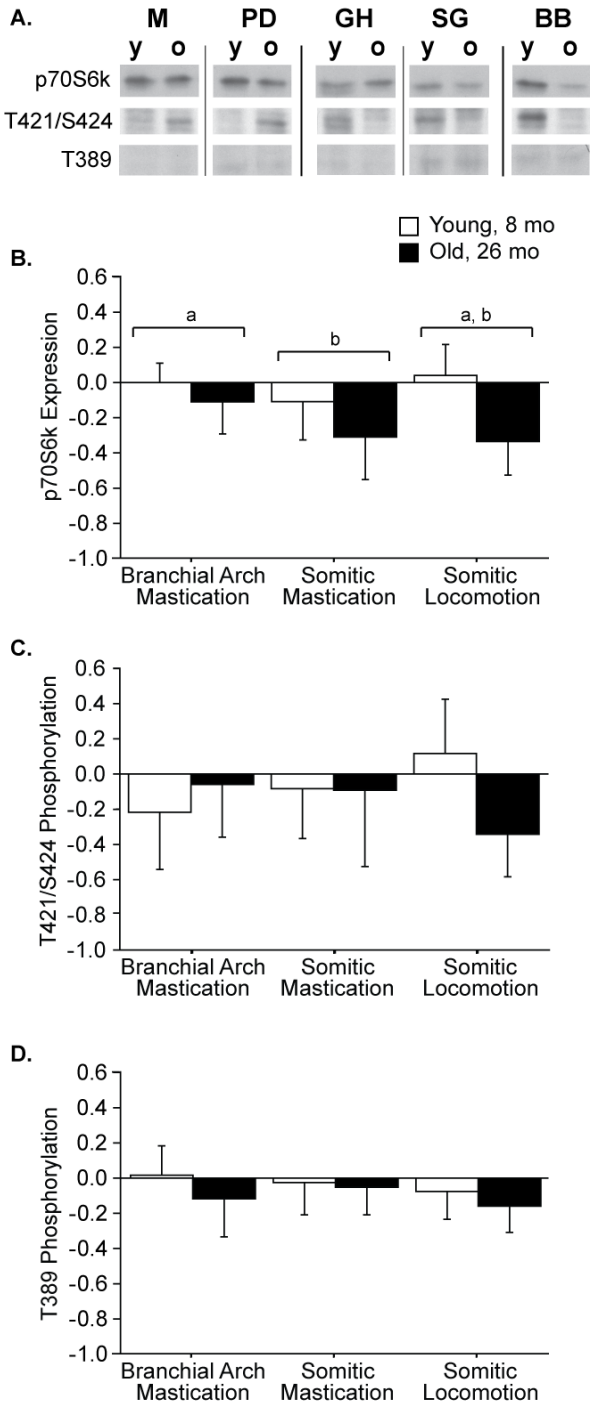

Figure 2.2 Expression and phosphorylation of p70S6k in young and old muscles by origin. Representative western blots (A) in which each antigen row is from a single blot, with the muscles rearranged for clarity. Expression of p70S6k (B) differs by muscle origin ($p=0.03$) and age ($p<0.0001$), but no significant interaction effect ($p=0.10$) was found. Origins designated by the same letter were statistically indistinguishable in post hoc T-tests. Phosphorylation of p70S6k on T421/S424 (C) had a significant interaction of age X origin ($p=0.03$), in which phosphorylation declines with age in somitic locomotion muscles, but is unchanged with age in branchial arch and somitic mastication muscles. No significant effects on phosphorylation of p70S6k on T389 were found (D). Data are presented as difference of logs from young averages, expressed as mean ± S.D.

MAP kinases

No main effects of muscle origin or age were found among MAP kinases (Figure 2.3), although interaction effects revealed origin-specific responses to aging for ERK and p38 phosphorylation. The significant origin X age interaction ($p=0.03$) shows that ERK phosphorylation declines with age in BB muscles while remaining unchanged in jaw and tongue muscles (Figure 2.3B), primarily because phosphorylation is exaggerated in the young muscle relative to all other groups. This effect was not seen in P (Table 2.6), and also appears to be unique to BB rather than to muscles of locomotion. The interaction effect ($p=0.002$) on p38 phosphorylation resulted from an increase with age in branchial arch muscles, with other groups remaining unchanged (Figure 2.3D), which suggest a greater sensitivity to stress in branchial arch muscles. Generally, phosphorylation of MAP kinases was slightly greater in the faster muscle from each origin, suggesting that the specific function or phenotype of the muscle is more important to MAPK signaling than is the generalized task.

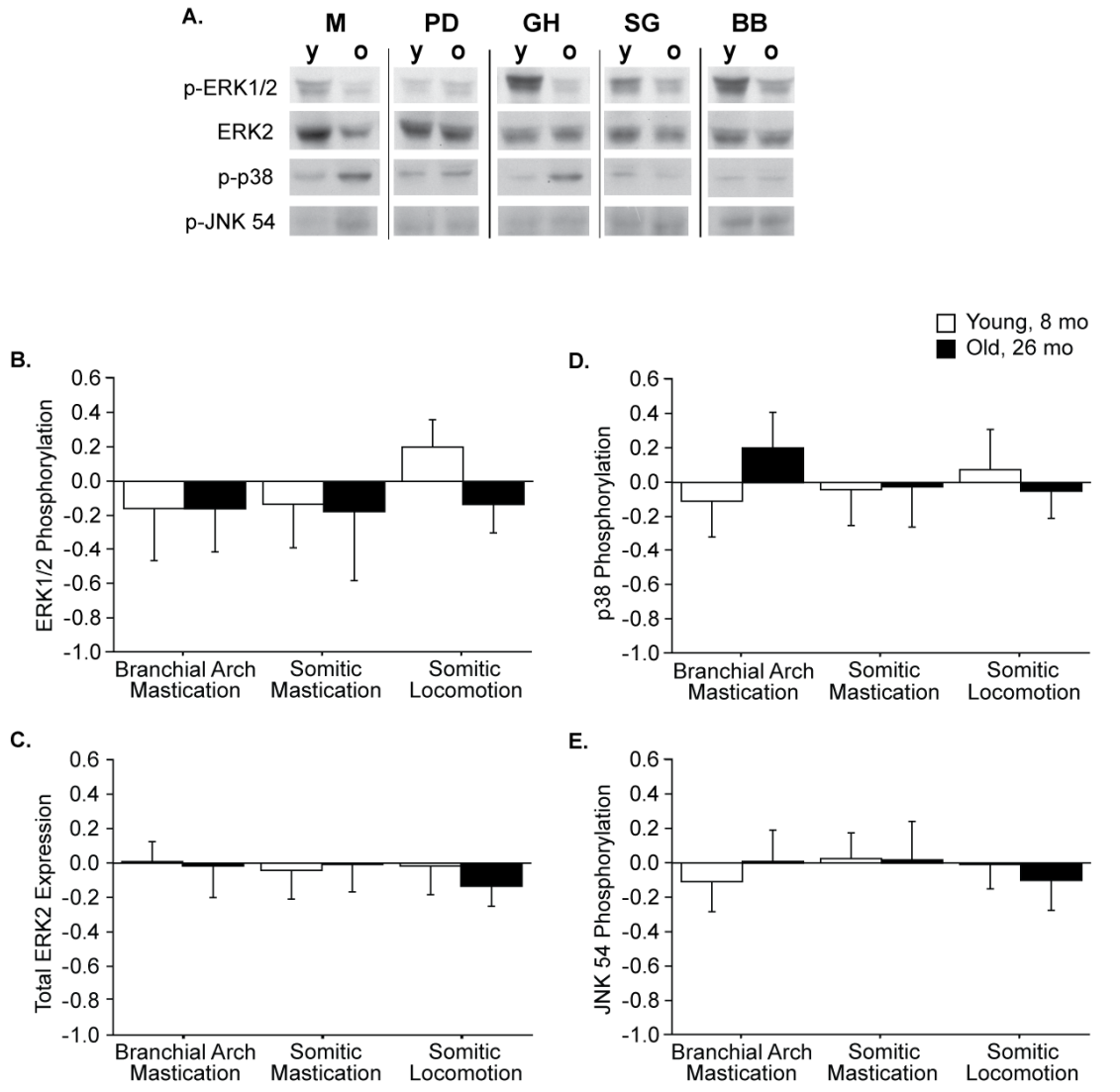

Figure 2.3 MAPK expression and phosphorylation in young and old muscles by origin. Representative western blots (A) in which each antigen row is from a single blot, with the muscles rearranged for clarity. A significant interaction effect (p=0.03) on ERK phosphorylation (B) indicates that the decline with age in somitic locomotion muscles is different than the conservation in mastication muscles. No effects on ERK2 expression (C) were found. The significant interaction effect (p=0.002) on phosphorylation of p38 (D) indicates that the increase with age in branchial arch muscles is different than the conservation seen in somitic muscles. No effects on JNK phosphorylation on T54 (E) were found. Data are presented as difference of logs from young averages, expressed as mean ± S.D..

Signaling in EOM and P muscles

EOM and P were separately analyzed to validate observations from the five core muscles. BA muscles showed exaggerated expression of Akt, which was not observed in EOM, but the BA-specific increase in JNK T54 phosphorylation was (p=0.03, Table 2.6).

The BB-specific phosphorylation of p70S6k$^{T421/S424}$ and ERK2 with age was not observed in P, and aged P showed significantly greater phosphorylation of JNK54 and expression of Akt (p=0.02 and p=0.016, respectively, Table 2.6).

Table 2.6 Summary of protein expression and phosphorylation in extraocular (EOM) and pectoralis (P) muscles of young (8 month) and old (26 month) F344 rats.

	EOM		**P**	
	Y	O	Y	O
p-ACC	1.00±0.4	1.45±1.5	1.00±0.3	1.34±0.7
Akt	1.00±0.3	0.78±0.3	1.00±0.3	1.59±0.5
p-Akt	1.00±0.5	1.32±1.1	1.00±0.3	0.92±0.5
Rel Akt	1.00±0.5	1.94±1.5	1.00±0.3	0.64±0.4
p70	1.00±0.4	0.99±0.7	1.00±0.3	0.92±0.5
p70$^{T421/S424}$	N.D.	N.D.	1.00±0.5	0.98±0.5
Rel T421	N.D.	N.D.	1.00±0.8	0.97±0.5
p70^{T389}	N.D.	N.D.	1.00±0.4	0.99±0.3
Rel T389	N.D.	N.D.	1.00±0.8	1.07±0.5
ERK2	1.00±0.5	1.17±0.7	1.00±0.2	1.11±0.6
p-ERK	1.00±0.3	0.83±0.5	1.00±0.7	1.09±0.4
Rel ERK	1.00±0.4	0.72±0.3	1.00±0.6	1.05±0.6
p-p38	1.00±0.3	0.79±0.4	1.00±0.4	1.45±0.5
p-JNK 46	1.00±0.7	0.63±0.3	1.00±0.2	1.09±0.4
p-JNK 54	1.00±0.3	1.84±0.6	1.00±0.3	1.69±0.6

Discussion

The key findings of the current study show p70S6k expression declines with age in all muscle groups; phosphorylation of ERK and p70S6k$^{T421/S424}$ is elevated in young BB muscles; Akt expression is elevated in branchial arch muscles; and p38

phosphorylation is much greater in aged branchial arch muscles. Factor analysis revealed coordinated phosphorylation of most signaling molecules, independent of fiber-type or developmental origin, and that this coordination breaks down with aging.

Statistical resolution of individual kinase differences may have been hampered by at least two constraints. First, these comparisons are among muscles in their basal or resting state, at which phosphorylation levels are expected to be low. Second, due to the nature of the dissections, there was a substantial lag between euthanasia and freezing of each muscle. During this time, endogenous phosphatases and proteases may have reduced differences among muscles. Specimens were chilled after euthanasia to minimize this activity as much as possible and pilot experiments indicated that basal phosphorylation was stable for at least an hour. However, one interpretation of factor 2 containing all of the phosphorylations is that samples varied in the preservation of phosphorylation.

Factor analysis identifies sets of correlations between all measures within each muscle and across all groups of muscles. The strongest correlations were between the MHC isoforms and distinguished between fast and slow muscles. The quantification of MHC content by Coomassie-stained gels was associated with variance of less than 20% for fast isoforms. In contrast, variance of kinase phosphorylations detected by Western blot ranged from a low of 20% to a high of 95% within a muscle. This difference in variance encourages the inclusion of MHC isoforms, and facilitates the resolution of systematic biological patterns, such as the shift from IIb to IIx/IIa with age. Coordination among kinases from the Akt-p70S6k cascade and the different MAP kinase cascades is consistent with the involvement of multiple pathways in growth signaling, and it is particularly interesting that this factor is increased in aged M and GH, muscles associated with jaw closing and tongue protrusion, but decreased in aged BB. This suggests that there may be activity dependent signaling within the muscles of mastication at a level too subtle to resolve by Western blot of individual kinases.

The goal of this study was to evaluate the influence of developmental and functional origin on growth signaling during aging. Aging is associated with a decline in systemic growth signals, muscle activity and with motor neuron degeneration that may differentially affect somitic and branchial arch muscles (Giovannini et al., 2008; Larsson and Ansved, 1995; Lynch et al., 2007; Nair, 2005). Such differences may contribute to declines up to 30% in hind limb muscle mass in F344 rats with age (Daw et al., 1988; Yu et al., 1982), while head, neck and tongue muscles of F344/BN or F344 show reductions of 15% or less in mass and force at equivalent age (Connor et al., 2008; Norton et al., 2001). Although we did not collect head, neck and tongue muscles intact enough to assess mass, EDL and soleus mass from these animals decreased by 19 and 26% respectively (data not shown), which is appropriate for this strain and age (Daw et al., 1988; Yu et al., 1982). BB from old animals were visibly smaller than from young animals and expected to be a forelimb correlate to the commonly studied fast hind limb muscles. Size differences of the tongue and jaw muscles were not as visibly distinct.

General effects of age

The effect of systemic changes on growth signaling was expected to be revealed by age-associated alterations in signaling molecule activation independent of origin. Expression of p70S6k declines in every muscle group of our 26 month-old Fischer 344 animals. Similar declines are seen in 30 and 36 month-old F344/Brown Norway (FBN) rats (Kinnard et al., 2005) and 27 month-old Sprague-Dawley rats (Kimball et al., 2004). Although the regulation of p70S6k phosphorylation and activation has been reported in detail, control of p70S6k expression has been less extensively reported. The phosphorylation of p70S6k shortly after exercise is correlated with eventual hypertrophy (Baar and Esser, 1999), and acute performance of high force contractions results in an extended period of p70S6k phosphorylation (Glover et al., 2008; Nader and Esser, 2001). In this study, factor analysis revealed p70S6k expression was greater in fast muscles

suggesting p70S6k signaling may be particularly important in muscles that stereotypically produce greater forces but are subject to infrequent activity. The general decline in p70S6k expression suggests that aged muscle may have reduced capacity to respond to maintenance signals provided by infrequent high force contractions.

Influence of lineage

The effect of lineage is revealed by differences between the branchial arch muscles and the somitic muscles. Branchial arch muscles displayed two unique features: hyperexpression of Akt and hyperphosphorylation of p38 with age. Head and neck muscles in general have several characteristics that differ from somitic limb muscles, including a unique myogenic program and increased myonuclear turnover (Evans et al., 2008; Noden and Francis-West, 2006). Masseter and extraocular muscles have a larger population of activated satellite cells than limb muscle, but also appear to undergo accelerated apoptosis, suggesting that these branchial arch muscles are subject to continual myonuclear turnover (Evans et al., 2008; McLoon et al., 2004)**.**

P38 is activated in response to cellular stress and important in cellular processes including myogenesis and apoptosis (Keren et al., 2006; Lluis et al., 2006). Phosphorylation of p38 overall was unchanged with age in somitic muscles, which is similar to other studies (Mylabathula et al., 2006), but in branchial arch muscles, p38 phosphorylation greatly increased with age. Hyperactivation of p38 is consistent with accelerated myonuclear turnover, and a more active population of satellite cells in the branchial arch muscles might contribute to preservation of function during aging. However, the unique developmental origin of the head and neck muscles may make them hypersensitive to cellular stresses. Further studies are needed to elucidate the role of p38 with age in these muscles.

Influence of physical activity

Activity was not measured in this study but qualitative observations from other studies are extremely consistent, and a reduction in locomotor activity is observed using any measure of home-cage or voluntary activity (Holloszy et al., 1985; Skalicky et al., 1996). In contrast, tasks of head, neck and tongue muscles - mastication, respiration, and swallowing - are required throughout life and show either minimal change (Connor et al., 2008) or even increased activity (Peng and Kang, 1984; Zhang et al., 2008). We hypothesized these relative changes in muscle activity with age based on muscle function (mastication versus locomotion) would reveal the effect of muscle activity on growth signaling. Although analysis of the five core muscles indicated that phosphorylation of ERK and p70S6k$^{T421/S424}$ declines with age only in somitic BB muscles, failure to confirm this with P suggests that home cage activity plays little role in supporting basal activation of growth signaling of young locomotor muscles. This is consistent with highly variable literature reports of basal ERK phosphorylation, including either no change (*pectoralis*, present study; *tibialis anterior* and *plantaris*, (Parkington et al., 2004)), increase (*extensor digitorum longus*, (Mylabathula et al., 2006)), or decrease (*biceps brachii*, present study) in limb muscles with age. Acutely, ERK phosphorylation is increased in response to electrical stimulation and is closely correlated with mechanical force (Martineau and Gardiner, 2001; Widegren et al., 2001; Wretman et al., 2001). Such acute, force-dependent responses may allow infrequent but intense activity to provide a transient stimulus and maintain muscle mass.

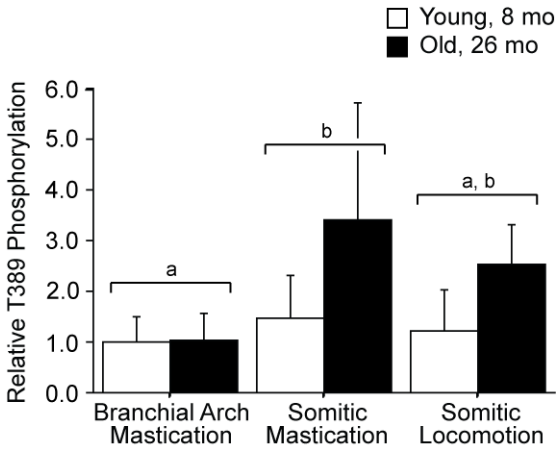

Figure 2.4 Relative phosphorylation of p70S6k on T389 to total p70S6k expression in young and old muscles by origin. Relative p70S6k phosphorylation differs by muscle origin ($p=0.01$) and age ($p=0.01$), but no significant interaction effect ($p=0.10$) was found. Origins designated by the same letter were indistinguishable in post hoc T-tests. Data are presented as difference of logs from young averages, expressed as mean ± S.D..

Separate Mechanisms Regulating Expression and Phosphorylation

Similar $p70S6k^{T389}$ phosphorylation in spite of down-regulation of p70S6k expression with age indicates a greater fraction of p70S6k molecules are active as reflected in relative phosphorylation status (Figure 2.4), and implies a decoupling of the control of expression and activity. Discoordination of p70S6k expression and T389 phosphorylation has been reported in other aging models (Kimball et al., 2004; Kinnard et al., 2005; Thomson and Gordon, 2006) suggesting the regulation of expression and post-translational control of phosphorylation may be regulated by independent processes. Phosphorylation of p70S6k at T389 is the residue most closely representative of activity (Pullen and Thomas, 1997; Weng et al., 1998) and is highly correlated with protein synthesis rate and muscle growth (Baar and Esser, 1999; Thomson and Gordon, 2006). Protein synthesis is higher in old animals despite losing muscle mass (Kimball et al., 2004), which is consistent with neutral or elevated p70S6k phosphorylation. We propose a feedback model for T389 phosphorylation, dependent on muscle force and a separate feedforward model for p70S6k expression dependent on systemic factors (Figure 2.5).

This suggests that functional overload stimulates phosphorylation and activation of p70S6k, whereas systemic factors promote cell growth possibly through acetyl-group modifications leading to stabilization of p70S6k protein (Fenton et al., 2010). Withdrawal of systemic factors, such as growth factors, associated with aging would then reduce the pool of p70S6k and limit the ability of muscle to increase protein synthesis in response to acute stimuli like exercise.

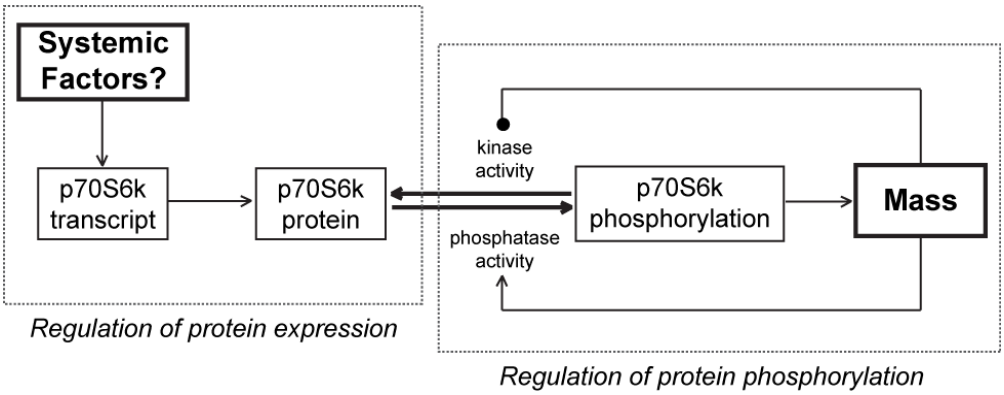

Figure 2.5 Suggested mechanism for regulation of p70S6k expression and phosphorylation. Schematic representation of a feed-forward mechanism in which systemic factors regulate p70S6k expression and a feed-back mechanism in which p70S6k phosphorylation and activation is regulated by muscle mass and modulated by muscle load. In aged muscle, maintaining p70S6k phosphorylation despite a decline in amount of p70S6k may require increased (mTOR) kinase activity. The age-related decline in p70S6k may limit the muscles' ability to respond to stimuli with increased mass.

Conclusions

In summary, this study provides a comparative analysis of the phosphorylation state of proteins associated with muscle growth in muscles with different functional roles, and different developmental origins. Phosphorylation within the mTOR and MAP kinase cascades was strikingly independent of age, developmental origin, or functional task, but an underlying coordination among phosphorylation of ERK, JNK T54, and p70S6k$^{T421/S424}$ and Akt was found. One unique signaling structure observed in branchial

arch muscles, characterized by hyperexpression of Akt and exaggerated phosphorylation of p38, may contribute to their exaggerated myonuclear turnover and relative sparing from sarcopenia. The discoordination of p70S6k expression and phosphorylation of T389 suggests these aspects are independently regulated, potentially by systemic factors and muscle load.

Acknowledgments

This work was supported by the National Institute of Health (NIH) grant, DC05017 and AG023902.

CHAPTER III

IMMEDIATE RESPONSE OF GROWTH-RELATED SIGNALING IS NOT DEPENDENT ON SUB-MAXIMAL FORCE LEVEL IN MOUSE *TIBIALIS ANTERIOR* FOLLOWING LOW DUTY CYCLE ACTIVATIONS

Abstract

High force contractions lead to muscle hypertrophy and attention has been drawn to the high forces involved, although both mechanical and metabolic stresses occur simultaneously. Both stimuli activate multiple cascades related to protein synthesis, and the contraction regimen may influence the resulting muscle growth. The present study aimed to alter force produced by the muscle, while minimizing metabolic stresses to test the hypothesis that growth-related signaling during isometric activation is dependent on the level of force. Mouse *tibialis anterior* muscles were subjected to 60 low duty cycle activations *in situ*. Muscle length, shortening velocity or stimulation pulse width were manipulated to produce sub-maximal forces and phosphorylation status of MAP kinases and Akt-mTOR-p70S6 kinase cascades were analyzed. Although three distinct force levels were produced and phosphorylation of ERK, Akt, and p70S6k changed substantially, no force dependent signaling could be resolved in this study. Phosphorylation of ERK appears to be the only one of the growth-related kinases examined whose phosphorylation is dependent on fiber-activation. These kinases are substantially removed from direct signal transduction events, but these results suggest that only ERK is directly dependent on an action potential, while the remainder of signaling at this level is strongly dependent on stimuli uncoupled from force production.

Introduction

Resistance training and high force contractions lead to muscle hypertrophy through a complex process involving increased protein synthesis, activation of satellite cells, and changes in gene regulation. The most dramatic aspect of high force contractions is the high force, and this force has been linked to activation of important growth related signaling cascades via growth factor-independent mechanisms (Hornberger and Chien, 2005; Hornberger et al., 2004; Spangenburg et al., 2008). Multiple midstream signaling cascades have been associated with these processes, including PI-3K-mTORC1-p70S6k and various MAP kinases. High frequency electrical stimulation (HFES) induces phosphorylation of p70S6k on the T389 residue, which represents mTORC1 activity and correlates to changes in muscle mass (Baar and Esser, 1999; Witkowski et al., 2010). MAP kinases (ERK1/2, p38, JNK) are phosphorylated after HFES, but each has a different correlation with force (Martineau and Gardiner, 2001; Wretman et al., 2001).

The response of muscle to force production appears to be specific to the conditions of force production. Biaxial, but not uniaxial stretch induces phosphorylation of p70S6k (Frey et al., 2009; Hornberger et al., 2005; Kumar et al., 2002). HFES of rat *tibialis anterior* (TA) induces phosphorylation of p70S6k sustained for 6 hours, while low frequency electrical stimulation (LFES) sustains p70S6k phosphorylation for only 3 hours (Nader and Esser, 2001). Akt phosphorylation is increased following long duration stimulations (Nader and Esser, 2001; Sakamoto et al., 2002) but not following short duration stimulations (Brozinick and Birnbaum, 1998). Eccentric activation induces substantially greater phosphorylation of JNK, ERK, and p70S6k than do concentric (Baar and Esser, 1999; Martineau and Gardiner, 2001; Wretman et al., 2001). These experiments support the theory that force level determines the cellular response of the muscle. However, differences in stimulation conditions used to alter force production also alter other potential signals, including AMP:ATP ratio and other markers of

metabolic cost. For example, reduced cross-bridge turnover during eccentric contractions results in greater force and mechanical stress at a lower metabolic cost than either isometric or concentric contractions (Beltman et al., 2004; Fenn and Latchford, 1933), and repeated activations, particularly long activations with short rest periods, reduce force generation through substrate and electrolyte depletion (Burke et al., 1973).

Force production cannot be decoupled from metabolic cost, but the relationship between force and cost is highly dependent on the conditions of stimulation. Fatiguing protocols (i.e. high work: rest ratio) intensify ATP turnover during contraction and may lead to failure to maintain or generate peak force, increases in ROS, AMP:ATP ratio or lactate concentrations, decreases in glycogen/glucose availability or pH (Burke et al., 1973; Fitts, 1994). For example, the HFES intervention that induced sustained p70S6k phosphorylation was associated with a greater reduction in muscle glycogen than the LFES intervention that induced only brief p70S6k phosphorylation (Nader and Esser, 2001). Similar HFES studies report increased AMP-activated protein kinase (AMPK) activity and that AMPK may inhibit mTORC1 activity (Thomson et al., 2008). The concentric and eccentric contractions used to infer that MAP kinase activation is proportional to force only sustained force for the first few contractions, reaching a nadir of 30-50% by the first minute (Martineau and Gardiner, 2001). Further, eccentric activations are uniquely associated with cell damage and calcium leakage (McCully and Faulkner, 1985; Yeung et al., 2003), which may trigger qualitatively different responses than isometric and concentric activation. Thus, studies linking growth signaling to high force activations may obscure the role of force-dependent signaling with closely correlated metabolic and traumatic signaling.

This study was designed to analyze force-related differences in phosphorylation state of kinases associated with growth-signaling under minimal metabolic load to test the hypothesis that MAP kinase signaling is related to peak muscle force. Brief stimulations with long rest periods were used to minimize ATP turnover and glycogen depletion. To

further decouple force and stimulation conditions, 3 target force levels of High (100%), Moderate (60%) and Low (30%) relative to maximum force (P_0) were obtained by adjusting muscle length, muscle shortening velocity or simulation pulse width. Compared to maximal isometric contractions, activations at short lengths (low force) consume similar ATP indicated by ATPase activity (a measure of cross-bridge cycling) and heat production (Fenn and Latchford, 1933; Gordon et al., 1966; Stephenson et al., 1989), suggesting that isometric force and metabolic cost are uncorrelated along the ascending limb of the length-tension relationship. By contrast, increasing the velocity of shortening (low force) results in nearly proportional increases in heat and cross-bridge cycling (Huxley, 1957a; Potma and Stienen, 1996; Potma et al., 1994) thus, force during shortening is negatively correlated with metabolic cost. Reducing the intensity of stimulation reduces the number of fibers recruited, reducing both ion transport and cross-bridge turnover, and should result in a direct correlation between force and metabolic cost. This design provides similar force levels with different ATP costs, and should allow separation of force-dependent and ATP turnover-dependent signaling.

The results do not support the existence of any molecular responses specific to force, but do reveal modules of correlated signaling. The response of molecules within the canonical Akt-mTORC1-p70S6k cascade were generally more muted than reported elsewhere, an outcome we attribute to our emphasis on low metabolic cost activations or to our focus on very rapid responses.

Material and methods

Animals

Male CFW Swiss-Webster mice (Crl:CFW (SW), Charles River, 26.2 g ± 2.0; n=8 per group) were housed in pairs on a 12/12 light cycle with food and water *ad libitum***.** Procedures were reviewed and approved by Institutional Animal Care and Use

Committee at Georgia Institute of Technology and performed in compliance with the Guide for Care and Use of Laboratory Animals.

Electrical Stimulation

A total of 70 animals were randomly assigned to one of 7 experimental or 2 control groups. Within the experimental groups, force was modulated by altering length (L), velocity (V) or pulse width (PW) to achieve Moderate or Low force levels: Mod- L, Low-L, Mod-V, Low-V, Mod-PW, or Low-PW. Maximal tension (High) is produced during isometric activations at optimum length (L_0) and supramaximal pulse width, so High-L, High-V, and High-PW groups represent identical conditions, and only one, lumped High group was used. Animals were anesthetized by intraperitoneal injection of a ketamine cocktail (90 mg/kg ketamine, 1 mg/kg acepromazine and 10 mg/kg xylazine). The *tibialis anterior* (TA) muscle was surgically exposed, the distal tendon released and tied to the arm of a force-measuring servo motor (Aurora Scientific), and the knee immobilized in a spring clamp. The peroneal nerve was isolated and mounted on hook electrodes. A series of twitch activations was used to determine the current (I_0) and muscle length (L_0) producing maximal twitch force (P_t). Activations start at L_0 and subsequent stimulation was 2x I_0, with the exception of pulse width groups in which stimulation was I_0. Maximal tetanic tension (P_0) was determined by 300 ms stimulation at 70 Hz at L_0. Muscles were then subjected to a series of 60 activations of 300 ms at 70 Hz over 15 minutes (15 s rest, 2% duty cycle) with force levels obtained using one of three methods described below. Throughout the stimulation protocol, muscles were wetted with 1X PBS (136.7 mM NaCl, 2.7 mM KCl, 1.4 mM KH_2PO_4, 4.3 mM Na_2HPO_4) or mineral oil to prevent desiccation. Immediately following electrical stimulation, animals were sacrificed by cervical dislocation, muscles dissected and immediately frozen in melting isopentane.

Length method: Short muscle lengths reduce the ability of the sarcomere to properly engage in cross-bridge formation and results in reduced force per fiber with a relatively constant metabolic load (Fenn and Latchford, 1933; Gordon et al., 1966; Stephenson et al., 1989). After the single tetanus to determine P_0, muscles were shortened to reduce force generation. Based on force-length curves generated in a separate set of pilot experiments, Mod-L muscles were shortened by 2 mm, and Low-L muscles were shortened by 3 mm. These lengths were adjusted on subsequent stimuli to obtain active tensions of 60±10% or 30±10% of P_0 (Table 3.1).

Velocity method: Increasing shortening velocity reduces force by limiting cross-bridge efficiency, but increases cross-bridge turnover rate, resulting in a higher energetic cost (Huxley, 1957a; Potma and Stienen, 1996; Potma et al., 1994). After determination of P_0, target force was set and isotonic activations were performed using the muscle servo in force control mode. The Low-V force was 38.7% P_0, and Mod-V force was 68.7% P_0 (Table 3.1).

Pulse width method: Modifying the number of fibers activated results in force and metabolic load that are proportional to activation level. Preliminary force-pulse width curves were used to estimate the pulse width at which the target force would be produced. Force was monitored and pulse width periodically adjusted during the series of tetani to maintain target isometric force levels of 30±10% and 60±10% (Table 3.1).

To provide a reference for the intensity of metabolic stress, an additional groups of animals (n=8) was subjected to a high duty cycle stimulation protocol that results in substantial glycogen depletion in rats (Nader and Esser, 2001). TA muscles were prepared as above but received 60 activation of 3 s at 70 Hz in 10 sets of 6 with 10 s of rest between repetitions and 60 s rest between sets (15% duty cycle). Unfortunately, post-hoc analysis of the force produced by this high duty cycle protocol revealed two response populations: one in which force was relatively maintained (>50% of P_0) throughout the 3 s stimulations (2/8 animals) and one in which force fell below 25% of

P_0, within the first second of stimulation (6/8 animals). Because greater changes in metabolic markers (e.g. ACC phosphorylation and glycogen content) occurred in muscles with better force maintenance during these stimulations, we attribute the rapid loss of force production to failure within the stimulation and neuromuscular conduction path. These stimulations were considered unreliable, but ACC phosphorylation and glycogen content measures can be found in Supplemental Material as positive controls for those assays.

Another group of animals (n=6) was subjected to a sham protocol in which the TA was exposed, attached to the force transducer as described above, and length adjusted to L_0 by a series of twitch activations. Animals were held in the apparatus for 15 min and the muscle bathed regularly in mineral oil, but did not receive stimulation.

Force Data

Muscle force during stimulation was digitized at 1000 Hz in 500 ms windows surrounding each 300 ms stimulation, for all protocols. Length change and velocity were also recorded in the velocity method. The resting, passive tension was subtracted from each trace, and tension records were normalized to the peak tension achieved during the maximal isometric activation. Average Peak Force (APF) for each animal was determined by averaging the peak tension achieved during each of the 60 activations. Force-time-integral (FTI) was determined by integrating force generated during all 60 activations. Sag was defined as the difference between force at the end of the 300 ms activation and the peak force achieved during that activation, and was averaged across all 60 activations. Length change (LC), in the velocity protocol, was the minimum length achieved during isotonic shortening. LC, in the length protocol, was the length at which stimulations were performed. Specific tension was determined according to the formula,

$$T_0=P_0 \rho L_f/m/\cos(\theta) \qquad (1)$$

where m is muscle mass, and ρ is muscle density, 1.06 g/cm^2 (Mendez and Keys, 1960). Values used for pennation angle (θ=11.7º) and fiber length (L_f=7.9 mm) were taken from the literature (Burkholder et al., 1994).

Western Blotting

Muscles were homogenized using a rotor-stator (TissueMizer, Fisher Scientific) in a low salt detergent buffer (50 mM Tris, pH 7.5; 30 mM NaCl; 5 mM EDTA, 1% Triton X-100 plus NaF, NaVO3 and protease inhibitors) to minimize myofilament extraction and cleared of debris at 15,000 × g. The protein concentration of the supernatant was measured by BCA assay (Pierce) according to manufacturer's protocol. Soluble protein (15 ug) was separated by SDS-PAGE, transferred to nitrocellulose membranes, and detected by Western blot. Primary antibody dilutions were: p-ERK$^{T202/T204}$ 1:3000; total ERK2 1:2500; p-JNK 1:500; p-p38$^{T180/Y182}$ 1:2000; p-Akt ^{S473} 1:2000; total Akt 1:2000; p-P70S6k $^{T421/S424}$ 1:2000; p-p70S6k ^{T389} 1:2500; pan p70 1:2000; p-ACC 1:1000; p-mTORC1 ^{S2448} 1:2000; p-FAK^{Y397} 1:2000 . All antibodies are purchased from Cell Signaling except JNK (Santa Cruz), FAK (Invitrogen) and total ERK2 (BD). Bands were visualized by enhanced chemiluminescence and quantified by scanning densitometry. Results are expressed as a ratio of the stimulated to the un-stimulated contralateral muscle. ERK2, p-JNK, p-p38, Akt, p70S6k, p-mTOR, and p-FAK are expressed as (IOD_{stim}/IOD_{unstim}) where IOD is the integrated optical density of the band, and stim/unstim refers to the stimulated and contralateral muscles, respectively. p-ERK, p-Akt and p-p70S6k are expressed as (IOD_{stim}/IOD_{unstim})/ $IOD_{stim\text{-}pan}/IOD_{unstim\text{-}pan}$), where pan refers to the corresponding non-phosphorylated, or total antigen. ACC phosphorylation was quantified by normalizing all of the bands on a gel to the average of the contralateral IOD from all animals on that gel. All gels were repeated at least twice, and the average of all repeats for each sample was used for analysis. Each blot included a

common positive control from insulin stimulated or eccentrically activated TA muscle for validation.

Glycogen Content

The distal portion (~20 mg) of the TA was weighed, digested in 30% KOH saturated with Na_2SO_4 for 20 min at 100°C and glycogen precipitated with 1.2 volumes of 95% EtOH for 30 min on ice as described by Lo (Lo et al., 1970). Glycogen was pelleted at 850 x g for 30 min then dissolved in deionized H_2O. Content was determined spectrophotometrically using 5% phenol followed by rapid addition of 96% H_2SO_4 and read at 490 nm.

Statistics

All values are expressed as means ± s.d. and statistical analyses were performed on StatView (Abacus Software). Glycogen content and ACC phosphorylation were analyzed by mixed-mode, two-way ANOVA, with stimulation (repeated: stimulated or contralateral) and method (factorial: length, velocity, pulse width, sham) as factors or by paired t-tests. Western blot ratios (stimulated:contralateral) were log transformed for statistical analysis although untransformed results are presented in tables and graphs. One Sample analysis of the pooled data (n=56) was used to determine whether stimulation had an overall effect on each antigen. Phosphorylation ratios were then analyzed by two-way ANCOVA (Method X APF) with a significance threshold of $p < 0.05$, followed by post hoc t-tests using the Bonferroni/Dunn correction for multiple comparisons. Because the one high force group is common to all stimulation methods and the software requires a fully populated data matrix, the high force data were replicated and represented in all methods. Replication of data increases the degrees of freedom used for statistical analysis and results in an over-estimate of significance. To account for this, F-values were recalculated using corrected degrees of freedom and p-

values recalculated using the F to p calculator at http://faculty.vassar.edu/lowry/tabs.html#f.

Because of the breadth of data obtained from each sample, factor analysis was used to extract principal components and identify potential common causes. Kinase ratios, APF and LC were included in this analysis with the anticipation that common causes within a group of kinases might allow resolution of more subtle mechanical effects than individual kinases. Factor scores were Varimax transformed and method-dependent differences in the orthogonal solutions were determined by 1-way ANOVA with a significance threshold of $p < 0.05$.

Table 3.1. Experimental Design and Measures. Stimulation protocol and characteristics of muscles producing 2 sub-maximal force levels (Moderate and Low) by 3 methods (Length, Velocity, Pulse Width) that will be compared to High force level. Data presented as mean ± s.d.

High Force (100% P_0)		**Moderate Force (60% P_0)**	**Low Force (30% P_0)**
60 isometric activations at optimal length (L_0) 70 Hz, 300 ms duration 15 s rest 0.1 ms pulse width Max force (P_0): **1.06 N** ±0.14 Force-Time: **20.4 kN***ms ±3.2 Specific Force: **3.1N/cm^2** ±0.6	**Length** *Average Peak force* *Intra-animal variability* *Force-Time Integral* *Specific Force* *Mode* *Length*	 **57.9%** ± 7.4 (0.72N) 3.1% ± 3.0 12.0 kN*ms ± 1.8 2.8 N/cm^2 ± 0.2 Isometric -1.84 mm ± 0.52	 **30.7%** ± 3.7 (0.38 N) 6.9% ± 4.7 4.8 kN*ms ± 2.0 2.5 N/cm^2 ± 0.2Isometric -2.54 mm ± 0.51
	Velocity *Average Peak force* *Intra-animal variability* *Force-Time Integral* *Specific Force* *Mode* *Length change* *Peak velocity*	 **68.7%** ± 0.8 (0.73 N) 1.1% ± 2.8 15.5 kN*ms ± 0.5 2.8 N/cm^2 ± 0.1 Concentric -0.8 mm ± 0.3 6.1 mm/s ± 1.4	 **38.6%** ± 1.1 (0.42 N) 0.17% ± 0.1 9.3 kN*ms ± 0.8 2.8 N/cm^2 ± 0.5 Concentric -2.1 mm ± 0.2 16.0 mm/s ± 1.5
	Pulse Width *Average Peak force* *Intra-animal variability* *Force-Time Integral* *Specific Force* *Mode* *Pulse Width*	 **62.9%** ± 6.0 (0.64 N) 7.1% ± 1.8 11.9 kN*ms ± 3.4 2.6 N/cm^2 ± 0.5Isometric at L_0 ~0.06 ms	 **29.3%** ± 3.8 (0.30 N) 10.0% ± 2.4 6.2 kN*ms ± 0.9 2.9 N/cm^2 ± 0.2Isometric at L_0 ~0.03 ms

Results

Force stimulus

Modulation of muscle length, shortening velocity or stimulation pulse width provided 3 methods by which 2 sub-maximal target force levels could be obtained and compared against high force (High) contractions (Figure 3.1A). Across methods, average peak force (APF) of all 60 activations was 99.5% ± 6.9% for High, 64.8± 5.3% for Moderate and 35.2± 5.8% of P_0 for Low force groups. Individual group results are detailed in Table 3.1.

Figure 3.1B depicts the force produced by stimulations in the High group plotted over the duration of the low duty cycle protocol and illustrates that short stimulations with long rest intervals minimizes fatigue and allows the muscle to repeatedly produce maximum force. The decline in peak force from the first contraction to the 60^{th} contraction ranged from 0-10% the High group and is similar to the intra-animal variability of all protocols (Table 3.1). Stimulation produced nearly fused tetanic activations with force ripple around 0.7% and sag of 2-10% of peak tension with the exception of Mod-P and Low-L in which sag was greater than 25% (Figure 3.1A). Muscles allowed to shorten isotonically in the V method achieved isometric equilibrium near the end of activation. The equilibrium length was consistently longer than the length required for isometric generation of the same force level, consistent with a persistent loss of tension (Abbott and Aubert, 1952) and indicating multiple ways for a muscle to produce the same force (Figure 3.1C).

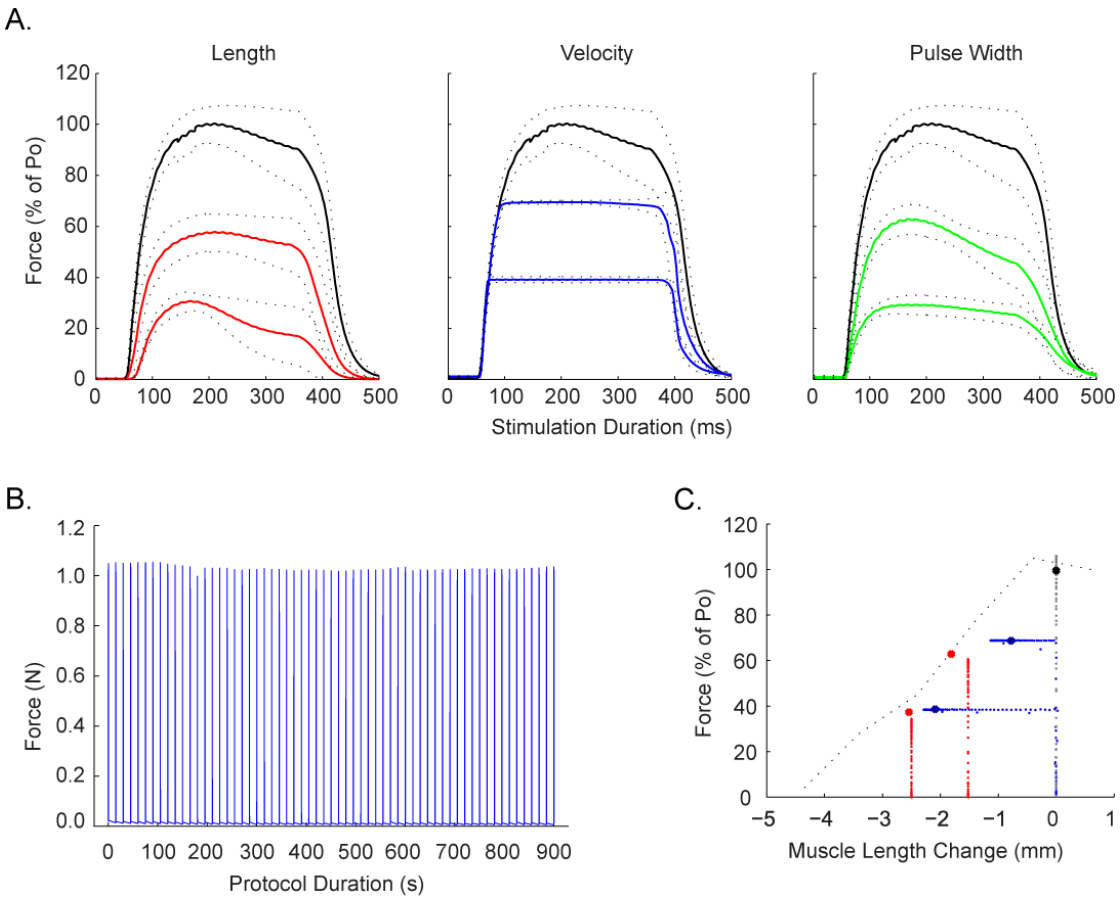

Figure 3.1 Stimulation protocols resulted in distinct force levels. A) Forces produced by each group were first averaged across all 60 activations for each muscle, normalized to the maximum force produced by each muscle, then averaged across all animals per group (n=8). Dashed lines represent ± s.d. among the animals for each group and the High Force group is replicated for comparison in each method. B) Representative low duty cycle protocol for the High force group where each 300 ms activation and 15 s rest period have been plotted sequentially for a single animal to show loss of force with repeated stimulation. C) Length-force histories for representative contractions, with each dot representing 5 ms. In L (red), muscles begin at short length, in High (black) and PW (not shown) at L_0, and force increases isometrically. In V (blue) muscles begin at L_0, force increases isometrically to the target force then length decreases isotonically. V muscles typically experience a brief isometric period at short length, followed by return to L_0 as the muscle relaxes. Dashed line represents force-length curve from pilot experiments. Bold dots indicate average length change and force produced by respective groups.

Minimal metabolic cost of stimulation

The stimulation regimen of 2% duty cycle was designed to minimize the changes in AMP:ATP ratio associated with repeated muscle activations. Acetyl-coA-carboxylase (ACC) is a primary physiological target of AMPK and its phosphorylation was used as an index of in vivo AMPK activity. Two-way repeated measures ANOVA showed

stimulation significantly increased ACC phosphorylation by 40% compared to unstimulated contralateral muscles (n=56, p<0.0001, Figure 3.2) however, there were no main effects of method or level of force. That is, the effect of stimulation on ACC phosphorylation could only be resolved in the pooled data, and suggests low energetic costs associated with this stimulation protocol. Likewise, an 8.7% reduction in glycogen content (p=0.0009, Figure 3.2) by stimulation could be resolved as a main effect in 2-way ANOVA, but not in any separate group. In two animals subjected to a high duty cycle (HDC, 15%) stimulation regimen glycogen content was reduced by 30% (Suppl. Figure 3.2S-B) and ACC phosphorylation was increased by 584% (Suppl. Figure 3.2S-A) compared to unstimulated contralateral muscles, however the small sample size prevented valid statistical analysis.

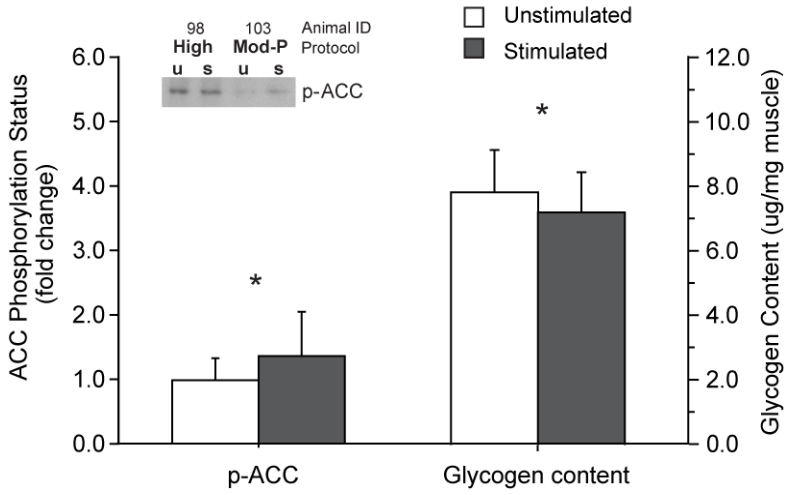

Figure 3.2 Metabolic Measures. Electrical stimulation (grey) increased ACC phosphorylation by 40% (n=56, p<0.0001) using low duty cycle (LDC) activations compared to paired unstimulated contralateral muscles. Above, representative western blots for ACC phosphorylation of unstimulated (u) and stimulated (s) muscles are shown for LDC (identified by protocol) from a single gel. Glycogen content decreased by 8.7% (n=56, p=0.0009) using LDC activations compared to paired unstimulated contralateral muscle. Data presented as mean of groups pooled ± s.d. * p<0.05 between stimulated and unstimulated by paired t-tests.

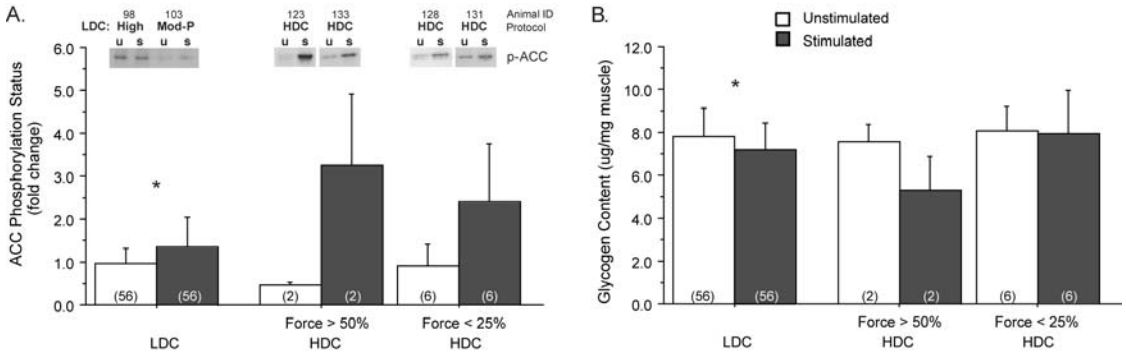

Figure 3.2S Metabolic Measures of Duty Cycles. Electrical stimulation (grey) increased ACC phosphorylation (A) by 40% ($p<0.0001$) in muscles subjected to LDC activations compared to unstimulated (white) contralateral muscles. Two populations emerged from HDC stimulations based on level of force maintenance throughout the long duration activations. When force was maintained at >50% of maximum through each 3 second stimulation, ACC phosphorylation increased by 584%. In muscles where force production fell to <25% of maximum, ACC phosphorylation was 262% greater than in unstimulated contralateral muscles. Representative western blots show ACC phosphorylation of unstimulated (u) and stimulated (s) muscles from LDC (identified by protocol) and both populations of HDC activations. Glycogen content (B) decreased by 8.7% ($p=0.0009$) in muscles subjected to LDC activations and 30% in muscle subjected to HDC activations in which force was maintained at >50% of maximum. By contrast, when force fell to <25% by the end of the long-duration activation, glycogen content of the stimulated muscle was unchanged (-1.5%) compared to unstimulated muscles. * $p<0.05$ between stimulated and unstimulated by paired t-test. No statistics were performed on either HDC population due to the inadequate samples. Numbers within each bar indicate the n of each group.

Autophosphorylation of focal adhesion kinase is not altered by force

One kinase widely implicated in mechanotransduction of force is focal adhesion kinase (FAK)(Fluck et al., 1999). Autophosphorylation on tyrosine 397 was not increased by electrical stimulation (1.2 ± 0.8 fold, $p=0.71$ by one-sample t-test; Figure 3.3). Two-way ANCOVA did identify a significant effect of force (APF $p= 0.03$), with positive slopes in all methods, but no specific group was significantly increased when analyzed by one-sample t-test. This suggests that high force isometric contractions only weakly contribute to FAK autophosphorylation.

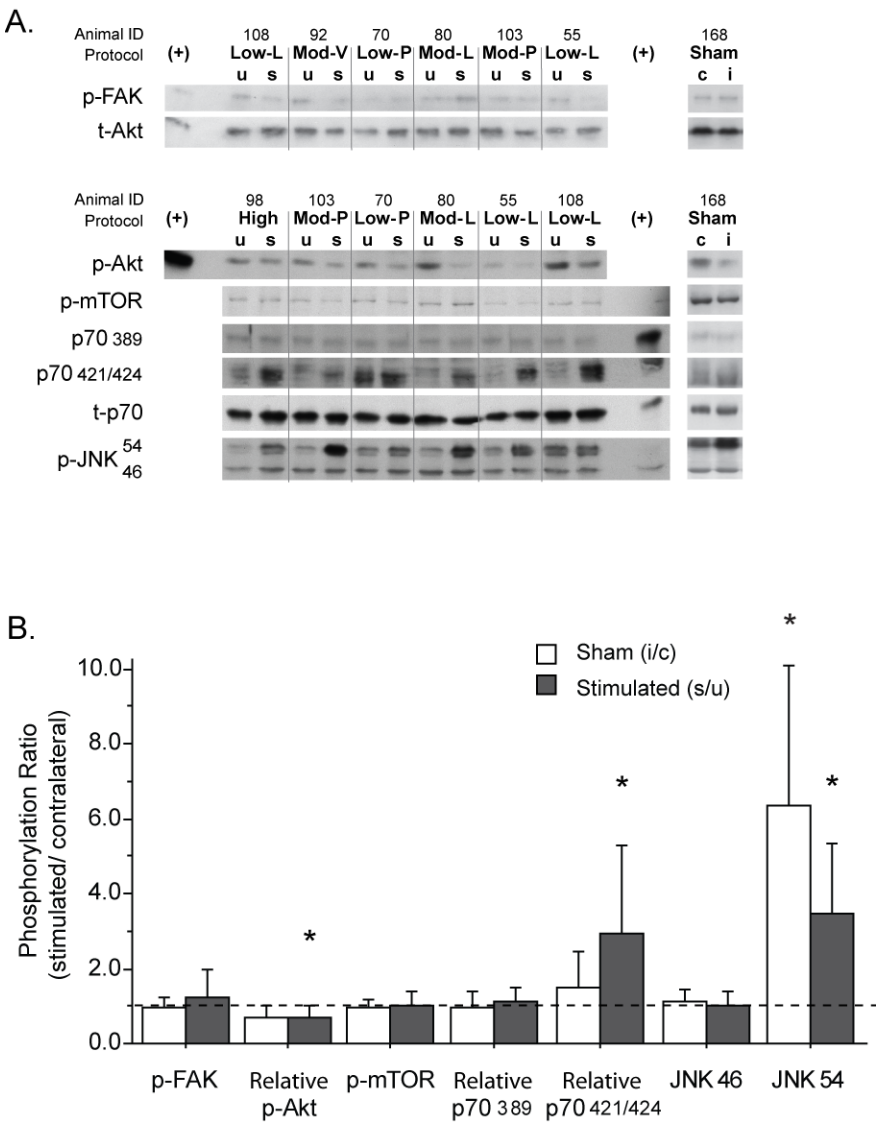

Figure 3.3. A) Representative western blots for contralateral, unstimulated (u) and stimulated (s) muscles. All blots shown are generated from a single set of muscles analyzed together on the same gel with positive controls from either insulin-stimulated or eccentric-activated control muscles. Unstimulated sham blots come from the same animal but were run on separate gels. B) Change in phosphorylation of selected targets induced by electrical stimulation (grey) or sham (open). Results are expressed as a ratio of the stimulated or sham to contralateral muscle. Horizontal dotted line indicates a ratio of 1.0. Data presented as mean ± s.d. * indicates significantly different than 1 by one-sample T-test on log transformed data.

Minimal signaling through Akt-mTOR-p70S6k cascade

Electrical stimulation significantly reduced Akt phosphorylation relative to contralateral control by an average of 32% ($p<0.0001$; Figure 3.3A), however, two-way ANCOVA revealed no systematic effects (Method $p=0.34$, APF $p=0.56$, Method X APF

p=0.68). Phosphorylation of mTOR (p=0.46) and its downstream target p70S6k T389 (p=0.67) were unchanged by stimulation (Figure 3.3A). Phosphorylation of p70S6k at T421/S424 was significantly increased (p<0.0001) by stimulation relative to contralateral muscle, and two-way ANCOVA found a trend for an effect of force (p=0.05). Closer inspection revealed that this trend was strongly influenced by a single extreme data point in Low-L group. Analysis without this point reduced significance of the force effect to 0.095.

Stimulation increases MAP kinases phosphorylation, independent of force

Phosphorylation of ERK, p38, and JNK 54 MAPKs was greater following stimulation (p<0.0001, p=0.0007, p<0.0001 respectively), without change in JNK 46 (p=0.36, Figure 3.3A), when data was pooled across groups and analyzed by one-sample t-tests. Two-way ANCOVA was unable to resolve any effect of modulation method or force in JNK 54 (p=0.55 or p=0.69, respectively), and sham animals showed a similar increase (6.3±3.8; p=0.01). By contrast, phosphorylation of p38 was unchanged (1.2-fold±0.6; p=0.96), and ERK was marginally increased (2.3-fold±0.5; p=0.0002) in the sham animals. ERK phosphorylation in Sham animals is similar to Low-P, but significantly different from the phosphorylation response seen in L and V methods (p<0.0001). Because the Low-P force was achieved by reducing the number of motor units recruited, it represents a treatment very similar to sham, with very few muscle fibers actually activated.

Two-way ANCOVA showed a trend for p38 phosphorylation to vary with modulation method (p=0.09). This appeared to result from exaggerated phosphorylation in a single low force point in the V method (Figure 3.4). Analysis without this outlier eliminated the effect of method (p=0.36) and uncovered a trend for a main effect of force (p=0.06, Figure 3.4 solid line). In neither analysis did an interaction effect appear (Method X APF p=0.23 including or p=0.55 excluding outlier). Detailed examination of

the outlying data point, including repeated Western blot, failed to uncover any justification for excluding it beyond being vastly different than all other samples. Regardless of its inclusion, there was at best very weak correlation between force and p38 phosphorylation.

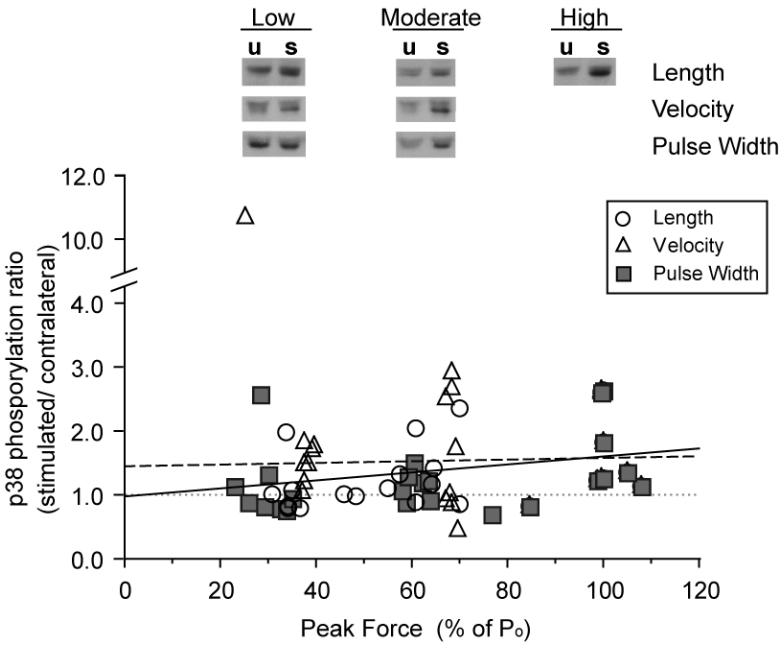

Figure 3.4 p38 MAPK Phosphorylation. Individual p38 phosphorylation ratios (stimulated/contralateral) are plotted against average peak force of respective muscle and identified by method: length (circles), velocity (triangles) and pulse width (squares). High force data was replicated and represented in all methods. Regression line for phosphorylation ratio and average peak force is shown including all data points (dashed line; R^2=0.032) or excluding the outlier (solid line; R^2=0.081). Horizontal dotted line indicates a ratio of 1.0 or no change in phosphorylation. Two-way ANCOVA indicates a trend for a significant main effect of force (solid line, p=0.06) however, no main effect or method (p=0.36) or interaction effect (Method X APF, p=0.55) was found. Representative western blots for p38 phosphorylation of contralateral, unstimulated (u) and stimulated (s) muscles for each method and force level are shown above in which blots from each method are from a single gel.

In contrast to other antigens, ERK phosphorylation varied substantially among groups. Two-way ANCOVA confirmed an interaction effect between force produced and method of force modulation (Method X APF p=0.028; Figure 3.5A). Under the pulse width method, regression analysis showed ERK2 phosphorylation was positively correlated with force (p=0.006), as expected. However, under the length method, ERK2

phosphorylation was negatively correlated with force (p=0.011), and no correlation was found under velocity modulation (p=0.95). The phospho-ERK2 measure is relative to pan-ERK2 intensity, which was homogeneous and unchanged from contralateral across most groups. However, the Low-L group only showed a 33% reduction in ERK2 content by one-sample t-test (p=0.0015, Figure 3.5B), and it was this reduction, rather than an elevation in the IOD of phospho-ERK, that produced the negative correlation within the Length method. The decrease in ERK2 content after just 15 minutes of electrical stimulation was unexpected. It was unique to ERK2 and was not present in any groups for total p70 or Akt (data not shown), so it seems unlikely to result from a systematic error in protein content. ERK2 content of the other groups were not significantly altered by stimulation (p>0.12), so it seems unlikely to result from a marginally significant effect coincidentally reaching significance in Low-L. Specific degradation of ERK2 in muscle activated at short length seems the least unlikely explanation.

Coordinated signaling is not correlated with force

No correlations with force were found among individual kinases, so factor analysis was used to identify statistically correlated sets of variables. The first 3 factors (Table 3.2) account for 59% of the population variance. APF appears in Factor 2, which also includes Length Change and FAK phosphorylation, but none of the growth-related kinases. As noted above, no change in FAK phosphorylation could be resolved in any group, nor in the pooled data, so the correlation identified here, and by 2-way ANCOVA represents an effect too weak to resolve by t-test on western blot data. Factor 1 contained most of the MAP kinases, with p38, JNK 46 being primary contributors and correlated with ERK, mTOR and FAK as weaker contributions. Factor 3 contained the components of the widely recognized Akt-mTOR-p70S6k cascade. So, factor analysis was able to identify recognized relationships among the sampled cascades, but failed to identify any distinct signaling molecule or module correlated with contractile force.

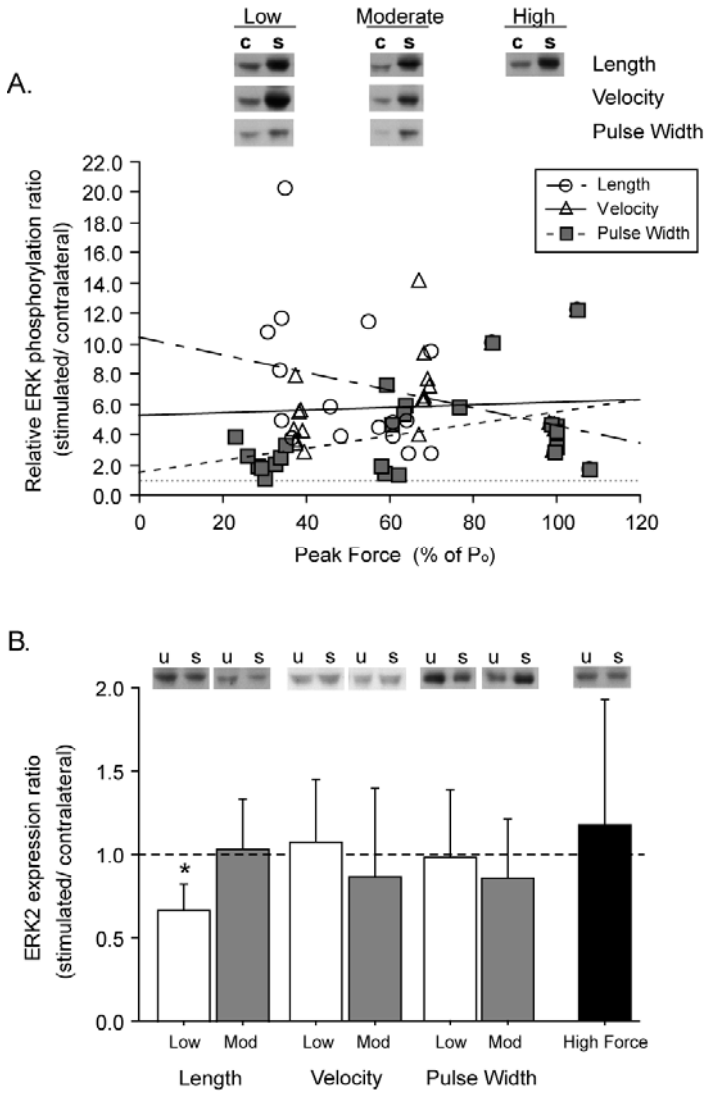

Figure 3.5 ERK MAPK Phosphorylation. A) Individual relative ERK phosphorylation ratios plotted against average peak force of respective muscle and identified by method. High force data was replicated and represented in all methods. Regression lines for phosphorylation ratio and average peak force modulated by length (circles, long dashed line; R^2=0.169), velocity (triangles, solid line; R^2=0.0004) and pulse width (squares, short dashed line; R^2=0.185) are shown. Two-way ANCOVA identifies an interaction effect (Method X APF, p=0.028), and a main effect of method (p=0.003) but no main effect of force (p=0.96) was found. Representative western blots for ERK phosphorylation of contralateral, unstimulated (u) and stimulated (s) muscles for each method and force level are shown above in which blots from each method are from a single gel. B) ERK2 expression ratio (stimulated/contralateral) is reduced by 33% when muscle is stimulated at short length (p=0.0015). Data presented as mean of group ± s.d. Horizontal dashed line indicates a ratio of 1.0 or no change in phosphorylation. (*) indicates significantly different than 1 by one-sample t-test on log-transformed data. Representative western blots for ERK2 expression shown above and labeled as in A.

Table 3.2 Common correlations. Orthogonal solutions of 3 factors identified by factor analysis of whole data set. Numbers in bold red indicate primary components of the given factor while numbers in red indicate weaker but correlated contributors to the factor

	Factor 1	Factor 2	Factor 3
Peak Force	-0.013	**0.941**	-0.039
L change	-0.015	0.551	0.084
p-ERK	0.342	0.261	0.094
p-p38	**0.858**	0.076	-0.048
p-JNK 46	**0.800**	-0.092	0.347
p-JNK 54	0.104	0.046	0.004
p-FAK	0.339	0.382	0.409
p-Akt	0.003	0.025	**0.791**
p-mTOR	0.551	-0.002	0.596
p70 $^{421/424}$	-0.126	-0.047	0.482
p70 ^{389}	0.201	-0.012	**0.856**
p-ACC	0.079	-0.089	0.098
Population Variance	20.6%	14.8%	23.5%

Discussion

The key finding of this study is that, although force production resulted in phosphorylation of ERK, JNK, and p70S6k$^{T421/S424}$, phosphorylation of these kinases was not dependent on the magnitude of sub-maximal force generation. Only ERK2 phosphorylation differed among the experimental groups, and these differences are independent of force.

Minimal changes in markers indicating metabolic costs

The non-fatiguing stimulation protocol used here successfully produced a range of repeatable forces with little metabolic stress. "Metabolic stress" is used in a very broad sense to represent cellular processes related to ATP consumption and resynthesis. ATP is required for contraction (cross-bridge cycling) and maintaining electrolyte balance (Na^+/K^+ and Ca^{2+} pump activity). The rate of oxygen consumption, even at 0ºC, may increase by six fold during contraction (Kushmerick and Paul, 1977), while Pi and ATP synthesis may remain elevated for thirty times as long as the contraction duration

(Challiss et al., 1989), so it is clear that maximal isometric activity imposes substantial and lasting energetic imbalance.

This project was designed to emphasize the direct effects of force production and minimize the confounding effects of indirect, secondary processes. This contrasts with many similar projects whose goal is to understand the integrative process by which strength training leads to muscle hypertrophy. Such integrative studies may employ stimulation protocols intended to mimic human exercise protocols (Nader and Esser, 2001), including relatively long stimulations with relatively short rest periods, sometimes divided into sets of repetitions. Protocols like this involve substantial metabolic load, as evidenced by the ~50-75% glycogen depletion reported by the Esser group. In two high duty cycle animals in which force was maintained through the long-duration stimulations, we did find a substantial increase in ACC phosphorylation, indicative of increased AMPK activity and metabolic stress, and glycogen depletion of 30%, both of which are substantially greater than in the low duty cycle stimulations.

Our stimulation protocol also differs from those interested in mechanical force as a signal that invoke eccentric activation to impose extremely high forces (Hentzen et al., 2006; Martineau and Gardiner, 2001; Wretman et al., 2001). Eccentric activations are uniquely associated with ultrastructural disruption, increased membrane permeability, and an inflammatory response (Friden and Lieber, 2001; McCully and Faulkner, 1985), which suggests eccentric activations may invoke a qualitatively different response, or an injury response separate from true mechanotransduction. For example, Martineau and Gardiner (2001) report that JNK phosphorylation is exponentially related to peak tension during concentric, isometric, and eccentric activations, because JNK phosphorylation after eccentric activation is nearly 80-fold higher than unstimulated muscle. Likewise, eccentric activation uniquely induces expression of myogenin and ankyrin-related proteins, even at the same force level (Hentzen et al., 2006). Although we did not directly assess tissue damage, our force modulation methods did not involve muscle

stretch or eccentric activations and we believe our muscles suffered minimal injury while inducing distinct mechanical force signals.

Minimal effects of force or stimulation on Akt-mTOR-p70 cascade

Independent of the force produced by the muscle or the method used, Akt phosphorylation decreased relative to contralateral muscle with no change in downstream mTOR or p70S6k^{T389} phosphorylation. The literature contains reports of either immediate increases (Nader and Esser, 2001; Sakamoto et al., 2002; Thomson et al., 2008) or decreases (Brozinick and Birnbaum, 1998; Deldicque et al., 2008; Widegren et al., 2001) in Akt phosphorylation. In the present study, a similar decrease in Akt^{S473} phosphorylation was seen in sham preparations, which suggests that some of the discrepancies may derive from differences in preparation and that activation of Akt is not an obligate response to high force contractions. The lack of response from Akt is in agreement with the hypothesis that load-induced muscle hypertrophy occurs via mTORC1 activation independent of the PI3K-Akt pathway (Goodman et al., 2010; Philp et al., 2011; Spangenburg et al., 2008).

Downstream of mTORC1, phosphorylation of p70S6k on T389 has been shown to follow several forms of mechanical stimulation, with some delay. Metabolically expensive HFES, particularly in combination with active lengthening, results in 2-5 fold increases in T389 phosphorylation within 3-6 hours (Burry et al., 2007; Nader and Esser, 2001), but stretch, even passive stretch, with nearly no force production nor metabolic stress, induces this phosphorylation as quickly as 30 minutes (Hornberger et al., 2005; Hornberger et al., 2004). The present 15 minute stimulation protocol may not be long enough to allow p70S6k^{T389} phosphorylation to develop, but the lack of a stretch component may also minimize this response. Burry and colleagues (2007) report no change in T389 phosphorylation following isometric activations, and Nader and Esser (2001) report HFES-increased p70S6k phosphorylation (not residue specific) only in the

eccentrically activated TA and not in the concentrically activated soleus. So, it appears that p70S6k, particularly on the T389 residue can be phosphorylated by stretch, even at low forces with little metabolic cost. This phosphorylation depends of the geometry of deformation, as we have seen that biaxial stretch of the same magnitude provokes T389 phosphorylation where uniaxial stretch does not (Hornberger et al., 2005). Based on the time course suggested by these studies (>30 min), T389 phosphorylation might not be expected in our 15 min protocol of LDC isometric activations, thus, whether force contributes to phosphorylation of downstream molecules, like T389, or not cannot be determined here. By contrast, the phosphorylation of p70S6k on T421/S424 did increase immediately in response to stimulation. These residues are not mTOR dependent nor related to muscle growth (Pearson et al., 1995; Thomson et al., 2008) but are required for subsequent T389 phosphorylation (Dufner and Thomas, 1999; Pullen and Thomas, 1997), suggesting that full activation of p70S6k requires integration of multiple signals.

Stimulation increases MAPK signaling

MAP kinases are not uniformly activated by force generation, and none of the MAPKs showed force dependence. The magnitude of phosphorylation reported here is consistent with similar isometric protocols, however reducing force to sub-maximal levels did not result in reduction of phosphorylation. Similar to Martineau and Gardiner we report little change in p38 phosphorylation following maximal isometric contractions, suggesting that activation of p38 is not an immediate or is a weak responder to force. Phosphorylation of JNK 54 is most dramatic following eccentric activations producing supramaximal forces and muscle damage (Boppart et al., 2001; Martineau and Gardiner, 2001; Russ and Lovering, 2006). In the present study, JNK 54 phosphorylation is comparable to that from isometric and concentric activations reported by Martineau and Gardiner, but in our hands, JNK 54 phosphorylation can be attributed to the surgical procedure and exposing the muscle. Eccentric activations produce significant damage to

muscle, and the dramatic phosphorylation of JNK54 after EC may reflect that injury more than the generated force. In cell culture, both cell damage and JNK phosphorylation are velocity dependent (Burkholder, 2003; Frey et al., 2009), suggesting that JNK phosphorylation may reflect cell damage or permeabilization more than force *per* se.

ERK signaling varies with stimulation intensity but is not force-dependent

In contrast to the other signaling molecules, phosphorylation of ERK did vary with stimulation conditions. The variation with force differed among the force modulation methods, and we conclude that ERK phosphorylation is not a force indicator. The ERK MAP kinase is of special interest because inhibition of ERK phosphorylation prevents both phosphorylation of p70S6k and hypertrophy following IGF-I infusion (Haddad and Adams, 2004). Overload-induced hypertrophy does not depend on IGF-I signaling (Spangenburg et al., 2008), but ERK may participate in both IGF-I dependent and IGF-I independent hypertrophy. Following 60 x 0.3 s maximal isometric activations, ERK phosphorylation was increased 5-fold relative to contralateral, similar to the 3-fold increase after 300 x 0.15 s trains (Martineau and Gardiner, 2001)and 2-fold changes after 60 x 3 s trains (Nader and Esser, 2001). This is also similar to the 4-fold increase reported after synergist ablation (Carlson et al., 2001) or IGF-I infusion (Haddad and Adams, 2004). However, we report 5.7-fold increase in ERK phosphorylation during concentric activations that produce 60% P_0, while Martineau and Gardiner report only 2-fold increase following concentric activations at 75% of P_0. The reason for this difference is not clear, although muscles in the present study were capable of producing the full tension throughout the stimulation protocol, where Martineau & Gardiner's muscles fatigued rapidly and produced less than 25% P_0 for the last 240 of 300 stimulations, so the true force to which their muscles respond is somewhat uncertain.

ERK phosphorylation appeared to vary with force, although in opposite directions, when modulated by stimulation pulse width and muscle length. By varying

stimulation pulse width, we alter the fraction of fibers recruited, and ERK phosphorylation might be expected, and was observed, to be proportional to force magnitude under pulse width modulation. Indeed, ERK phosphorylation in Low-P was indistinguishable from sham, and suggests that ERK phosphorylation may reflect fiber activation more than force production. Mechanisms dependent on depolarization immediately suggest calcium-dependent processes, and the Raf-ERK cascade can be activated by calcium-dependent processes like PKC (Kumar et al., 2002).

The negative correlation between ERK phosphorylation and force modulated by length is interesting because it results from the decrease in ERK2 content seen only in the Low-L group. That is, the IOD of phospho-ERK in Low-L is similar to the IOD of phospho-ERK in High, but because we report IOD-phospho/IOD-pan, ERK phosphorylation is elevated. No other group shows a decline in ERK2 content, and there were no changes in p70 or Akt content in any group. We did not expect total protein expression to change over the course of a 15-minute protocol, and validated this observation several ways to ensure there was no systematic technical variability in a single group. Samples were processed in random order so Low-L samples were not homogenized together, did not have protein contents assayed together, and were not run on the same gels. The order of samples on each gel was randomized, so Low-L ERK2 samples are not systematically subject to edge effects or other blot inhomogeneities, and the results reported represent averages from two independent blots. Therefore, we suspect maximal activation of muscle at such short length causes a rapid reduction in ERK2 content, although the mechanism for this is unclear.

Growth-related signaling independent of fiber activation

The homogeneity of phosphorylation across different stimulation intensities was unexpected. That is, looking only within the PW groups, it was expected that activation of more fibers would be associated with higher levels of phosphorylation, and this was

found only for ERK phosphorylation. For all other kinases, their phosphorylation and presumptive activation was apparently independent of whether the particular fiber was activated, which suggests that the signal most directly responsible for growth-related signaling during high force contractions is external to the fiber. It also suggests that this signal saturates at relatively low force or activation levels. We considered three possibly mechanisms: release of paracrine factors, deformation-dependent signaling, and environmental conditions. High force contractions are associated with release of autocrine or paracrine factors, such as IGF-I, bFGF and PGF2α, which may link force generation by one fiber to growth signaling in its neighbors (Clarke et al., 1993; McKoy et al., 1999; Trappe et al., 2001). It is possible that high sensitivity to released growth factors result in saturation of the response, even at 30% force level, and 70 Hz stimulation is much greater than physiological firing rates (Hennig and Lomo, 1985). Muscle deformation occurs in response to force production and similar deformations occur in all fibers. In the isometric muscle, this deformation is small and positively correlated with force, and in L and V groups it is much larger and negatively correlated with force. Insensitivity to deformation might explain the lack of effect of PW, but it should be manifest in L and V. Force generation by a muscle is associated with increased heat production, transiently reduced and persistently increased blood flow. Muscle is sensitive to temperature and small changes in temperature can drive changes in gene expression, morphology and function (Rome et al., 1985). The low duty cycle stimulation protocol used in the present study should minimize temperature changes, and temperature change would be expected to correlate with stimulation intensity.

Hypertrophic signaling may require more than high forces

Human high force training regimens are sometimes described as “strength” training, involving low volume, very high force contractions, or as “hypertrophic” training, involving high volume but moderate force contractions. The stimulation

protocol used in this study design is more closely related to the low volume-high force strength training hypertrophy protocols. The primary differences between these protocols are force level and rest period. Hulmi *et al.* report differential signaling with greater activation of a number of molecules in the hypertrophy protocol compared to strength protocol (Hulmi et al., 2010), however, the time point assayed was later than assayed here. In that study, metabolic changes and/or volume of load may be important cell signaling stimuli. The 60 activations used here would be expected to also result in some degree of muscle hypertrophy. Dow *et al.* found that 50 contractions per day (equivalent to ~2 contractions per hour) are sufficient to restore (~94% of control) the muscle mass lost due to denervation (Dow et al., 2004). Further, similar increases in protein synthesis (Kumar et al., 2009) and eventual hypertrophy after training (Campos et al., 2002) suggest that the stimuli/signals for muscle growth are more complex and that force itself, though required, is not exclusive (Hulmi et al., 2010; Wernbom et al., 2008).

Summary

Although three distinct force levels were produced by multiple methods, no force dependent signaling emerged in this study. Phosphorylation of ERK appears to be the only one of the growth-related kinases examined whose phosphorylation is dependent on fiber-activation. Fatiguing muscle activations increase the metabolic stresses and may contribute to the signals observed in other studies. Signaling molecules that respond to force likely do exist, however, the MAPK and Akt signaling cascades analyzed here appear too far downstream and have already integrated a number of other signals that obscure any strict dependence on force production.

Acknowledgments

This work was supported by the National Institute of Health (NIH) grant, DC05017.

CHAPTER IV

TEMPORAL CHARACTERISTICS OF HIGH FREQUENCY ELECTRICAL STIMULATION INFLUENCE PHOSPHORYLATION OF FAK, P38 AND MTOR IN MOUSE *TIBIALIS ANTERIOR*

Abstract

High force contractions (HFC) activate multiple cascades related to protein synthesis. Although some studies have suggested force-dependent activation of various growth-related kinases, we previously found no correlation between force magnitude and several members of these signaling cascades when metabolic stress was minimized. HFC impose both mechanical and metabolic stresses, and the present study aimed to alter metabolic stress produced by the muscle to test the hypothesis that MAP kinase signaling during isometric activation is influenced by the work-to-rest ratio (duty cycle, DC) and increased metabolic costs. Mouse *tibialis anterior* muscles were subjected to low duty cycle (LDC, 1.5%) or high DC (HDC, 15%) *in situ* isometric activations of either short (0.3s) or long duration (3s) to manipulate ATP turnover. The phosphorylation status of MAP kinases and Akt-mTOR-p70S6 kinase cascades were analyzed. Force-time integrals were ~5X greater in HDC than LDC and fatigue was evident in HDC groups. ACC phosphorylation, indicative of AMPK activity, was greater in HDC protocols indicating greater energetic stress. p38 phosphorylation was also greater in HDC than LDC, which could reflect either force or energy-depletion dependent signaling. Phosphorylation of ACC, FAK and mTOR increased dramatically only in HDC with long activations, demonstrating the importance of metabolic load on the immediate response to HFC. Combined with our previous observation of force-independent signaling, we

conclude that metabolic stress is a major contributor to high force-related signaling, and that DC is not sufficient to predict metabolic stress.

Introduction

Skeletal muscle readily adapts to demands imposed by performance requirements. Resistance exercise and high force contractions (HFC) are anabolic signals and result in hypertrophy through a complex process involving increased protein synthesis, activation of satellite cells, and changes in gene regulation (Adams et al., 2002; Bodine et al., 2001; Wong and Booth, 1990). The most prominent aspect of HFC is the high force and this force has been linked to activation of important growth related signaling cascades. Effectors of mTORC1 are activated in response to high force but not low force contractions and closely associated with changes in mass (Baar and Esser, 1999), and activation of MAPK signaling has been correlated to peak tension (Martineau and Gardiner, 2001). Unlike studies using eccentric activation to obtain high forces, we found no correlation between sub-maximal force and immediate signaling molecules . That study emphasized low duty cycle activations to minimize disturbances of energy metabolism, and had several points of difference with previous, high duty cycle experiments. Metabolic costs are inherent to force production so the inconsistency in signaling responses suggests that metabolic components of force production may contribute to growth-related signaling.

The complexity of HFC results in the combination of mechanical and metabolic stress-related signaling. For example, the HFC stimulation regimen used by Thomson et al (2008) increased AMPK activity, as measured by phosphorylation of downstream target, acetyl-co-carboxylase (ACC), concomitantly with increases in growth related signaling such as increased Akt, p70S6k, and 4EBP1. A decrease in eEF2 phosphorylation, often attributed to AMPK-mediated processes, was not observed until 20 minutes later, coinciding with AMPK activity returning to baseline. The limited

studies on blood flow restriction suggest that metabolite accumulation may enhance growth related signaling similar to that seen in HFC (Fry et al., 2010; Fujita et al., 2007). However, these studies do not specifically compare HFC to LFC with blood flow restriction. Human resistance training suggests high load with metabolic stress is important for hypertrophic response (Hulmi et al., 2010). It is not clear whether or how metabolic stress contributes to high force contraction signaling.

AMP-activated kinase (AMPK) integrates signals that perturb the energy balance of the cell and limit or inhibit ATP synthesis (e.g. low glycogen, hypoxia). AMPK is allosterically regulated by AMP concentrations and when activated inhibits energy-consuming tasks like protein synthesis. Many studies support the role of AMPK activity in the inhibition growth-related signal and protein synthesis (Lantier et al., 2010; Mounier et al., 2011; Thomson et al., 2008). For example, increased AMPK phosphorylation status with age is associated with reduced response to compensatory overload (Gordon et al., 2008; Thomson and Gordon, 2005). Artificial activation of AMPK by the AMP mimetic AICAR diminishes contraction-induced increases in mTORC1 signaling (Thomson et al., 2008). Reduced glycogen levels, which increase AMPK activity, prevent contraction induced Akt signaling (Creer et al., 2005). The effect of AMPK activity on MAP kinases is less clear although both are immediately activated in response to HFC and AICAR treatment (Williamson et al., 2006). Mild ischemia increases reactive oxygen species (ROS) and AMPK but also activates MAP kinases, presumably in response to different aspects of ischemia. So, AMPK activity is associated with processes that generally reduce or prevent muscle protein synthesis, but exercise interventions that promote muscle protein synthesis also activate AMPK. This raises the question whether AMPK activity during force production contributes to or antagonizes growth related signaling.

This study was designed to analyze phosphorylation state of kinases activated by HFC under various stimulation parameters to test the hypothesis that metabolic stress

contributes to growth-related MAP kinase signaling. Maximal isometric activations of either short duration or long duration stimulations were compared under high duty cycle, fatiguing and low duty cycle, non-fatiguing stimulation protocols. Thus, this design induces metabolic stress in two ways, both of which are expected to be related to ATP consumption and resynthesis and accumulation of metabolic byproducts. The results reveal an unexpected decoupling between markers of metabolic load and contraction-induced force decline. Signaling through MAPK and mTORC1 cascades was more closely correlated with markers of metabolic load than with force decline, which indicates the muscle stimulation pattern strongly influences the intracellular response to force production (HFC).

Material and Methods

Animals

Male CFW Swiss-Webster mice (Crl:CFW (SW), Charles River, 26.2 g ± 2.0; n=8 per group) were housed in pairs on a 12/12 light cycle with food and water *ad libitum***.** Procedures were reviewed and approved by Institutional Animal Care and Use Committee at Georgia Institute of Technology and performed in compliance with the Guide for Care and Use of Laboratory Animals.

Electrical Stimulation

A total of 32 animals were randomly assigned to one of 4 experimental groups determined by duty cycle (low, LDC, or high, HDC) and stimulation duration (0.3 s, short, or 3 s, long). Animals were anesthetized by intraperitoneal injection of a ketamine cocktail (90 mg/kg ketamine, 1 mg/kg acepromazine and 10 mg/kg xylazine). The *tibialis anterior* (TA) muscle was surgically exposed, the distal tendon released and tied to the arm of a force-measuring servo motor (Aurora Scientific), and the knee immobilized in a spring clamp. The peroneal nerve was isolated and mounted on hook

electrodes. A series of twitch activations was used to determine the current (I_0) and muscle length (L_0) producing maximal twitch force (P_t). Muscles were then subjected to a series of maximal isometric activations at 70 Hz at 2x I_0 over 20 minutes using one of four stimulation regimens described below. Throughout the stimulation protocol, muscles were wetted with 1X PBS (136.7 mM NaCl, 2.7 mM KCl, 1.4 mM KH_2PO_4, 4.3 mM Na_2HPO_4) or mineral oil to prevent desiccation. Immediately following electrical stimulation, animals were sacrificed by cervical dislocation, muscles dissected and immediately frozen in melting isopentane.

In order to test the contribution of metabolic stress to high force contraction signaling, duty cycle (DC) and stimulation duration (StimDur) were chosen as the controlled variables. Therefore the number of activations per groups differs. Low duty cycle (1.5% work: rest) short, 0.3 s stimulations (LDC-short) requires 60 activations whereas LDC long, 3s stimulations (LDC-long) requires only 6 activations over the 20 min. High duty cycle (15% work: rest) 0.3 s stimulations (HDC-short) results in 600 activations whereas HDC 3 s stimulations (HDC-long) results in 60 activations. HDC activations were performed as 10 sets of 6 or 60 activations with 1 min rest between each set.

Force Data

Muscle force during stimulation was digitized at 1000 Hz in 500 ms or 3500 ms windows surrounding each 300 ms or 3000 ms stimulation, respectively. The resting, passive tension was subtracted from each trace, and tension records were normalized to the peak tension achieved during the first activation. Force-time-integral (FTI) was determined by integrating force generated during all activations. Sag is a measure of the force loss during a single activation and was defined as the difference between force at the end of the activation and the peak force achieved during that activation, normalized to the peak tension during that activation, and was averaged across all activations. Fatigue

(F) is a measure of loss of force between activations. Because force frequently increased during the first few contractions, F was defined as the peak force produced during the final activation divided by the peak force produced during the entire protocol. Fatigue Sum, FS, combines both aspects of force loss by estimating the total force that should be produced by a muscle based on its P_0 and stimulation time (i.e. 18 s in LDC or 180 s in HDC) and calculates the difference in percent from the total force actually produced. That is, (FTI-TF) / TF*100 where total force, TF= P_0 * 18 or 180. Specific tension was determined according to the formula,

$$T_0 = P_0 \frac{\rho L_f}{m \cos(\theta)}$$

where m is muscle mass, and ρ is muscle density, 1.06 g/cm^2 (Mendez and Keys, 1960). Values used for pennation angle (θ=11.7º) and fiber length (L_f=7.9 mm) were taken from the literature (Burkholder et al., 1994).

Inclusion criteria. The force decline during long stimulation duration varied greatly among animals. Post-hoc analysis of the forces produced suggested two populations of responses. In one group force was maintained above 50% throughout the long-duration stimulations while in the other group force was fell by more than 74% during the 3s stimulation. This later group failed to maintain force even for the initial 300ms of the activation thus do not consider them credible for analysis. Based on this evaluation, we applied an inclusion criteria to muscles of all groups which required that force decline, or sag, across all activations average no more than 15% within the first 300ms and no more than 50% by the end of the 3s activations.

Table 4.1 Stimulation parameter and force measures for low and high duty cycle protocols. Data presented as mean ± s.d.

Duty Cycle	Low, 1.5%		High, 15%	
Stimulation Duration	0.3 s	3 s	0.3 s	3 s
Rest, s	20.3	240	0.85	10
Contraction Number	60	6	600	60
FTI, N*s	24.2±3	16.8±5	97.9±16	141.2±21
Specific Force, N/cm3	5.53±0.8	5.84±0.8	6.24±1.5	5.8±0.4
Number of animals	4	3	5	2
Group	LDC-short	LDC-long	HDC-short	HDC-long

Western Blotting

Muscles were homogenized using a rotor-stator (TissueMizer, Fisher Scientific) in a low salt detergent buffer (50 mM Tris, pH 7.5; 30 mM NaCl; 5 mM EDTA, 1% Triton X-100 plus NaF, NaVO3 and protease inhibitors) to minimize myofilament extraction and cleared of debris at 15,000 × g. The protein concentration of the supernatant was measured by BCA assay (Pierce) according to manufacturer's protocol. Soluble protein (15 ug) was separated by SDS-PAGE, transferred to nitrocellulose membranes, and detected by Western blot. Primary antibody dilutions were: p-ERK$^{T202/T204}$ 1:3000; total ERK2 1:2500; p-JNK 1:500; p-p38$^{T180/Y182}$ 1:2000; p-Akt ^{S473} 1:2000; total Akt 1:2000; p-P70S6k $^{T421/S424}$ 1:2000; p-p70S6k ^{T389} 1:2500; pan p70 1:2000; p-ACC 1:1000; p-mTORC1 ^{S2448} 1:2000; p-FAK^{Y397} 1:2000 . All antibodies are purchased from Cell Signaling except JNK (Santa Cruz), FAK (Invitrogen) and total ERK2 (BD). Bands were visualized by enhanced chemiluminescence and quantified by scanning densitometry. Results are expressed as a ratio of the stimulated to the un-stimulated contralateral muscle, which was always loaded in an adjacent lane of the same gel. ERK2, p-JNK, p-p38, Akt, p70S6k, p-mTOR, and p-FAK are expressed as (IOD_{stim}/IOD_{unstim}) where IOD is the integrated optical density of the band, and stim/unstim refers to the stimulated and contralateral muscles, respectively. p-ERK, p-

Akt and p-p70S6k are expressed as (IOD_{stim}/IOD_{unstim})/ ($IOD_{stim-pan}/IOD_{unstim-pan}$), where pan refers to the corresponding non-phosphorylated, or total antigen. ACC phosphorylation was quantified by normalizing all of the bands on a gel to the average of the contralateral IOD from all animals on that gel. Each blot included a common positive control from insulin stimulated or eccentrically activated TA muscle for validation.

Glycogen Content

The distal portion (~20 mg) of the TA was weighed, digested in 30% KOH saturated with Na_2SO_4 for 20 min at 100°C and glycogen precipitated with 1.2 volumes of 95% EtOH for 30 min on ice as described by Lo (Lo et al., 1970). Glycogen was pelleted at 850 x g for 30 min then dissolved in deionized H_2O. Content was determined spectrophotometrically using 5% phenol followed by rapid addition of 96% H_2SO_4 and read at 490 nm.

Statistics

All values are expressed as means ± s.d. and statistical analyses were performed on StatView (Abacus Software). Glycogen content was analyzed by three-way, mixed mode, repeated measures ANOVA, with stimulated/contralateral as a repeated measure and DC/StimDur as factors. Western blot ratios (stimulated:contralateral) were log transformed for statistical analysis although untransformed results are presented in tables and graphs. Phosphorylation ratios were analyzed by two-way ANOVA (StimDur X DC) with a significance threshold of $p < 0.05$, followed by post hoc t-tests using the Bonferroni/Dunn correction for multiple comparisons.

Because of the breadth of data obtained from each sample, factor analysis was used to extract principal components and identify potential common causes. Kinase ratios, FTI, Glycogen ratio, FS and F were included in this analysis with the anticipation that common causes within a group of kinases might allow resolution of more subtle

mechanical effects than individual kinases. Factor scores were Varimax transformed and method-dependent differences in the orthogonal solutions were determined by 1-way ANOVA with a significance threshold of $p < 0.05$. Regression analysis was performed on components of the identified factors.

Results

Force stimulus

Maintenance of force during the stimulation regimen was substantially different among protocols (Figure 4.1). Peak force (PF) produced by the first contraction was similar in all groups, averaging 1.03N ± 0.1. Force often increased during the first few contractions (e.g. Fig 4.1A) and the maximum force produced during the protocol. P_0, for all animals averaged 1.2 N ± 0.2. However, the pattern of force decline with repeated stimulation was unique to each protocol. Force-time integral (FTI) was expected to be greater in the HDC groups, but two way ANOVA revealed a significant interaction effect ($p=0.005$), in which the long stimulation duration caused greater force decline during the low duty cycle program (LDC-long: 16.8 ± 5 N*s) than short stimulation (LDC-short: 24.2 ± 3 N*s), but was force-sparing at high duty cycle, , (HDC-long: 141.2 ± 21 N*s, HDC-short: 97.9 ± 16 N*s; Table 4.1, Figure 4.2A). The dramatic failure to maintain force between successive activations in the HDC-short group, was anticipated to reflect the greater metabolic load associated with duration of activations for the same total contraction time (Bergstrom and Hultman, 1988; Hogan et al., 1998).

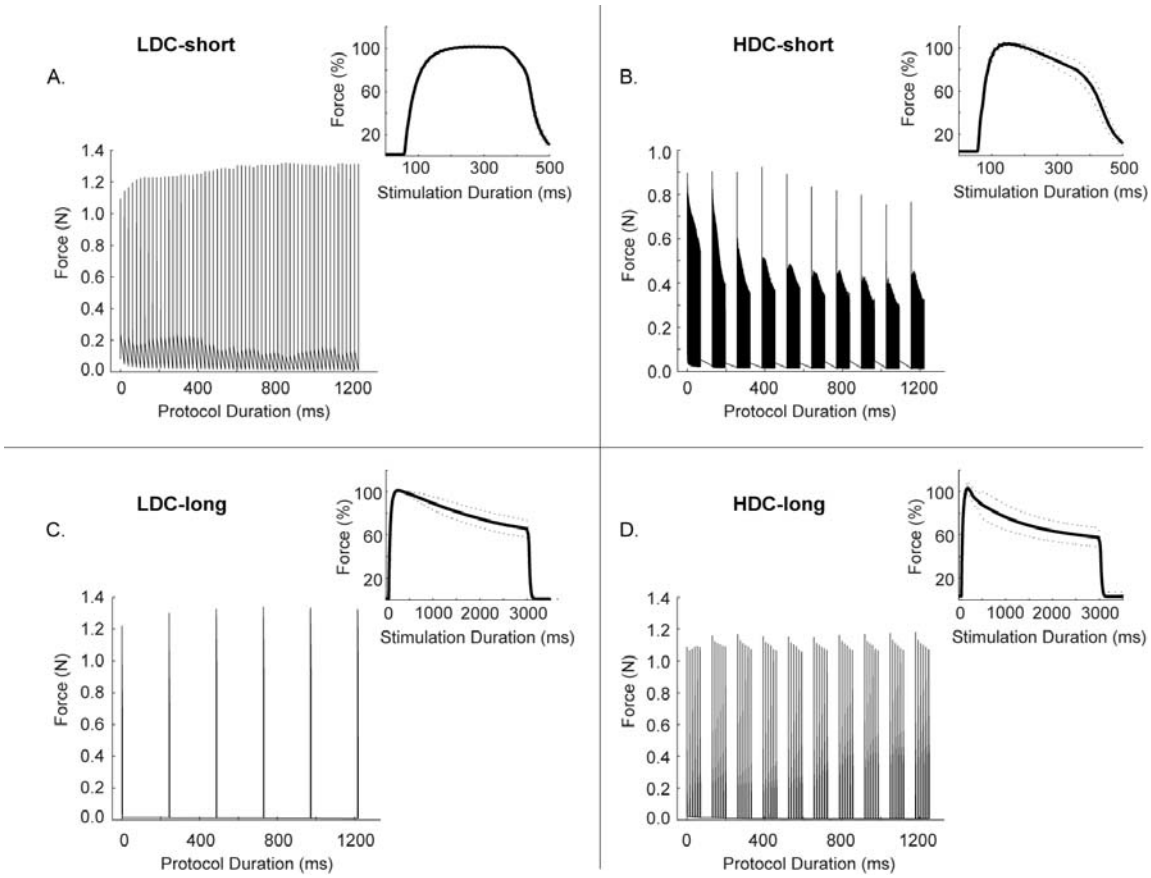

Figure 4.1 Stimulation protocol and Force Traces. Representative duty cycle protocols where each 300 ms (A,B) or 3 s (C, D) activation has been plotted sequentially separated by corresponding rest duration (see Table 4.1) for a single animal to show loss of force with repeated stimulation. Insets: Representative forces traces produced by stimulation protocol. Force of each activation was normalized to the maximum force produced by that muscle then averaged across all 6-60 or 600 activations. Dashed lines represent ± s.d. A) LDC-short, B) HDC-short, C) LDC-long and D) HDC-long.

In order to assess the ability to maintain force throughout the contraction, the decline in force by the end of stimulation, sag, was determined (see Methods). The LDC-short group showed sag of only 5.4% ± 2.7 in the first activation or when averaged across all activations. In the HDC-short group, sag in the first activation averaged 10 ± 8% however across all 600 activations sag increased to 31 ± 22%. The decline in force during long contractions was much greater. Sag, after 3s stimulation, was 40 ± 13% in both the LDC and HDC groups.

The decline in peak force between successive activations was also highly dependent on stimulation protocol. The LDC stimulation regimen was able to maintain

PF from contraction to contraction, and frequently demonstrated potentiation during the protocol. The HDC stimulations resulted in substantial loss of force between contractions within one set, an average of 16% decline in PF per set in the long activations and a 58% decline in PF with short activations, with some recovery during the one-minute rest between sets. The pattern of rapid force decline within a set was most striking in the HDC-short group, in which the inter-set rest was only able to restore force production for a single activation, all subsequent activations being at substantially reduced and similar forces. This effect can be seen, but is greatly muted in the intuitively more stressful long activations. Fatigue (F) was calculated by dividing the peak force generated by the final activation by the overall peak force generated. Two-way ANOVA revealed main effects for DC ($p<0.0001$) and StimDur ($p=0.019$, Figure 4.2B) and an interaction effect for Fatigue (DC X StimDur $p= 0.019$) suggesting a dependence on stimulation pattern.

To assess the net effect of both forms of force decline, we calculated a maximum force-time potential by multiplying peak force by the total stimulation time (TF, see Methods). Fatigue sum (FS) was then calculated by subtracting the calculated TF from the actual FTI, then dividing by the calculated TF. The decline in force within the long stimulations is more evident with this measure, as seen in LDC-long where TF over the course of the protocol was not achieved and in the reduced difference between HDC-short and HDC-long. Two-way ANOVA revealed an interaction effect for FS (DC X StimDur $p= 0.010$), resulting from the maintenance of force in LDC-short, but the dramatic force loss in the HDC-short group, which was only able to generate 53% of its theoretical FTI. A main effect was found for DC ($p=0.0005$) but, in contrast to the F measure, not for StimDur ($p=0.11$, Figure 4.2C).

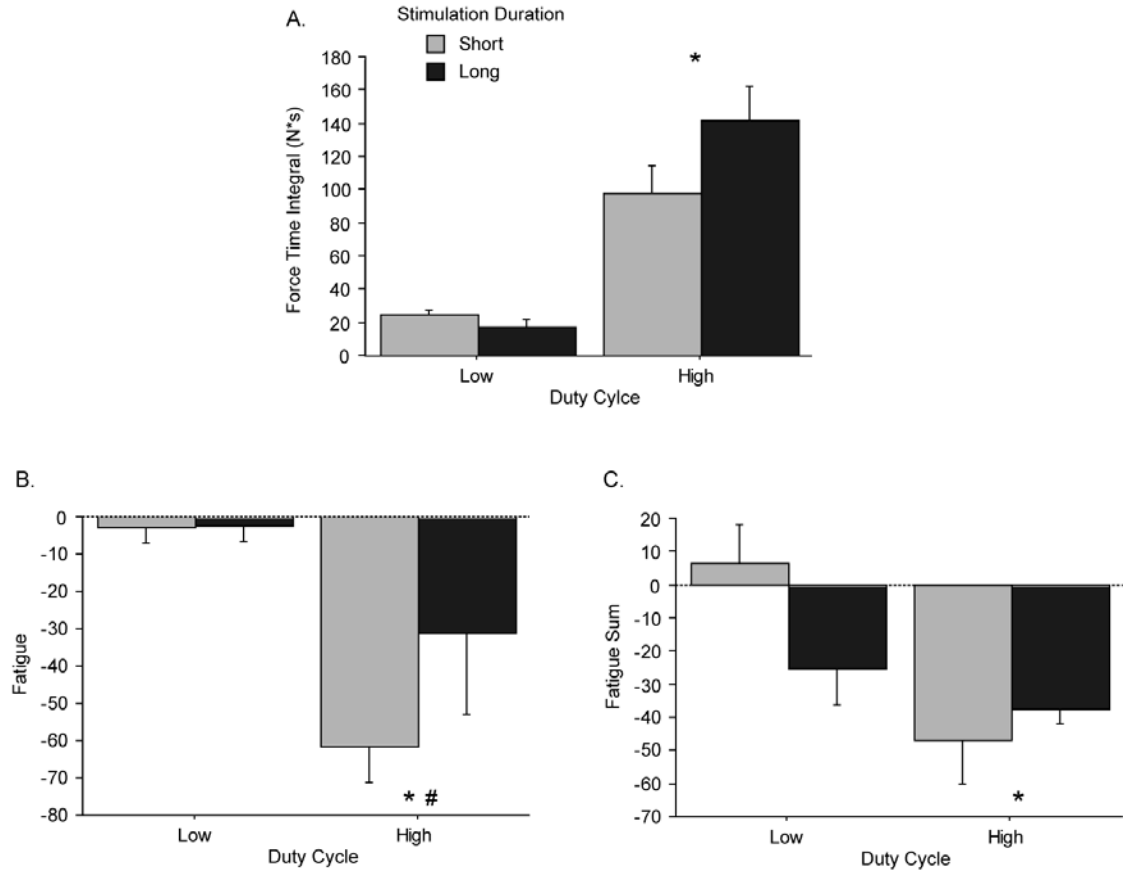

Figure 4.2 Functional Measures of Metabolic Stress. A) Force-time integral (FTI), B) Fatigue (F), C) Fatigue Sum (FS) of short duration (gray) and long duration (black) activations by DC. Data presented as mean ± s.d. * indicates significant main effect of DC and # indicates a main effect of StimDur on log transformed data.

Markers of metabolic stress

Glycogen content and acetyl-coA-carboxylase (ACC) phosphorylation were used to assess metabolic and energy stress associated with the different protocols. ACC is a primary physiological target of AMPK and its phosphorylation was used as an index of *in vivo* AMPK activity. ACC phosphorylation was significantly increased by stimulation relative to the contralateral control in all groups ($p<0.0001$). Two-way ANOVA showed a significant interaction effect ($p=0.023$) between duty cycle (DC) and stimulation duration (StimDur), due to extremely high phosphorylation in the HDC-long group (Figure 4.3A). This also drove a main effect of duty cycle (DC, $p=0.0008$) and stimulation duration (StimDur, $p=0.023$). Glycogen content in the HDC-long stimulated

muscles averaged 30% less than that of contralateral control muscles, although this could not be distinguished from the -12% decline in HDC-short group. Glycogen depletion in the LDC groups was less than 3% (Figure 4.3B). Three-way mixed mode, repeated measures ANOVA found a main effect of DC (p=0.037) but not StimDur (p=0.37) or an interaction effect (DC X StimDur p=0.22). In contrast to the fatigue measures, these data indicate that the HDC-long stimulation is the most energetically demanding regimen. Metabolic stress signaling was similar across the other three conditions, HDC-short being only slightly and not resolvably elevated from the LDC groups.

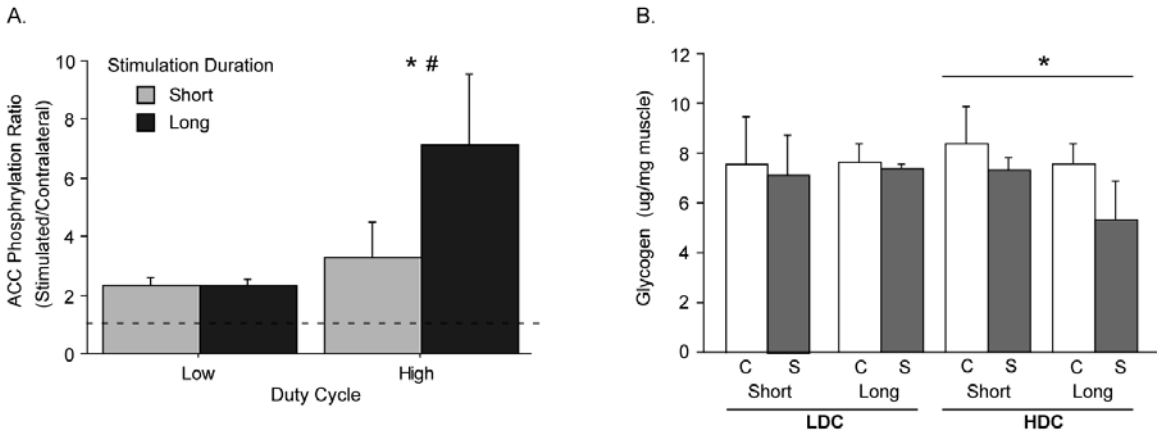

Figure 4.3 Biochemical Measures of Metabolic Stress. A) ACC phosphorylation was expressed as a ratio of the stimulated to contralateral muscle for short duration (gray) and long duration (black) activations by DC. Horizontal dotted line indicates a ratio of 1.0. B) Glycogen content of contralateral (c, white) and stimulated (s, gray) muscles. Data presented as mean ± s.d. * indicates significant main effect of DC and # indicates a main effect of StimDur on log transformed data.

Focal adhesion kinase and MAP kinase phosphorylation

Phosphorylation of FAK, ERK2, and p38 showed a similar pattern as ACC phosphorylation, while JNK54 was reversed. Autophosphorylation of FAK on T397 was increased specifically in the HDC-long group (DC X StimDur p=0.015). This drove a main effect for DC (p=0.011) and trend for a main effect of StimDur (p=0.091, Figure 4.4A). Phosphorylation of ERK, p38 and p54 JNK was increased relative to contralateral in all groups, while p46 JNK was unchanged (Figure 4.4B, C, and D). Within the MAPK cluster, there were no systematic effects of stimulation protocol, with the exception that

two-way ANOVA revealed a significant effect of DC on p38 phosphorylation (p=0.0006, Figure 4.4C). Regression analysis shows a positive correlation between p38 phosphorylation and FTI (R=0.770, R^2=0.593, p=0.001) but only a moderate correlation with fatigue (R=0.476, p=0.09). In contrast, p54 JNK phosphorylation was more strongly correlated with F (R=0.581, R^2=0.338, p=0.03) than with FTI (R=0.408).

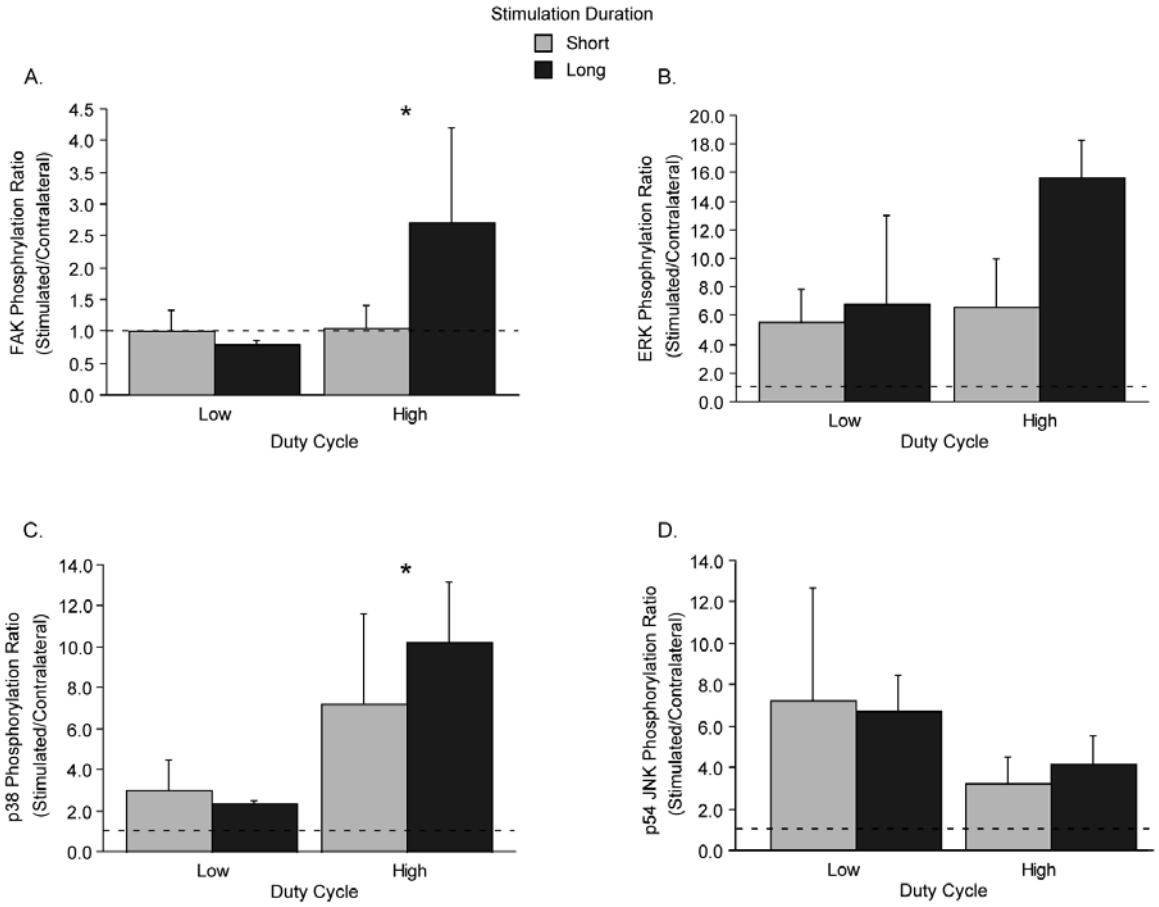

Figure 4.4 Phosphorylation of FAK and MAP kinases. Phosphorylations are expressed as a ratio of the stimulated to contralateral muscle for short duration (gray) and long duration (black) activations by DC. A) Phosphorylation of FAK was greater in HDC-long indicated by a significant interaction effect DC X StimDur, p=0.015). B) ERK phosphorylation was increased in all groups but no main effects were found (DC, p=0.08; StimDur, p=0.16). C) p38 phosphorylation was greater in HDC protocols compared to LDC protocols (DC, p=0.006). D) p54 JNK phosphorylation was increased in all groups but no main effects were found (DC, p=0.11; StimDur, p=0.49). Horizontal dotted line indicates a ratio of 1.0. Data presented as mean ± s.d. * indicates significant main effect of DC on log transformed data.

Signaling through Akt-mTOR-p70S6k cascade

Phosphorylation through the mTOR cascade correlated with ACC phosphorylation but not with fatigue. Phosphorylation of mTOR increased with both duty cycle and stimulus duration, and was noticeably greater in HDC-long. Two-way ANOVA found main effects of DC ($p=0.001$) and StimDur ($p=0.014$), however the interaction effect was not statistically resolvable (DC X StimDur $p=0.39$). The increase in p70S6k T389 in HDC-long is strongly influenced by an extreme data point and low n for the group. Phosphorylation of mTOR and its downstream target p70S6k T389 were unchanged by LDC stimulations, but phosphorylation of p70S6k T421/S424, within the autoinhibitory domain, increased with both duty cycle and stimulation duration. Two-way ANOVA reveals a main effect of DC ($p=0.026$) and StimDur ($p=0.023$), but these appear to be independent, as there was no interaction effect ($p=0.31$). These responses appear not to require Akt phosphorylation, which was reduced in all groups by greater than 17% relative to contralateral controls with the greatest decline in LDC-long (62%). Two-way ANOVA could not resolve a main effect of DC ($p=0.22$) or StimDur ($p=0.91$) however a trend for an interaction effect is present (DC X StimDur $p=0.15$), due to the exaggerated decline in LDC-long and muted decline in HDC-long.

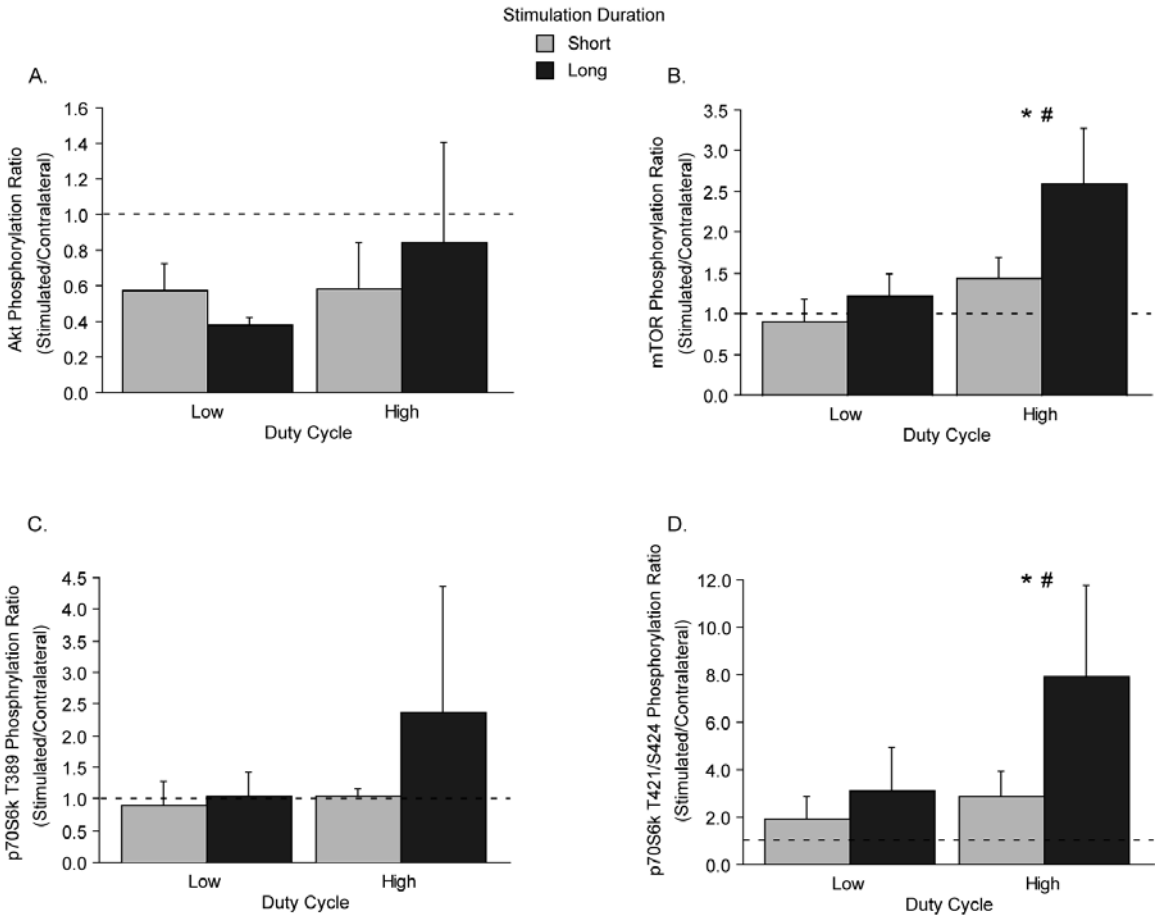

Figure 4.5 Phosphorylation of Akt, mTOR and p70S6k. Phosphorylations are expressed as a ratio of the stimulated to contralateral muscle for short duration (gray) and long duration (black) activations by DC. A) Akt phosphorylation. B) mTOR phosphorylation. C) p70S6k T389 phosphorylation . D) p70S6k T421/S424 phosphorylation. Horizontal dotted line indicates a ratio of 1.0. Data presented as mean ± s.d. * indicates significant main effect of DC and # indicates a main effect of StimDur on log transformed data.

Coordinated signaling

Factor analysis was performed to identify statistically correlated sets of variables from within this large data set and includes all of the kinases presented as well as FTI, F, FS, and glycogen content as a ratio of stimulated/contralateral. The first 2 factors account for greater than 89% of the population variance. Factor 1, 63% of the variance, included the force and fatigue measures with nearly all the signaling molecules: ACC (0.833), mTOR (0.857), pFAK (0.801), p38 (0.819) and p70S6k$^{T421/S424}$ (0.760)

phosphorylation along with FTI (0.929) and glycogen content ratio (-0.686) with minor contribution from pAkt (0.564), p70S6k^{T389} (0.631), ERK (0.541) and F (-0.488), FS (-0.510). Factor 1 represents an activity-dose measure, increasing with FTI (duty cycle) and being reduced by glycogen depletion and factors contributing to ACC phosphorylation. The combination of signaling molecules corroborates the observation that most signaling molecules are highly phosphorylated in the HDC-long group and minimally altered in the LDC groups. Factor 2, 27% of the population variance, contains p54 JNK (0.821) phosphorylation along with F (0.749) and FS (0.710) with weaker contribution also from pAkt, pFAK and p70S6k^{T389} (<0.614). The two factors appear to define two signaling modules: one including ACC, mTOR, FAK, p38, and p70S6k and closely correlated with activity; and one including p54 JNK negatively coupled with force loss during a contraction. Within factor 1, one imagines that glycogen depletion, ACC phosphorylation and fatigue measures are linked through ATP depletion and processes intended to restore ATP. FAK, mTOR, p38, and p70S6k are more often associated with force dependent signaling, but the contribution of energy depletion, particularly in the differences between HDC-short and HDC-long, reveals at least a contribution of force dynamics (Frey et al., 2009), if not a direct contribution from ATP homeostasis. The correlation between JNK and measures of fatigue (F, FS) suggests activation of JNK is reduced by processes evoked at exhaustion.

A.

	Factor 1	Factor 2
Fatigue, F	-.488	**.749**
Fatigue Sum, FS	-.510	**.710**
p-ERK	.541	.012
p70 T421/S424	**.760**	.186
p70 T389	.631	.427
p-Akt	.564	.614
p-P38	**.819**	-.052
p54 JNK	-.115	**.821**
p-ACC	**.833**	-.099
p-mTOR	**.857**	-.012
p-FAK	**.801**	.480
FTI, N*s	**.929**	-.258
Glycogen ratio	-.686	-.071

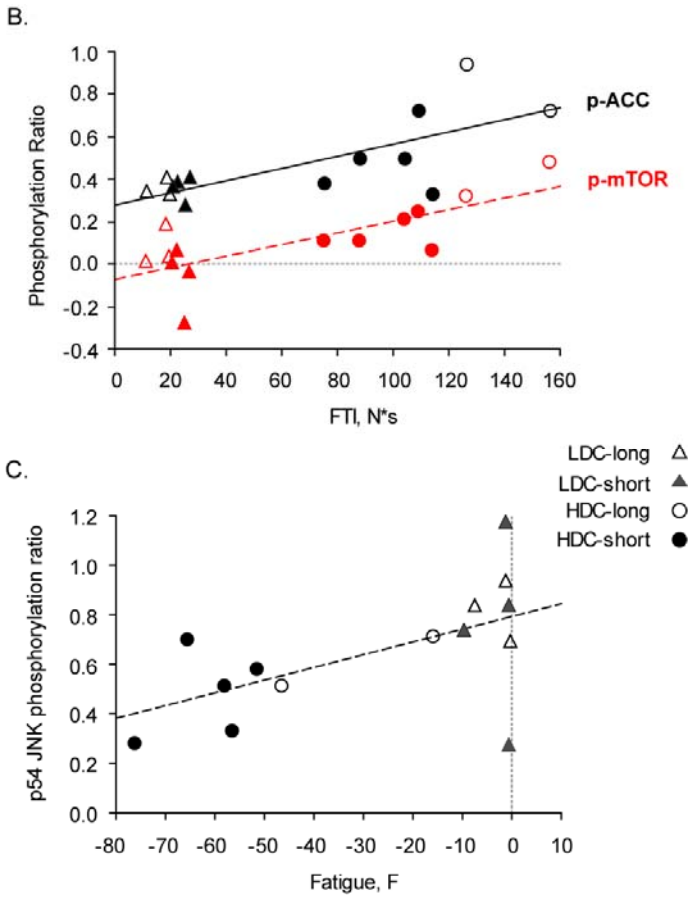

Figure 4.6 Correlated signaling. A) Orthogonal solutions of 2 factors identified by factor analysis of the whole data set. Numbers in bold indicate primary components of the given factor. B) Regression line for correlated components from factor 1. Phosphorylation of ACC and mTOR each correlated with FTI (R^2=0.551, p=0.002 and R^2=0.575, p=0.002, respectively). ACC and mTOR phosphorylation also strongly correlated, R^2=0.632, p=0.0007. C) Regression line for correlated components of factor 2. Phosphorylation of p54 JNK correlated with the measure, Fatigue. R^2= 0.338, p=0.03.

Discussion

High force contractions were produced under conditions that produced a variety of metabolic loads, as evaluated by glycogen depletion and AMPK activity. Interestingly, these measures were not were not altered in both HDC groups. The key finding in this study is that most signaling correlated closely with biochemical measures of metabolic costs, and were increased by long activations performed with relatively short rest. Specifically, FAK, p38 MAPK, p70S6k$^{T421/S424}$ and mTOR phosphorylation

appeared concomitantly with increased ACC phosphorylation and decreased glycogen content.

Metabolic stress and force

The stimulation protocols employed here were aimed at varying the metabolic costs associated with repetitive activations. "Metabolic stress" refers to the acute depletion of ATP and increased glycolytic and mitochondrial flux required to restore ATP. These complex processes are grossly indicated by AMPK activity and glycogen depletion. In this general sense, it was expected that higher duty cycle would increase metabolic stress by driving ATP to a low concentration without a sufficient rest period for resynthesis, and that short duration contractions would increase metabolic stress by driving greater consumption of ATP. Muscles in the HDC protocols received the same total number of pulses (i.e. 70Hz for 180s, or 12600 pulses), ten-fold greater than the LDC protocol (i.e. 70Hz for 18s, 1260 pulses), grouped in trains of either 21 or 210.

The HDC-long used in this study is similar to the protocol used by many HFES studies (Nader and Esser, 2001; Parkington et al., 2003; Thomson et al., 2008; Wong and Booth, 1990; Wong and FW, 1990). Glycogen depletion reported in the rats used in previous work has ranged from 60-70% (Nader and Esser, 2001; Russ, 2008), is substantially greater than the 30% reported in the mice of the present study. AMPK phosphorylation is reportedly unchanged (Atherton et al., 2005; Thomson et al., 2008), however, similar to the present study, ACC phosphorylation, which is more reflective of AMPK activity is increased (Thomson et al., 2008). Taken together, the altered markers of metabolic costs resulting from the HDC-long group here is consistent with that seen in the existing literature. Short duration activations have been reported to be more metabolically strenuous than long duration, with greater levels and release of lactate (Hogan et al., 1998). By contrast, the present study finds lower glycogen depletion and less indication of AMPK activity during short activations.

Measures of metabolic stress did not correlate well with measures of contraction-induced force decline, particularly within the high duty cycle protocols. Muscle contraction increases the rate at which ATP is hydrolyzed, resulting in increased AMP and metabolic byproducts, but also blocks blood flow. ATP can be regenerated through the phosphocreatine (PCr) system, glycolysis, and mitochondrial respiration. These systems are believed to form a hierarchy of speed and capacity, with the PCr system being capable of regenerating a small amount of ATP very rapidly, but that is depleted within approximately 10s, while glycolysis generates a moderate amount of ATP sustainable for only a few minutes and mitochondrial respiration being capable of greatest regeneration, but turns on much more slowly.

Within the LDC protocols, it was expected that temporary metabolic imbalances induced by stimulation would have ample rest for recovery processes to replenish ATP levels and minimize activation of AMPK. During LDC-short, force is maintained through each individual contraction and through the complete series. This suggests that ATP and PCr stores are sufficient for 300ms activations, and that the 20s rest, 67x the contraction duration, between activations is sufficient to restore high energy phosphate balance. Force does decline during the 3s activations of LDC-long, likely due to depletion of PCr stores. To match the 1.5% DC used with short contractions, long duration contractions were separated by 240s (4 min), which is sufficient time to restore PCr levels (Challiss et al., 1989). Force decline in the LDC groups was minimal, correlating with expectations of metabolite depletion, but neither measure of metabolic stress indicated any significant change.

Within the HDC protocols, it was expected that greater metabolic imbalances induced by stimulation would exceed the capacity of recovery processes to replenish ATP, require activation of AMPK, and result in loss of force generating capacity. For long duration activations, increasing DC to 15% reduces the rest period from 240s to 10s, or just 3.3x the stimulation duration, and the effect on metabolic stress markers is

dramatic. The decline in peak force with consecutive activations is also evident (average of -16%), suggesting that substrate depletion may be responsible for the force decline. For short duration activations, increasing DC to 15% reduces the rest period from 20s to 1s, but markers of metabolic stress are only slightly elevated from the LDC and unstimulated muscles. However, force decline is greatest in this group, and appears unrelated to the metabolic stress markers. This protocol was expected to produce the greatest metabolic stress so there seems to be a disconnect between functional and metabolic markers of metabolic stress. With total contraction time equal in HDC groups, short duration activations are energetically more costly (Bergstrom and Hultman, 1988; Hogan et al., 1998). As ATP demand increases, oxygen consumption and glycolytic rates are elevated and this would be anticipated to increase AMP level, thus AMPK. Both authors report short duration activations produce substantially greater concentrations of lactate and increased acidosis. However, the contribution of these byproduct in fatigue is under debate (Lamb et al., 2006). The accumulation of glycolytic byproducts may slow the forward rate of ATP generation by glycolysis, reducing apparent metabolic demands. Although near-peak force is generated the first contraction of each set, the decline in force during the second activation becomes more pronounced with each set, suggesting progressive depletion of a required substrate or accumulation of an inhibitory substance. Minimal glycogen depletion and ACC phosphorylation in this group suggest that the force decline is not related to metabolic imbalance, but may have the effect of reducing ATP consumption. p54 JNK phosphorylation is the only molecule assayed with a close correlation to fatigue and in which phosphorylations from HDC-short are different from those of the other groups (Figure 4.6C) further suggesting that the decline in force may be more related to reducing ATP demand. This illustrates the difficulty in experimentally distinguishing metabolic and mechanical components of HFES, because measures of both metabolic load and force in the HDC-short group are smaller than in the HDC-long

group, despite identical stimulation times. In this case, that correlation appears to result from a non-metabolic inhibition of force production in the HDC-short group.

Intracellular signaling

Mechanical, energetic, and oxidative stresses activate similar intracellular signaling cascades and can potentially contribute to the increased signaling in HDC-long. Similar to our previous study and others, repetitive muscle activation resulted in immediate phosphorylation of p38, ERK and p54 JNK MAP kinases and the T421/S424 residue of p70S6k (Martineau and Gardiner, 2001; Nader and Esser, 2001; Thomson et al., 2008). In this study, with widely varying metabolic loads, phosphorylation of those residues (except JNK) is found to correlate closely with markers of metabolic load or FTI. While we believe this results from a common, metabolite-driven mechanism activating a network containing AMPK, p38, ERK2, and mTOR, there are alternative explanations. Blood flow is occluded during tetanic activation, so HDC muscles undergo frequent, transient ischemia-reperfusion events, which may contribute to generation of reactive oxygen species (ROS). Among the signaling molecules, p38 and $p70S6k^{T421/S424}$ were most sensitive to phosphorylation in HDC-long. Phosphorylation of p38 has been linked to transition to a more oxidative phenotype though production of ROS and activation of PGC-1α. Hulmi et al found p38 was increased when sub-maximal loads were repetitively lifted with short rests compared to near maximum loads lifted with long rests, suggesting that the increase in p38 may be due to the larger metabolic load. In contrast, Wretman (2001) suggested that ERK, but not p38, phosphorylation during HFES was attributable to reactive oxygen species (ROS), because ERK phosphorylation could be prevented by various antioxidants.

Interestingly phosphorylation of FAK and mTOR were also correlated with glycogen depletion and ACC phosphorylation. These molecules might be most directly linked with force, FAK because it is part of the integrin complex that transmits force and

mTOR because it has been linked to HFC-induced hypertrophy. HDC-long has the greatest FTI and the greatest ACC phosphorylation, so FAK and mTOR phosphorylation correlate with either "force" or "energy depletion". In HDC-short and LDC-long, FTI takes on intermediate values, while ACC phosphorylation falls to LDC-short levels. In these intermediate groups, FAK and mTOR phosphorylation also falls to LDC-short levels, suggesting that they are more responsive to the energetic signal than to the force signal. The 2.5-fold increase in mTOR seen here is similar to the 1.3-fold increase seen by Parkington (2004) using a similar protocol. $mTOR^{S2448}$ is canonically phosphorylated by Akt however, Akt phosphorylation is reduced compared to contralateral control muscles. ERK may contribute to mTOR activity however this is not due to direct phosphorylation but through inhibition of TSC1/2.

Summary

The present results demonstrate that the immediate response of muscle to HFES is highly dependent on the temporal characteristics of that stimulation. Contraction-induced signaling integrates potentially conflicting force and metabolic stimuli to allow simultaneous increase in AMPK activity (ACC phosphorylation) along with mTORC1 signaling, despite the negative feedback between these pathways. The immediate response of muscle is only slightly dependent on the magnitude of force generation, absent eccentric action, but both the total duration of stimulation and the temporal distribution of that stimulation strongly influence the metabolic load perceived by the muscle and the extent of ERK, p38, and p70S6k activation.

Acknowledgments

This work was supported by the National Institute of Health (NIH) grant, DC05017.

CHAPTER V

CONCLUSION

Summary

Force production by a muscle is critical to maintaining proper function and overall health of a human or animal. Muscle adapts to muscle loading with hypertrophy and to unloading conditions with atrophy. Disuse atrophy is thought to be a primary contributor to sarcopenia and in the aging population, resistance-like exercises can attenuate this progression to sarcopenia.

This project was performed under the overall hypothesis that the hypertrophic adaptation of muscle acts to maintain the homeostatic state of PF/CSA. An increase in CSA would allow the muscle to perform the same force load under less stress as that load is distributed across a larger area. This hypothesis then implies that the muscle can sense mechanical changes, specifically changes in force. A few mechanisms have been suggested, however a link from force production to growth related signaling cascades responsible for regulating protein synthesis is not conclusive. Previous studies that found force generation to be related to intracellular signaling are confounded by different metabolic stress imposed and difference in the metabolic capacity of the muscles being compared (Baar and Esser, 1999; Martineau and Gardiner, 2001; Wretman et al., 2001). This project took two approaches to better understand activity-driven and force-driven intracellular signaling associated with regulating muscle mass. The first approach employed a general survey of muscles and compared growth related signaling in muscles with differing changes in activity with age. The second approach utilized an *in situ* muscle preparation in which force production or metabolic cost were specifically controlled and analyzed intracellular signaling in response to varied force level or

metabolic demands. The goal of this project was to better understand the contribution of contractile force production to the intracellular signaling cascades that mediate protein synthesis.

The first study was performed under the hypothesis that mechanotransduction is preserved in aged muscles that retain force requirements. Limb muscles are subject to reduced activity as well as reduced growth factor and other age-related systemic processes. Comparisons made solely to young animals do not accurately address the role of muscle activity in regulating growth related signaling as they are in a more anabolic environment. Because some craniofacial muscles have been suggested to be sarcopenia-resistant and have minimal changes in activity with age this study looked to compare, within animals, phosphorylation status of signaling molecules of muscles that undergo different changes in activity with age. Craniofacical muscles are developmentally different from limb muscle. The inclusion of head and neck muscle derived from somites but with similar activity maintenance as branchial arch derived craniofacial muscle thus offers a more appropriate comparison of muscle activity responsive signaling. In addition, the results extend the body of knowledge available on head and neck muscles, as kinase data is minimal.

No conclusive activity-dependent signaling emerged, however, coordinated signaling seemed to breakdown with age. Similar to other aging studies, the elevated phosphorylation status of $p70^{T389}$ in old muscle suggests increased protein synthesis despite losing muscle mass (Kimball et al., 2004). Together this alludes to idea that independent processes may regulate expression and post-translational control of phosphorylation. The relative changes in muscle activity with age based on muscle function were expected to reveal the effect of muscle activity on growth signaling. While phosphorylation of ERK and $p70S6k^{T421/S424}$ were lower only in biceps muscles of aged animals, suggesting activity dependence, this was not confirmed in pectoralis muscles.

Because no activity depend molecule was found, the goal of the second study was to specifically modulate force produced in a single muscle.

The second study was performed under the hypothesis that activation of MAPK signaling correlates with peak muscle tension independent of metabolic influences by directly altering the force produced by the muscle with low duty cycle activations. Sub-maximal forces can be produced by multiple mechanisms due to intrinsic muscle properties. Producing similar force levels by modulating muscle length, velocity of shortening and stimulation pulse width illustrates the same force level can be produced in many ways and allows analysis of force level independent of modulation method. In other words, if force-dependent activation exists within the signaling cascade assessed, it would emerge across all methods. Contrary to the hypothesis, none of the signaling molecules analyzed showed force-dependence across all methods. Regression analysis found a weak dependence on force for FAK and p38 phosphorylation however maximum isometric force did not statistically increase phosphorylation. ERK phosphorylation varied with force only when force was modulated in the pulse width method suggesting phosphorylation is dependent on fiber-activation. The conclusion from this study is that force, *per se*, is not a primary modulator of growth-related signaling and that MAP kinase and Akt cascades may already reflect substantial signal integration

Because a clear force-dependent molecule did not emerge, the third study was performed under the hypothesis that metabolic stress associated with repetitive high force contractions contributes to MAPK phosphorylation. Prolonging the stimulation duration or increasing the frequency at which stimulations are applied is expected increase the metabolic stress involved with contraction. This increased stress is expected to be related to ATP consumption and resynthesis and accumulation of metabolic byproducts. The coordinated signaling among FAK, mTOR, p38, and p70S6k along with correlations with ACC and glycogen suggests energy depletion, specific to stimulation pattern, contributes to the immediate response high force contraction signaling.

The overall conclusion of this project is that these signaling molecules that have previously been implicated in force-dependent signaling lie much too downstream to relay strict force-dependent signaling. That metabolic cost is inherent in force production and the finding that metabolic stress contributes to many of the signaling molecules analyzed suggests that the MAPK and Akt signaling cascades analyzed here appear too far removed from the initial mechanical stimuli and have already integrated a number of other co-varying signals.

Implications

The link between mechanically induced signaling and changes in protein synthesis leading to increased muscle mass, by all indications, involves mTORC1 and activation of downstream proteins. The idea that upstream signaling cascades that input onto mTORC1 may be differentially sensitive to contraction-related signaling seemed an attractive possibility, especially given that evidence seemed to exist to support this. The conclusion that metabolic stress contributes to high force contraction signaling through the MAPK and Akt signaling cascades emphasizes the complex integration of stimuli in cell signaling.

In contrast to previous work, the results of this project show that no MAPK can be related solely to the tension produced by the muscle. Contraction mode is associated with differing metabolic costs and co-varying signals. Mechanical stretch can activate MAPK and Akt including mTOR and p70S6k in the absence of metabolic cost and with minimal force production (Hornberger and Chien, 2005; Hornberger et al., 2004; Kumar et al., 2002; Sakamoto et al., 2003). Therefore passive and active force production activates or associates with pathways that converge on these cascades.

One of the striking features of mechanical signaling is that extremely transient application of force can drive long-term adaptive processes. As few as 50 contractions per day are required to sufficiently restore the muscle mass lost due to denervation (Dow

et al., 2004). Thus, even the smallest dose interventions, the 60 activations used in the second study and in the LDC-S and HDC-L groups in the third study, would be expected to result in muscle hypertrophy despite differences in change of intracellular signaling between LDC and HDC-L groups. In animals, Adams showed that concentric, isometric and eccentric achieved similar hypertrophy following 20 days of training. In humans, eccentric activations are generally thought to induce great hypertrophy particularly in type II fibers. However, not all studies come to this conclusion (Mayhew et al., 1995) and the consensus among training studies seems to imply that resulting muscle hypertrophy is similar among the different contraction modes but activity dependent effect occur (Jones and Rutherford, 1987; Wernbom et al., 2007).

In the context of human resistance training, the results of the third study fall in line with the distinction made between "strength" training, involving low volume, very high force contractions, or as "hypertrophic" training, involving high volume but moderate force contractions. The primary differences between these protocols are the rest period between contractions. The reduced rest period utilized in the hypertrophic training studies presumably allows for greater metabolic imbalance and contributes to the increased signaling (Hulmi et al., 2010). However, in both cases, it is difficult to distinguish contribution of metabolic load and volume of load, as volume is inevitably greater.

Future Directions

The results from this group of studies, particularly the second and third studies combined, offer some potential follow-up projects for the future. High forces produced by HFC were not sufficient to alter intracellular signaling but required the addition of moderate metabolic stress. The importance of the combination of metabolic and mechanical signaling is not clear. Protein synthesis and hypertrophy were not measured. It would be of interest to determine whether HFC +/- moderate metabolic stress would

result in similar or different end adaptations after chronic application of stimulations (i.e. training) and whether any of the molecules altered by the stimulation regimen could be correlated to that end result if it were different. However, the challenge of controlling variables remains. For example, HDC and LDC had very different FTI. Equalizing FTI however would either reduce or prolong stimulation time, depending on duty cycle and stimulation duration used.

The HDC-short group was interesting and revealed that metabolic stress that activates stress-related signaling can be different from the stress that causes force decline. Here it would also be of interest to better assess the metabolic changes that occur during these different stimulation protocols.

The goal of this project was to understand contraction-induced signaling. Proteins that respond to force to activate signaling cascades likely do exist, but it is clear from this study that direct detection of mechanotransduction lies upstream from the MAP kinase cascades. A future direction for this research would be to analyze potential force sensors that are more directly associated with force production. It is known that FAK can signal through Akt and MAPK. Although the autophosphorylation site of FAK analyzed in this project was weakly dependent on force, a potential role for FAK signaling, and other components of focal adhesions, including Src, in response to force still exists. As a member of focal adhesions situated in the membrane, FAK is in a position to respond to membrane deformations arising from intracellular or extracellular sources. The titin kinase domain of titin is also in a prime position to directly respond to force, particularly active force, produced by the contractile apparatus. Interest in understanding the mechanics of titin kinase have grown and revealed the domain is mechanically active. A recent study mutated the kinase domain region and found sub-maximal force but not maximal force production was reduced however myopathy was eventually expected highlighting its role in sarcomere structure and the challenges in its study (Ottenheijm et

al., 2009). It remains unclear what the role of titin kinase is. As a serine/threonine kinase, there is potential to signal to interact with the growth-related signaling cascades.

FAK and titin kinase appear prime contenders and implicated as force transducers however, muscles in which these kinase domains are mutated or absent have not been challenged with an overload signal. Muscle specific induction (Cre/Lox-Tamoxofin models) of proteins with genetically modified kinase domains would retain any role these kinases may have in development and, as adults, allow specific assessment of their role in force-dependent signaling.

REFERENCES

(2009). American College of Sports Medicine. Position Stand: Progression models in resistance training for healthy adults. *Med Sci Sports Exerc* **41**, 687-708.

Abbott, B. C. and Aubert, X. M. (1952). The force exerted by active striated muscle during and after change of length. *J Physiol* **117**, 77-86.

Adams, G. R., Caiozzo, V. J., Haddad, F. and Baldwin, K. M. (2002). Cellular and molecular responses to increased skeletal muscle loading after irradiation. *American Journal of Physiology* **283**, C1182-95.

Adams, G. R. and Haddad, F. (1996). The relationships among IGF-1, DNA content, and protein accumulation during skeletal muscle hypertrophy. *Journal of Applied Physiology* **81**, 2509-16.

Adams, G. R., Haddad, F. and Baldwin, K. M. (1999). Time course of changes in markers of myogenesis in overloaded rat skeletal muscles. *Journal of Applied Physiology* **87**, 1705-12.

Adams, G. R. and McCue, S. A. (1998). Localized infusion of IGF-I results in skeletal muscle hypertrophy in rats. *Journal of Applied Physiology* **84**, 1716-22.

Agarkova, I. and Perriard, J. C. (2005). The M-band: an elastic web that crosslinks thick filaments in the center of the sarcomere. *Trends in Cell Biology* **15**, 477-85.

Anjum, R. and Blenis, J. (2008). The RSK family of kinases: emerging roles in cellular signalling. *Nat Rev Mol Cell Biol* **9**, 747-758.

Armstrong, R., Marum, P., Tullson, P. and Saubert, C. (1979). Acute hypertrophic response of skeletal muscle to removal of synergists
J Appl Physiol **46**, 835-842.

Aronson, D., Violan, M. A., Dufresne, S. D., Zangen, D., Fielding, R. A. and Goodyear, L. J. (1997). Exercise stimulates the mitogen-activated protein kinase pathway in human skeletal muscle. *Journal of Clinical Investigation* **99**, 1251-7.

Ashley, C. C. and Ridgway, E. B. (1969). Aspects of the relationship between membrane potential, calcium transient and tension in single barnacle muscle fibres. *J Physiol* **200**, 74P-6P.

Atherton, P. J., Babraj, J., Smith, K., Singh, J., Rennie, M. J. and Wackerhage, H. (2005). Selective activation of AMPK-PGC-1alpha or PKB-TSC2-mTOR signaling can explain specific adaptive responses to endurance or resistance training-like electrical muscle stimulation. *FASEB J* **19**, 786-8.

Baar, K. and Esser, K. (1999). Phosphorylation of $p70^{S6k}$ correlates with increased skeletal muscle mass following resistance exercise. *Am J Physiol Cell Physiol* **45**, C120-C127.

Balnave, C. and Allen, D. (1995). Intracellular calcium and force in single mouse muscle fibres following repeated contractions with stretch. *J Physiol* **488**, 25-36.

Banga, I., Guba, F. and Szent-Gyorgyi, A. (1947). Nature of myosin. *Nature* **159**, 194.

Barany, M. (1967). ATPase activity of myosin correlated with speed of muscle shortening. *Journal of General Physiology* **50**, Suppl:197-218.

Barbara, J. G. and Clarac, F. (2011). Historical concepts on the relations between nerves and muscles. *Brain Res* **1409**, 3-22.

Barclay, C. J., Lichtwark, G. A. and Curtin, N. A. (2008). The energetic cost of activation in mouse fast-twitch muscle is the same whether measured using reduced filament overlap or N-benzyl-p-toluenesulphonamide. *Acta Physiol (Oxf)* **193**, 381-91.

Baumgartner, R., Wayne, S., Waters, D., Janssen, I., Gallagher, D. and Morley, J. (2004). Sarcopenic Obesity Predicts Instrumental Activities of Daily Living Disability in the Elderly. *Obes Res* **12**, 1995-2004.

Baumgartner, R. N., Koehler, K. M., Gallagher, D., Romero, L., Heymsfield, S. B., Ross, R. R., Garry, P. J. and Lindeman, R. D. (1998). Epidemiology of sarcopenia among the elderly in New Mexico. *Am J Epidemiol* **147**, 755-763.

Baylor, S. M. and Hollingworth, S. (2003). Sarcoplasmic reticulum calcium release compared in slow-twitch and fast-twitch fibres of mouse muscle. *J Physiol* **551**, 125-38.

Beltman, J. G., van der Vliet, M. R., Sargeant, A. J. and de Haan, A. (2004). Metabolic cost of lengthening, isometric and shortening contractions in maximally stimulated rat skeletal muscle. *Acta Physiol Scand* **182**, 179-87.

Berger, R. A. (1962). Effect of varied weight training programs on strength. *Research Quarterly* **33**, 168-181.

Bergstrom, M. and Hultman, E. (1988). Energy cost and fatigue during intermittent electrical stimulation of human skeletal muscle. *J Appl Physiol* **65**, 1500-5.

Biolo, G., Maggi, S. P., Williams, B. D., Tipton, K. D. and Wolfe, R. R. (1995). Increased rates of muscle protein turnover and amino acid transport after resistance exercise in humans. *American Journal of Physiology* **268**, E514-20.

Blaauw, B., Canato, M., Agatea, L., Toniolo, L., Mammucari, C., Masiero, E., Abraham, R., Sandri, M., Schiaffino, S. and Reggiani, C. (2009). Inducible activation of Akt increases skeletal muscle mass and force without satellite cell activation. *FASEB J* **23**, 000-000.

Blix, M. (1893). Die Lange und die Spannung des Muskels. *Scandinavian Archive for Physiology* **4**, 399-409.

Bodine, S., Stitt, T., Gonzalez, M., Kline, W., Stover, G., Bauerlein, R., Zlotchenko, E., Scrimgeourt, A., Lawrence, J., Glass, D. et al. (2001). Akt/mTOR pathway is a crucial regulator of skeletal muscle hypertrophy and can prevent muscle atrophy in vivo. *Nat Cell Biol* **3**, 1014-1019.

Bolster, D. R., Crozier, S. J., Kimball, S. R. and Jefferson, L. S. (2002). AMP-activated protein kinase suppresses protein synthesis in rat skeletal muscle through down-regulated mammalian target of rapamycin (mTOR) signaling. *J Biol Chem* **277**, 23977-80.

Bolster, D. R., Kubica, N., Crozier, S. J., Williamson, D. L., Farrell, P. A., Kimball, S. R. and Jefferson, L. S. (2003). Immediate response of mammalian target of rapamycin (mTOR)-mediated signalling following acute resistance exercise in rat skeletal muscle. *Journal of Physiology* **553**, 213-20.

Booth, F. and Thomason, D. (1991). Molecular and Cellular Adaptation of Muscle in Response to Exercise: Perspectives of Various Models. *Physiol Rev* **71**, 541-574.

Boppart, M. D., Hirshman, M. F., Sakamoto, K., Fielding, R. A. and Goodyear, L. J. (2001). Static stretch increases c-Jun NH2-terminal kinase activity and p38 phosphorylation in rat skeletal muscle. *American Journal of Physiology* **280**, C352-8.

Borisov, A. B., Raeker, M. O., Kontrogianni-Konstantopoulos, A., Yang, K., Kurnit, D. M., Bloch, R. J. and Russell, M. W. (2003). Rapid response of cardiac obscurin gene cluster to aortic stenosis: differential activation of Rho-GEF and MLCK and involvement in hypertrophic growth. *Biochemical and Biophysical Research Communications* **310**, 910-8.

Borisov, A. B., Sutter, S. B., Kontrogianni-Konstantopoulos, A., Bloch, R. J., Westfall, M. V. and Russell, M. W. (2006). Essential role of obscurin in cardiac myofibrillogenesis and hypertrophic response: evidence from small interfering RNA-mediated gene silencing. *Histochem Cell Biol* **125**, 227-38.

Bottinelli, R., Canepari, M., Reggiani, C. and Stienen, G. J. (1994). Myofibrillar ATPase activity during isometric contraction and isomyosin composition in rat single skinned muscle fibres. *J Physiol* **481 (Pt 3)**, 663-75.

Brozinick, J. T., Jr. and Birnbaum, M. J. (1998). Insulin, but not contraction, activates Akt/PKB in isolated rat skeletal muscle. *J Biol Chem* **273**, 14679-82.

Burd, N. A., West, D. W., Staples, A. W., Atherton, P. J., Baker, J. M., Moore, D. R., Holwerda, A. M., Parise, G., Rennie, M. J., Baker, S. K. et al. (2010). Low-load high volume resistance exercise stimulates muscle protein synthesis more than high-load low volume resistance exercise in young men. *PLoS One* **5**, e12033.

Burke, R., Levine, D., Tsairis, P. and Zajac, F. (1973). Physiological types and histochemical profiles in motor units of the cat gastrocnemius. *J Physiol* **234**, 723-748.

Burkholder, T. J. (2003). Permeability of C2C12 myotube membranes is influenced by stretch velocity. *Biochemical and Biophysical Research Communications* **305**, 266-70.

Burkholder, T. J., Fingado, B., Baron, S. and Lieber, R. L. (1994). Relationship between muscle fiber types and sizes and muscle architectural properties in the mouse hindlimb. *J Morphol* **221**, 177-90.

Burry, M., Hawkins, D. and Spangenburg, E. (2007). Lengthening contractions differentially affect p70s6k phosphorylation compared to isometric contractions in rat skeletal muscle. *Eur J Appl Physiol* **100**, 409-415.

Caiozzo, V. J., Baker, M. J., Huang, K., Chou, H., Wu, Y. Z. and Baldwin, K. M. (2003). Single-fiber myosin heavy chain polymorphism: how many patterns and what proportions? *Am J Physiol Regul Integr Comp Physiol* **285**, R570-80.

Calalb, M. B., Polte, T. R. and Hanks, S. K. (1995). Tyrosine phosphorylation of focal adhesion kinase at sites in the catalytic domain regulates kinase activity: a role for Src family kinases. *Molecular and Cellular Biology* **15**, 954-63.

Campos, G. E., Luecke, T. J., Wendeln, H. K., Toma, K., Hagerman, F. C., Murray, T. F., Ragg, K. E., Ratamess, N. A., Kraemer, W. J. and Staron, R. S. (2002). Muscular adaptations in response to three different resistance-training regimens: specificity of repetition maximum training zones. *Eur J Appl Physiol* **88**, 50-60.

Cargnello, M. and Roux, P. P. (2011). Activation and function of the MAPKs and their substrates, the MAPK-activated protein kinases. *Microbiol Mol Biol Rev* **75**, 50-83.

Carlson, C., Fan, Z., Gordon, S. and Booth, F. (2001). Time course of the MAPK and PI3-kinase response within 24 h of skeletal muscle overload. *J Appl Physiol* **91**, 2079-2087.

Caspersen, C. J., Pereira, M. A. and Curran, K. M. (2000). Changes in physical activity patterns in the United States, by sex and cross-sectional age. *Med Sci Sports Exerc* **32**, 1601-9.

Challiss, R. A., Blackledge, M. J., Shoubridge, E. A. and Radda, G. K. (1989). A gated 31P-n.m.r. study of bioenergetic recovery in rat skeletal muscle after tetanic contraction. *Biochemical Journal* **259**, 589-92.

Chalmers, G. R., Roy, R. R. and Edgerton, V. R. (1992). Variation and limitations in fiber enzymatic and size responses in hypertrophied muscle. *J Appl Physiol* **73**, 631-41.

Chen, C. S. (2008). Mechanotransduction - a field pulling together? *J Cell Sci* **121**, 3285-92.

Chesley, A., MacDougall, J., Tarnopolsky, M., Atkinson, S. and Smith, K. (1992). Changes in human muscle protein synthesis after resistance exercise. *J Appl Physiol* **73**, 1383-1388.

Chicurel, M. E., Chen, C. S. and Ingber, D. E. (1998). Cellular control lies in the balance of forces. *Current Opinion in Cell Biology* **10**, 232-9.

Clarke, M. S. and Feeback, D. L. (1996). Mechanical load induces sarcoplasmic wounding and FGF release in differentiated human skeletal muscle cultures. *FASEB Journal* **10**, 502-9.

Clarke, M. S., Khakee, R. and McNeil, P. L. (1993). Loss of cytoplasmic basic fibroblast growth factor from physiologically wounded myofibers of normal and dystrophic muscle. *Journal of Cell Science* **106 (Pt 1)**, 121-33.

Cobb, M. (2002). Timeline: exorcizing the animal spirits: Jan Swammerdam on nerve function. *Nat Rev Neurosci* **3**, 395-400.

Coffey, V., Zhong, Z., Shield, A., Canny, B., Chibalin, A., Zierath, J. and Hawley, J. (2006). Early signaling responses to divergent exercise stimuli in skeletal muscle from well-trained humans. *FASEB J* **20**, 190-192.

Connor, N., Ota, F., Nagai, H., Russell, J. and Leverson, G. (2008). Differences in age-related alterations in muscle contraction properties in rat tongue and hindlimb. *J Speech Lang Hear Res* **51**, 818-827.

Cox, G. A., Sunada, Y., Campbell, K. P. and Chamberlain, J. S. (1994). Dp71 can restore the dystrophin-associated glycoprotein complex in muscle but fails to prevent dystrophy. *Nat Genet* **8**, 333-9.

Creer, A., Gallagher, P., Slivka, D., Jemiolo, B., Fink, W. and Trappe, S. (2005). Influence of muscle glycogen availability on ERK1/2 and Akt signaling after resistance exercise in human skeletal muscle. *J Appl Physiol* **99**, 950-956.

Crow, M. T. and Kushmerick, M. J. (1982). Chemical energetics of slow- and fast-twitch muscles of the mouse. *Journal of General Physiology* **79**, 147-66.

Daw, C. K., Starnes, J. W. and White, T. P. (1988). Muscle atrophy and hypoplasia with aging: impact of training and food restriction. *J Appl Physiol* **64**, 2428-2432.

Deldicque, L., Atherton, P., Patel, R., Theisen, D., Nielens, H., Rennie, M. and Francaux, M. (2008). Decrease in Akt/PKB signalling in human skeletal muscle by resistance exercise. *Eur J Appl Physiol* **104**, 57-65.

Deshmukh, A. S., Treebak, J. T., Long, Y. C., Viollet, B., Wojtaszewski, J. F. and Zierath, J. R. (2008). Role of adenosine 5'-monophosphate-activated protein kinase subunits in skeletal muscle mammalian target of rapamycin signaling. *Mol Endocrinol* **22**, 1105-12.

Dow, D. E., Cederna, P. S., Hassett, C. A., Kostrominova, T. Y., Faulkner, J. A. and Dennis, R. G. (2004). Number of contractions to maintain mass and force of a denervated rat muscle. *Muscle Nerve* **30**, 77-86.

Dreyer, H. C., Fujita, S., Cadenas, J. G., Chinkes, D. L., Volpi, E. and Rasmussen, B. B. (2006). Resistance exercise increases AMPK activity and reduces 4E-BP1 phosphorylation and protein synthesis in human skeletal muscle. *J Physiol* **576**, 613-24.

Drummond, M., Fry, C., Glynn, E., Dreyer, H., Dhanani, S., Timmerman, K., Volpi, E. and Rasmussen, B. (2009). Rapamycin administration in humans blocks the contraction-induced increase in skeletal muscle protein synthesis. *J Physiol* **587.7**, 1535-1546.

Du, J., Guan, T., Zhang, H., Xia, Y., Liu, F. and Zhang, Y. (2008). Inhibitory crosstalk between ERK and AMPK in the growth and proliferation of cardiac fibroblasts. *Biochemical and Biophysical Research Communications* **368**, 402-407.

Dufner, A. and Thomas, G. (1999). Ribosomal S6 Kinase Signaling and the Control of Translation. *Exp Cell Res* **253**, 100-109.

Engelhardt, W. A. and Ljubimowa, M. N. (1939). Myosine and adenosinetriphosphatase. *Nature* **144**, 668-669.

Engelman, J. A., Chu, C., Lin, A., Jo, H., Ikezu, T., Okamoto, T., Kohtz, D. S. and Lisanti, M. P. (1998). Caveolin-mediated regulation of signaling along the p42/44 MAP kinase cascade in vivo. A role for the caveolin-scaffolding domain. *FEBS Letters* **428**, 205-11.

Evans, M., Morine, K., Kulkarni, C. and Barton, E. R. (2008). Expression profiling reveals heightened apoptosis and supports fiber size economy in the murine muscles of mastication. *Physiol Genomics* **35**, 86-95.

Fenn, W. O. (1923). A quantitative comparison between the energy liberated and the work performed by the isolated sartorius muscle of the frog. *J Physiol* **58**, 175-203.

Fenn, W. O. (1924). The relation between the work performed and the energy liberated in muscular contraction. *J Physiol* **58**, 373-95.

Fenn, W. O. and Latchford, W. B. (1933). The effect of muscle length on the energy for maintenance of tension. *J Physiol* **80**, 213-9.

Fenton, T. R., Gwalter, J., Ericsson, J. and Gout, I. T. (2010). Histone acetyltransferases interact with and acetylate p70 ribosomal S6 kinases *in vitro* and *in vivo*. *Int J Biochem Cell Biol* **42**, 359-366.

Fitts, R. (1994). Cellular Mechanisms of Muscle Fatigue. *Physiol Rev* **74**, 49-81.

Fluck, M., Carson, J. A., Gordon, S. E., Ziemiecki, A. and Booth, F. W. (1999). Focal adhesion proteins FAK and paxillin increase in hypertrophied skeletal muscle. *American Journal of Physiology* **277**, C152-62.

Flueck, M. and Goldspink, G. (2010). COUNTERPOINT: IGF IS NOT THE MAJOR PHYSIOLOGICAL REGULATOR OF MUSCLE MASS. *Journal of Applied Physiology* **108**, 1821-1823.

Ford-Speelman, D., Roche, J., Bowman, A. and Bloch, R. (2009). The Rho-Guanine Nucleotide Exchange Factor Domain of Obscurin Activates RhoA Signaling in Skeletal Muscle. *Mol Biol Cell* **20**, 3905-3917.

Frey, J. W., Farley, E. E., O'Neil, T. K., Burkholder, T. J. and Hornberger, T. A. (2009). Evidence that mechanosensors with distinct biomechanical properties allow for specificity in mechanotransduction. *Biophys J* **97**, 347-56.

Friden, J. and Lieber, R. L. (2001). Eccentric exercise-induced injuries to contractile and cytoskeletal muscle fibre components. *Acta Physiol Scand* **171**, 321-6.

Frontera, W. R., Meredith, C. N., O'Reilly, K. P., Knuttgen, H. G. and Evans, W. J. (1988). Strength conditioning in older men: skeletal muscle hypertrophy and improved function. *J Appl Physiol* **64**, 1038-1044.

Fry, C. S., Glynn, E. L., Drummond, M. J., Timmerman, K. L., Fujita, S., Abe, T., Dhanani, S., Volpi, E. and Rasmussen, B. B. (2010). Blood flow restriction exercise stimulates mTORC1 signaling and muscle protein synthesis in older men. *J Appl Physiol* **108**, 1199-209.

Fujita, S., Abe, T., Drummond, M. J., Cadenas, J. G., Dreyer, H. C., Sato, Y., Volpi, E. and Rasmussen, B. B. (2007). Blood flow restriction during low-intensity resistance exercise increases S6K1 phosphorylation and muscle protein synthesis. *J Appl Physiol* **103**, 903-10.

Gan, B., Yoo, Y. and Guan, J. L. (2006). Association of focal adhesion kinase with tuberous sclerosis complex 2 in the regulation of s6 kinase activation and cell growth. *J Biol Chem* **281**, 37321-9.

Gao, X., Zhang, Y., Arrazola, P., Hino, O., Kobayashi, T., Yeung, R. S., Ru, B. and Pan, D. (2002). Tsc tumour suppressor proteins antagonize amino-acid-TOR signalling. *Nat Cell Biol* **4**, 699-704.

Gardiner, E. N. (2002). Athletics in the Ancient World: Dover Publications.

Gardiner, P., Michel, R., Browman, C. and Noble, E. (1986). Increased EMG of rat plantaris during locomotion following surgical removal of its synergists. *Brain Res* **380**, 114-21.

Garma, T., Kobayashi, C., Haddad, F., Adams, G., Bodell, P. and Baldwin, K. (2007). Similar acute molecular responses to equivalent volumes of isometric, lengthening, or shortening mode resistance exercise. *J Appl Physiol* **102**, 135-143.

Gasser, H. S. and Hill, A. V. (1924). The dynamics of muscular contraction. *Proceedings of the Royal Society of London. Series B: Biological Sciences* **96**, 398-437.

Gautel, M. (2011). The sarcomeric cytoskeleton: who picks up the strain? *Current Opinion in Cell Biology* **23**, 39-46.

Gautsch, T., Anthony, J., Kimball, S., Paul, G., Layman, D. and Jefferson, L. (1998). Availability of eIF4E regulates skeletal muscle protein synthesis during recovery from exercise. *Am J Physiol Cell Physiol* **274**, 406-414.

Giovannini, S., Marzetti, E., Borst, S. E. and Leeuwenburgh, C. (2008). Modulation of GH/IGF-1 axis: potential strategies to counteract sarcopenia in older adults. *Mech Age Develop* **129**, 593-601.

Glover, E. I., Oates, B. R., Tang, J. E., Moore, D. R., Tarnopolsky, M. A. and Phillips, S. M. (2008). Resistance exercise decreases eIF2Bepsilon phosphorylation and potentiates the feeding-induced stimulation of p70S6K1 and rpS6 in young men. *Am J Physiol Reg Integr Comp Physiol* **295**, R604-R610.

Goldberg, A., Etlinger, J., Goldspink, D. and Jablecki, C. (1975). Mechanism of work-induced hypertrophy of skeletal muscle. *Med Sci Sports* **7**, 185-198.

Goldberg, A. L. (1967). Work-induced growth of skeletal muscle in normal and hypophysectomized rats. *American Journal of Physiology* **213**, 1193-8.

Goldberg, A. L. and Goodman, H. M. (1969). Relationship between growth hormone and muscular work in determining muscle size. *The Journal of Physiology* **200**, 655-666.

Goldspink, D., Cox, V., Smith, S., Eaves, L., Osbaldeston, N., Lee, D. and Mantle, D. (1995). Muscle growth in response to mechanical stimuli. *American Journal of Physiology* **268**, 288-297.

Goldspink, G. and Howells, K. F. (1974). Work-induced hypertrophy in exercised normal muscles of different ages and the reversibility of hypertrophy after cessation of exercise. *J Physiol* **239**, 179-93.

Goldstein, M. A., Schroeter, J. P. and Michael, L. H. (1991). Role of the Z band in the mechanical properties of the heart. *The FASEB Journal* **5**, 2167-2174.

Goodman, C. A., Mayhew, D. L. and Hornberger, T. A. (2011). Recent progress toward understanding the molecular mechanisms that regulate skeletal muscle mass. *Cell Signal* **23**, 1896-906.

Goodman, C. A., Miu, M. H., Frey, J. W., Mabrey, D. M., Lincoln, H. C., Ge, Y., Chen, J. and Hornberger, T. A. (2010). A phosphatidylinositol 3-kinase/protein kinase B-independent activation of mammalian target of rapamycin signaling is sufficient to induce skeletal muscle hypertrophy. *Mol Biol Cell* **21**, 3258-68.

Goodyear, L., Chang, P.-Y., Sherwood, D., Dufresne, S. and Moller, D. (1996). Effects of exercise and insulin on mitogen-activated protein kinase signaling pathways in rat skeletal muscle. *Am J Physiol Endocrinol Metab* **271**, E403-E408.

Gordon, A. M., Huxley, A. F. and Julian, F. J. (1966). The variation in isometric tension with sarcomere length in vertebrate muscle fibres. *J Physiol* **184**, 170-92.

Gordon, S., Lake, J., Westerkamp, C. and Thomson, D. (2008). Does AMP-Activated Protein Kinase Negatively Mediate Aged Fast-Twitch Skeletal Muscle Mass? *Exerc Sport Sci Rev* **36**, 179-186.

Gordon, S. E., Fluck, M. and Booth, F. W. (2001). Selected Contribution: Skeletal muscle focal adhesion kinase, paxillin, and serum response factor are loading dependent. *J Appl Physiol* **90**, 1174-83; discussion 1165.

Grater, F., Shen, J., Jiang, H., Gautel, M. and Grubmuller, H. (2005). Mechanically induced titin kinase activation studied by force-probe molecular dynamics simulations. *Biophys J* **88**, 790-804.

Haddad, F. and Adams, G. (2004). Inhibition of MAP/ERK kinase prevents IGF-I induced hypertrophy in rat muscles. *J Appl Physiol* **96**, 203-210.

Han, Y. S., Geiger, P. C., Cody, M. J., Macken, R. L. and Sieck, G. C. (2003). ATP consumption rate per cross bridge depends on myosin heavy chain isoform. *J Appl Physiol* **94**, 2188-96.

Hardie, D. G. and Hawley, S. A. (2001). AMP-activated protein kinase: the energy charge hypothesis revisited. *Bioessays* **23**, 1112-9.

Hargreaves, M. and Spriet, L. L. (2006). Exercise metabolism: Human Kinetics.

Hather, B. M., Tesch, P. A., Buchanan, P. and Dudley, G. A. (1991). Influence of eccentric actions on skeletal muscle adaptations to resistance training. *Acta Physiol Scand* **143**, 177-85.

Henneman, E. (1957). Relation between size of neurons and their susceptibility to discharge. *Science* **126**, 1345-7.

Henneman, E. and Olson, C. B. (1965). Relations between Structure and Function in the Design of Skeletal Muscles. *J Neurophysiol* **28**, 581-98.

Hennig, R. and Lomo, T. (1985). Firing patterns of motor units in normal rats. *Nature* **314**, 164-6.

Hentzen, E. R., Lahey, M., Peters, D., Mathew, L., Barash, I. A., Friden, J. and Lieber, R. L. (2006). Stress-dependent and -independent expression of the myogenic regulatory factors and the MARP genes after eccentric contractions in rats. *J Physiol* **570**, 157-67.

Hilber, K., Sun, Y. B. and Irving, M. (2001). Effects of sarcomere length and temperature on the rate of ATP utilisation by rabbit psoas muscle fibres. *J Physiol* **531**, 771-80.

Hill, A. V. (1938). The Heat of Shortening and the Dynamic Constants of Muscle. *Proceedings of the Royal Society of London. Series B, Biological Sciences* **126**, 136-195.

Hogan, M. C., Ingham, E. and Kurdak, S. S. (1998). Contraction duration affects metabolic energy cost and fatigue in skeletal muscle. *American Journal of Physiology* **274**, E397-402.

Holloszy, J. O., Smith, E. K., Vining, M. and Adams, S. (1985). Effect of voluntary exercise on longevity of rats. *Journal of Applied Physiology* **59**, 826-831.

Holm, L., van Hall, G., Rose, A. J., Miller, B. F., Doessing, S., Richter, E. A. and Kjaer, M. (2010). Contraction intensity and feeding affect collagen and myofibrillar protein synthesis rates differently in human skeletal muscle. *Am J Physiol Endocrinol Metab* **298**, E257-69.

Homsher, E. and Kean, C. J. (1978). Skeletal muscle energetics and metabolism. *Annual Review of Physiology* **40**, 93-131.

Horman, S., Browne, G., Krause, U., Patel, J., Vertommen, D., Bertrand, L., Lavoinne, A., Hue, L., Proud, C. and Rider, M. (2002). Activation of AMP-activated protein kinase leads to the phosphorylation of elongation factor 2 and an inhibition of protein synthesis. *Curr Biol* **12**, 1419-23.

Hornberger, T. and Esser, K. (2004). Mechanotransduction and the regulation of protein synthesis in skeletal muscle. *Proc Nutr Soc* **63**, 331-335.

Hornberger, T., Sukhija, K., Wang, X.-R. and Chien, S. (2007). mTOR is the Rapamycin-Sensitive Kinase that Confers Mechanically-Induced Phosphorylation of the Hydrophobic Motif Site Thr(389) in p70S6k. *FEBS Letters* **581**, 4562-4566.

Hornberger, T. A., Armstrong, D. D., Koh, T. J., Burkholder, T. J. and Esser, K. A. (2005). Intracellular signaling specificity in response to uniaxial vs. multiaxial stretch: implications for mechanotransduction. *American Journal of Physiology* **288**, C185-94.

Hornberger, T. A. and Chien, S. (2005). Mechanical stimuli and nutrients regulate rapamycin-sensitive signaling through distinct mechanisms in skeletal muscle. *Journal of Cellular Biochemistry*.

Hornberger, T. A., Stuppard, R., Conley, K. E., Fedele, M. J., Fiorotto, M. L., Chin, E. R. and Esser, K. A. (2004). Mechanical stimuli regulate rapamycin-sensitive signalling by a phosphoinositide 3-kinase-, protein kinase B- and growth factor-independent mechanism. *Biochemical Journal* **380**, 795-804.

Horowits, R. and Podolsky, R. J. (1987). The positional stability of thick filaments in activated skeletal muscle depends on sarcomere length: evidence for the role of titin filaments. *Journal of Cell Biology* **105**, 2217-23.

Hortobagyi, T., Hill, J. P., Houmard, J. A., Fraser, D. D., Lambert, N. J. and Israel, R. G. (1996). Adaptive responses to muscle lengthening and shortening in humans. *J Appl Physiol* **80**, 765-72.

Hulmi, J. J., Walker, S., Ahtiainen, J. P., Nyman, K., Kraemer, W. J. and Hakkinen, K. (2010). Molecular signaling in muscle is affected by the specificity of resistance exercise protocol. *Scand J Med Sci Sports*.

Huxley, A. F. (1957a). Muscle structure and theories of contraction. *Progress in Biophysics and Biophysical Chemistry* **7**, 255-318.

Huxley, A. F. (1971). The activation of striated muscle and its mechanical response. *Proceedings of the Royal Society of London. Series B: Biological Sciences* **178**, 1-27.

Huxley, A. F. and Niedergerke, R. (1954). Structural changes in muscle during contraction; interference microscopy of living muscle fibres. *Nature* **173**, 971-3.

Huxley, A. F. and Simmons, R. M. (1971). Proposed mechanism of force generation in striated muscle. *Nature* **233**, 533-8.

Huxley, A. F. and Taylor, R. E. (1958). Local activation of striated muscle fibres. *Journal of Physiology* **144**, 426-41.

Huxley, H. E. (1957b). The double array of filaments in cross-striated muscle. *Journal of Biophysical and Biochemical Cytology* **3**, 631-48.

Inoki, K., Zhu, T. and Guan, K. L. (2003). TSC2 mediates cellular energy response to control cell growth and survival. *Cell* **115**, 577-90.

Janssen, I., Baumgartner, R., Ross, R., Rosenberg, I. and Roubenoff, R. (2004a). Skeletal muscle cutpoints associated with elevated physical disability risk in older men and women. *Am J Epidemiol* **159**, 413-421.

Janssen, I., Shepard, D., Katzmarzyk, P. and Roubenoff, R. (2004b). The healthcare costs of sarcopenia in the United States. *J Am Geriatr Soc* **52**, 80-85.

Jones, D. and Rutherford, O. (1987). Human Muscle Strength Training: The Effects of Three Different Regimes and the Nature of the Resultant Changes. *J Physiol* **391**, 1-11.

Jones, D. A., Rutherford, O. M. and Parker, D. F. (1989). Physiological changes in skeletal muscle as a result of strength training. *Q J Exp Physiol* **74**, 233-56.

Karagounis, L. G. and Hawley, J. A. (2010). Skeletal muscle: increasing the size of the locomotor cell. *Int J Biochem Cell Biol* **42**, 1376-9.

Karlsson, H. K., Nilsson, P. A., Nilsson, J., Chibalin, A. V., Zierath, J. R. and Blomstrand, E. (2004). Branched-chain amino acids increase p70S6k phosphorylation in human skeletal muscle after resistance exercise. *Am J Physiol Endocrinol Metab* **287**, E1-7.

Katsumi, A., Naoe, T., Matsushita, T., Kaibuchi, K. and Schwartz, M. A. (2005). Integrin Activation and Matrix Binding Mediate Cellular Responses to Mechanical Stretch. *Journal of Biological Chemistry* **280**, 16546-16549.

Katsumi, A., Orr, A. W., Tzima, E. and Schwartz, M. A. (2004). Integrins in mechanotransduction. *J Biol Chem* **279**, 12001-4.

Katz, B. (1939). The relation between force and speed in muscular contraction. *Journal of Physiology* **96**, 45-64.

Keren, A., Tamir, Y. and Bengal, E. (2006). The p38 MAPK signaling pathway: a major regulator of skeletal muscle development. *Mol Cell Endocrinol* **252**, 224-230.

Kimball, S. R. (2006). Interaction between the AMP-Activated Protein Kinase and mTOR Signaling Pathways. *Med Sci Sports Exerc* **38**, 1958-1964.

Kimball, S. R., O'Malley, J. P., Anthony, J. C., Crozier, S. J. and Jefferson, L. S. (2004). Assessment of biomarkers of protein anabolism in skeletal muscle during the life span of the rat: sarcopenia despite elevated protein synthesis. *Am J Physiol Endocrinol Metab* **287**, E772-E780.

Kinnard, R. S., Mylabathula, D. B., Uddemarri, S., Rice, K. M., Wright, G. L. and Blough, E. R. (2005). Regulation of p70S6k, GSK-3beta, and calcineurin in rat striated muscle during aging. *Biogerontology* **6**, 173-184.

Klitgaard, H. (1988). A model for quantitative strength training of hindlimb muscles of the rat. *J Appl Physiol* **64**, 1740-5.

Klossner, S., Durieux, A. C., Freyssenet, D. and Flueck, M. (2009). Mechano-transduction to muscle protein synthesis is modulated by FAK. *Eur J Appl Physiol* **106**, 389-98.

Kojic, S., Medeot, E., Guccione, E., Krmac, H., Zara, I., Martinelli, V., Valle, G. and Faulkner, G. (2004). The Ankrd2 protein, a link between the sarcomere and the nucleus in skeletal muscle. *J Mol Biol* **339**, 313-25.

Kontrogianni-Konstantopoulos, A., Jones, E. M., van Rossum, D. B. and Bloch, R. J. (2003). Obscurin Is a Ligand for Small Ankyrin 1 in Skeletal Muscle. *Molecular Biology of the Cell* **14**, 1138-1148.

Krause, W. (1869). Die Motorischen Endplatten der qeurgestriefen Muskelfasern. Hannover: Hahn'sche Hofbuchhandlung.

Kubica, N., Bolster, D. R., Farrell, P. A., Kimball, S. R. and Jefferson, L. S. (2005). Resistance exercise increases muscle protein synthesis and translation of eukaryotic initiation factor 2Bepsilon mRNA in a mammalian target of rapamycin-dependent manner. *J Biol Chem* **280**, 7570-80.

Kuhne, W. (1864). Untersuchungen über das Protoplasma und die Contractility. Leipzig: W. Engelmann.

Kumar, A., Chaudhry, I., Reid, M. and Boriek, A. (2002). Distinct signaling pathways are activated in response to mechanical stress applied axially and transversely to skeletal muscle fibers. *J Biol Chem* **277**, 46493-46503.

Kumar, V., Selby, A., Rankin, D., Patel, R., Atherton, P., Hildebrandt, W., Williams, J., Smith, K., Seynnes, O., Hiscock, N. et al. (2009). Age-related differences in the dose-response relationship of muscle protein synthesis to resistance exercise in young and old men. *J Physiol* **587**, 211-7.

Kushmerick, M. J. and Paul, R. J. (1977). Chemical energetics in repeated contractions of frog sartorius muscles at 0 degrees C. *J Physiol* **267**, 249-60.

Lamb, G. D., Stephenson, D. G., Bangsbo, J. and Juel, C. (2006). Point:Counterpoint: Lactic acid accumulation is an advantage/disadvantage during muscle activity. *Journal of Applied Physiology* **100**, 1410-1412.

Lange, S., Auerbach, D., McLoughlin, P., Perriard, E., Schafer, B. W., Perriard, J. C. and Ehler, E. (2002). Subcellular targeting of metabolic enzymes to titin in heart muscle may be mediated by DRAL/FHL-2. *J Cell Sci* **115**, 4925-36.

Lange, S., Xiang, F., Yakovenko, A., Vihola, A., Hackman, P., Rostkova, E., Kristensen, J., Brandmeier, B., Franzen, G., Hedberg, B. et al. (2005). The kinase domain of titin controls muscle gene expression and protein turnover. *Science* **308**, 1599-603.

Lantier, L., Mounier, R., Leclerc, J., Pende, M., Foretz, M. and Viollet, B. (2010). Coordinated maintenance of muscle cell size control by AMP-activated protein kinase. *FASEB J* **24**, 3555-61.

Larsson, L. and Ansved, T. (1995). Effects of ageing on the motor unit. *Prog Neurobiol* **45**, 397-458.

Laurent, G., Sparrow, M. and Millward, D. (1978). Changes in rates of protein synthesis and breakdown during hypertrophy of the anterior and posterior latissimus dorsi muscles. *Biochemical Journal* **176**, 407-417.

Lluis, F., Perdiguero, E., Nebreda, A. R. and Munoz-Canoves, P. (2006). Regulation of skeletal muscle gene expression by p38 MAP kinases. *Trends Cell Biol* **16**, 36-44.

Lo, S., Russell, J. C. and Taylor, A. W. (1970). Determination of glycogen in small tissue samples. *J Appl Physiol* **28**, 234-6.

Long, Y. C., Widegren, U. and Zierath, J. R. (2004). Exercise-induced mitogen-activated protein kinase signalling in skeletal muscle. *Proc Nutr Soc* **63**, 227-232.

Lowe, D. A. and Alway, S. E. (2002). Animal models for inducing muscle hypertrophy: are they relevant for clinical applications in humans? *J Orthop Sports Phys Ther* **32**, 36-43.

Lymn, R. W. and Taylor, E. W. (1971). Mechanism of adenosine triphosphate hydrolysis by actomyosin. *Biochemistry* **10**, 4617-24.

Lynch, G. S., Schertzer, J. D. and Ryall, J. G. (2007). Therapeutic approaches for muscle wasting disorders. *Pharmacol Ther* **113**, 461-487.

Ma, X. M. and Blenis, J. (2009). Molecular mechanisms of mTOR-mediated translational control. *Nat Rev Mol Cell Biol* **10**, 307-18.

MacAuley, D. (1994). A history of physical activity, health and medicine. *J R Soc Med* **87**, 32-5.

Mack, P. J., Kaazempur-Mofrad, M. R., Karcher, H., Lee, R. T. and Kamm, R. D. (2004). Force-induced focal adhesion translocation: effects of force amplitude and frequency. *Am J Physiol Cell Physiol* **287**, C954-62.

Martineau, L. C. and Gardiner, P. F. (2001). Insight into skeletal muscle mechanotransduction: MAPK activation is quantitatively related to tension. *Journal of Applied Physiology* **91**, 693-702.

Martonosi, A. N. (2000). Animal electricity, Ca2+ and muscle contraction. A brief history of muscle research. *Acta Biochim Pol* **47**, 493-516.

Mayhew, D. L., Hornberger, T. A., Lincoln, H. C. and Bamman, M. M. (2011). Eukaryotic initiation factor 2B epsilon induces cap-dependent translation and skeletal muscle hypertrophy. *J Physiol* **589**, 3023-37.

Mayhew, D. L., Kim, J. S., Cross, J. M., Ferrando, A. A. and Bamman, M. M. (2009). Translational signaling responses preceding resistance training-mediated myofiber hypertrophy in young and old humans. *J Appl Physiol* **107**, 1655-1662.

Mayhew, T. P., Rothstein, J. M., Finucane, S. D. and Lamb, R. L. (1995). Muscular adaptation to concentric and eccentric exercise at equal power levels. *Med Sci Sports Exerc* **27**, 868-73.

McBride, A. and Hardie, D. G. (2009). AMP-activated protein kinase--a sensor of glycogen as well as AMP and ATP? *Acta Physiol (Oxf)* **196**, 99-113.

McCarthy, J. J., Mula, J., Miyazaki, M., Erfani, R., Garrison, K., Farooqui, A. B., Srikuea, R., Lawson, B. A., Grimes, B., Keller, C. et al. (2011). Effective fiber hypertrophy in satellite cell-depleted skeletal muscle. *Development* **138**, 3657-66.

McCully, K. K. and Faulkner, J. A. (1985). Injury to skeletal muscle fibers of mice following lengthening contractions. *J Appl Physiol* **59**, 119-26.

McKendrick, L., Morley, S. J., Pain, V. M., Jagus, R. and Joshi, B. (2001). Phosphorylation of eukaryotic initiation factor 4E (eIF4E) at Ser209 is not required for protein synthesis in vitro and in vivo. *Eur J Biochem* **268**, 5375-85.

McKoy, G., Ashley, W., Mander, J., Yang, S. Y., Williams, N., Russell, B. and Goldspink, G. (1999). Expression of insulin growth factor-1 splice variants and structural genes in rabbit skeletal muscle induced by stretch and stimulation. *J Physiol* **516 (Pt 2)**, 583-92.

McLoon, L. K., Rowe, J., Wirtschafter, J. D. and McCormick, K. M. (2004). Continuous myofiber remodeling in uninjured extraocular myofibers: myonuclear turnover and evidence for apoptosis. *Muscle and Nerve* **29**, 707-715.

Mendez, J. and Keys, A. (1960). Density and composition of mammalian muscle. *Metabolism* **9**, 184-188.

Miranda, L., Horman, S., De Potter, I., Hue, L., Jensen, J. and Rider, M. (2008). Effects of contraction and insulin on protein synthesis, AMP-activated protein kinase and phosphorylation state of translation factors in rat skeletal muscle. *Pflugers Arch* **455**, 1129-1140.

Miyazaki, M. and Esser, K. A. (2009). Cellular mechanisms regulating protein synthesis and skeletal muscle hypertrophy in animals. *J Appl Physiol* **106**, 1367-73.

Moore, D. R., Atherton, P. J., Rennie, M. J., Tarnopolsky, M. A. and Phillips, S. M. (2011a). Resistance exercise enhances mTOR and MAPK signalling in human muscle over that seen at rest after bolus protein ingestion. *Acta Physiol (Oxf)* **201**, 365-72.

Moore, S. F., Hunter, R. W. and Hers, I. (2011b). mTORC2 Protein-mediated Protein Kinase B (Akt) Serine 473 Phosphorylation Is Not Required for Akt1 Activity in Human Platelets. *J Biol Chem* **286**, 24553-60.

Morpurgo, B. (1897). Ueber Activitats-Hypertrophie der willkurlichen Muskeln. *Virchows Arch Path Anat Physiol* **150**, 522-554.

Mounier, R., Lantier, L., Leclerc, J., Sotiropoulos, A., Foretz, M. and Viollet, B. (2011). Antagonistic control of muscle cell size by AMPK and mTORC1. *Cell Cycle* **10**, 2640-6.

Mylabathula, D. B., Rice, K. M., Wang, Z., Uddemarri, S., Kinnard, R. S. and Blough, E. R. (2006). Age-associated changes in MAPK activation in fast- and slow-twitch skeletal muscle of the F344/NNiaHSD X Brown Norway/BiNia rat model. *Experimental Gerontology* **41**, 205-14.

Nader, G. A. and Esser, K. A. (2001). Intracellular signaling specificity in skeletal muscle in response to different modes of exercise. *Journal of Applied Physiology* **90**, 1936-42.

Nair, K. S. (2005). Aging muscle. *Am J Clin Nutr* **81**, 953-963.

Nave, B. T., Ouwens, M., Withers, D. J., Alessi, D. R. and Shepherd, P. R. (1999). Mammalian target of rapamycin is a direct target for protein kinase B: identification of a convergence point for opposing effects of insulin and amino-acid deficiency on protein translation. *Biochemical Journal* **344 Pt 2**, 427-31.

Needham, D. M. (1942). The adenosinetriphosphatase activity of myosin preparations. *Biochemical Journal* **36**, 113-20.

Noden, D. and Francis-West, P. (2006). The differentiation and morphogenesis of craniofacial muscles. *Dev Dyn* **235**, 1194-1218.

Norton, M., Verstegeden, A., Maxwell, L. C. and McCarter, R. M. (2001). Constancy of masseter muscle structure and function with age in F344 rats. *Archives of oral biology* **46**, 139-146.

Ohanna, M., Sobering, A., Lapointe, T., Lorenzo, L., Praud, C., Petroulakis, E., Sonenberg, N., Kelly, P., Sotiropoulos, A. and Pende, M. (2005). Atrophy of S6K1(-/-) skeletal muscle cells reveals distinct mTOR effectors for cell cycle and size control. *Nat Cell Biol* **7**, 286-294.

Olha, A. E., Jasmin, B. J., Michel, R. N. and Gardiner, P. F. (1988). Physiological responses of rat plantaris motor units to overload induced by surgical removal of its synergists. *J Neurophysiol* **60**, 2138-51.

Orr, A. W., Helmke, B. P., Blackman, B. R. and Schwartz, M. A. (2006). Mechanisms of mechanotransduction. *Dev Cell* **10**, 11-20.

Ottenheijm, C. A., Hidalgo, C., Rost, K., Gotthardt, M. and Granzier, H. (2009). Altered contractility of skeletal muscle in mice deficient in titin's M-band region. *J Mol Biol* **393**, 10-26.

Pardo, J. V., Siliciano, J. D. and Craig, S. W. (1983). A vinculin-containing cortical lattice in skeletal muscle: transverse lattice elements ("costameres") mark sites of attachment between myofibrils and sarcolemma. *Proceedings of the National Academy of Sciences* **80**, 1008-1012.

Parkington, J. D., LeBrasseur, N. K., Siebert, A. P. and Fielding, R. A. (2004). Contraction-mediated mTOR, p70S6k, and ERK1/2 phosphorylation in aged skeletal muscle. *Journal of Applied Physiology* **97**, 243-8.

Parkington, J. D., Siebert, A. P., LeBrasseur, N. K. and Fielding, R. A. (2003). Differential activation of mTOR signaling by contractile activity in skeletal muscle. *American Journal of Physiology - Regulatory, Integrative and Comparative Physiology* **285**, R1086-R1090.

Parsons, J. T. (2003). Focal adhesion kinase: the first ten years. *J Cell Sci* **116**, 1409-16.

Patterson, S. W., Piper, H. and Starling, E. H. (1914). The regulation of the heart beat. *The Journal of Physiology* **48**, 465-513.

Pearson, R. B., Dennis, P. B., Han, J. W., Williamson, N. A., Kozma, S. C., Wettenhall, R. E. and Thomas, G. (1995). The principal target of rapamycin-induced p70s6k inactivation is a novel phosphorylation site within a conserved hydrophobic domain. *EMBO Journal* **14**, 5279-5287.

Pearson, S. J., Young, P., Macaluso, A., Devito, G., Nimmo, M. A., Cobbold, M. and Harridge, S. D. R. (2002). Muscle function in elite master weightlifters. *Med Sci Sports Exerc* **34**, 119-1206.

Pende, M., Um, S. H., Mieulet, V., Sticker, M., Goss, V. L., Mestan, J., Mueller, M., Fumagalli, S., Kozma, S. C. and Thomas, G. (2004). S6K1-/- /S6K2-/- Mice Exhibit Perinatal Lethality and Rapamycin-Sensitive 5 $^{\llcorner}$ -Terminal Oligopyrimidine mRNA Translation and Reveal a Mitogen-Activated Protein Kinase-Dependent S6 Kinase Pathway. *Molecular and Cellular Biology* **24**, 3112-3124.

Peng, M. T. and Kang, M. (1984). Circadian rhythms and patterns of running-wheel activity, feeding and drinking behaviors of old male rats. *Physiol Behav* **33**, 615-20.

Phillips, S. (2007). Resistance exercise: good for more than just Grandma and Grandpa's muscles. *Appl Physiol Nutr Metab* **32**, 1198-1205.

Philp, A., Hamilton, D. L. and Baar, K. (2011). Signals mediating skeletal muscle remodeling by resistance exercise: PI3-kinase independent activation of mTORC1. *J Appl Physiol* **110**, 561-8.

Potma, E. J. and Stienen, G. J. (1996). Increase in ATP consumption during shortening in skinned fibres from rabbit psoas muscle: effects of inorganic phosphate. *J Physiol* **496 (Pt 1)**, 1-12.

Potma, E. J., Stienen, G. J., Barends, J. P. and Elzinga, G. (1994). Myofibrillar ATPase activity and mechanical performance of skinned fibres from rabbit psoas muscle. *J Physiol* **474**, 303-17.

Proctor, D. N., Balagopal, P. and Nair, K. S. (1998). Age-related sarcopenia in humans is associated with reduced synthetic rates of specific muscle proteins. *J Nutr* **128**, 351S-355S.

Proud, C. (2007). Signalling to translation: how signal transduction pathways control the protein synthetic machinery. *Biochemical Journal* **403**, 217-234.

Puchner, E., Alexandrovich, A., Kho, A., Hensen, U., Schafer, L., Brandmeier, B., Grater, F., Grubmuller, H., Gaub, H. and Gautel, M. (2008). Mechanoenzymatics of titin kinase. *PNAS* **105**, 13385-13390.

Pullen, N. and Thomas, G. (1997). The modular phosphorylation and activation of p70s6k. *FEBS Letters* **410**, 78-82.

Pyronnet, S. (2000). Phosphorylation of the Cap-Binding Protein eIF4E by the MAPK-activated protein kinase Mnk1. *Biochem Pharmacol* **60**, 1237-1243.

Rahnert, J. A., Luo, Q., Balog, E. M., Sokoloff, A. J. and Burkholder, T. J. (2011). Changes in growth-related kinases in head, neck and limb muscles with age. *Exp Gerontol* **46**, 282-91.

Rahnert, J. A., Sokoloff, A. J. and Burkholder, T. J. (2010). Sarcomeric myosin expression in the tongue body of humans, macaques and rats. *Cell Tissues Organs* **191**, 431-442.

Ramsey, R. W. and Street, S. F. (1940). The isometric length-tension diagram of isolated skeletal muscle fibers of the frog. *Journal of Cellular and Comparative Physiology* **15**, 11-34.

Rando, T. A. (2001). The dystrophin-glycoprotein complex, cellular signaling, and the regulation of cell survival in the muscular dystrophies. *Muscle Nerve* **24**, 1575-94.

Redpath, N. T., Price, N. T., Severinov, K. V. and Proud, C. G. (1993). Regulation of elongation factor-2 by multisite phosphorylation. *Eur J Biochem* **213**, 689-99.

Renganathan, M., Messi, M. a. L. and Delbono, O. (1998). Overexpression of IGF-1 Exclusively in Skeletal Muscle Prevents Age-related Decline in the Number of Dihydropyridine Receptors. *Journal of Biological Chemistry* **273**, 28845-28851.

Rome, L. C., Morgan, D. L. and Julian, F. J. (1985). Stimulation rate, potentiators, and sarcomere length-tension relationship of muscle. *American Journal of Physiology* **249**, C497-502.

Russ, D. (2008). Active and passive tension interact to promote Akt signaling with muscle contraction. *Med Sci Sports Exerc* **40**, 88-95.

Russ, D. and Lovering, R. (2006). Influence of activation frequency on cellular signalling pathways during fatiguing contractions in rat skeletal muscle. *Exp Physiol* **91**, 957-966.

Ryder, J. W., Fahlman, R., Wallberg-Henriksson, H., Alessi, D. R., Krook, A. and Zierath, J. R. (2000). Effect of contraction on mitogen-activated protein kinase signal transduction in skeletal muscle. Involvement Of the mitogen- and stress-activated protein kinase 1. *J Biol Chem* **275**, 1457-62.

Sahlin, K., Tonkonogi, M. and Soderlund, K. (1998). Energy supply and muscle fatigue in humans. *Acta Physiol Scand* **162**, 261-6.

Sakamoto, K., Aschenbach, W., Hirshman, M. and Goodyear, L. (2003). Akt signaling in skeletal muscle: regulation by exercise and passive stretch. *Am J Physiol Endocrinol Metab* **285**, E1081-E1088.

Sakamoto, K. and Goodyear, L. J. (2002). Invited review: intracellular signaling in contracting skeletal muscle. *Journal of Applied Physiology* **93**, 369-83.

Sakamoto, K., Hirshman, M., Aschenbach, W. and Goodyear, L. (2002). Contraction Regulation of Akt in Rat Skeletal Muscle. *J Biol Chem* **277**, 11910-11917.

Sawada, Y. and Sheetz, M. P. (2002). Force transduction by Triton cytoskeletons. *Journal of Cell Biology* **156**, 609-15.

Schiaffino, S. and Reggiani, C. (2011). Fiber types in mammalian skeletal muscles. *Physiol Rev* **91**, 1447-531.

Shah, J., Anthony, J., KimballI, S. and Jefferson, L. (2000). 4E-BP1 and S6K1: translational integration sites for nutritional and hormonal information in muscle. *Am J Physiol Endocrinol Metab* **279**, E715-E729.

Sheikh, F., Raskin, A., Chu, P. H., Lange, S., Domenighetti, A. A., Zheng, M., Liang, X., Zhang, T., Yajima, T., Gu, Y. et al. (2008). An FHL1-containing complex within the cardiomyocyte sarcomere mediates hypertrophic biomechanical stress responses in mice. *Journal of Clinical Investigation* **118**, 3870-80.

Shende, P., Plaisance, I., Morandi, C., Pellieux, C., Berthonneche, C., Zorzato, F., Krishnan, J., Lerch, R., Hall, M. N., Ruegg, M. A. et al. (2011). Cardiac raptor ablation impairs adaptive hypertrophy, alters metabolic gene expression, and causes heart failure in mice. *Circulation* **123**, 1073-82.

Sherwood, D., Dufresne, S., Markuns, J., Cheatham, B., Moller, D., Aronson, D. and Goodyear, L. (1999). Differential regulation of MAP kinase, p70S6K, and Akt by contraction and insulin in rat skeletal muscle. *Am J Physiol Endocrinol Metab* **39**, E870-E878.

Shima, H., Pende, M., Chen, Y., Fumagalli, S., Thomas, G. and Kozma, S. C. (1998). Disruption of the p70(s6k)/p85(s6k) gene reveals a small mouse phenotype and a new functional S6 kinase. *EMBO Journal* **17**, 6649-6659.

Skalicky, M., Bubna-Littitz, H. and Viidik, A. (1996). Influence of physical exercise on aging rats: I. Life-long exercise preserves patterns of spontaneous activity. *Mechanisms of Ageing and Development* **87**, 127-139.

Soderlund, K. and Hultman, E. (1991). ATP and phosphocreatine changes in single human muscle fibers after intense electrical stimulation. *American Journal of Physiology* **261**, E737-41.

Spangenburg, E. E., Le Roith, D., Ward, C. W. and Bodine, S. C. (2008). A functional insulin-like growth factor receptor is not necessary for load-induced skeletal muscle hypertrophy. *J Physiol* **586**, 283-91.

Spangenburg, E. E. and McBride, T. A. (2006). Inhibition of stretch-activated channels during eccentric muscle contraction attenuates p70S6K activation. *Journal of Applied Physiology* **100**, 129-35.

Stephenson, D. G., Stewart, A. W. and Wilson, G. J. (1989). Dissociation of force from myofibrillar MgATPase and stiffness at short sarcomere lengths in rat and toad skeletal muscle. *J Physiol* **410**, 351-66.

Sturrock, R. R. (1987). Changes in the number of neurons in the mesencephalic and motor nuclei of the trigeminal nerve in the ageing mouse brain. *J Anat* **151**, 15-25.

Swammerdam, J. and Flloyd, T. (1978). The book of nature: Arno Press.

Sweeney, H. L., Kushmerick, M. J., Mabuchi, K., Gergely, J. and Sreter, F. A. (1986). Velocity of shortening and myosin isozymes in two types of rabbit fast-twitch muscle fibers. *American Journal of Physiology - Cell Physiology* **251**, C431-C434.

Szent-Gyorgyi, A. (1945). Studies on muscles. *Acta Physiol Scand* **Suppl XXV**, 1-115.

Szent-Gyorgyi, A. G. (2004). The early history of the biochemistry of muscle contraction. *Journal of General Physiology* **123**, 631-41.

Szulc, P., Duboeuf, F., Marchand, F. and Delmas, P. D. (2004). Hormonal and lifestyle determinants of appendicular skeletal muscle mass in men: the MINOS study. *Am J Clin Nutr* **80**, 496-503.

Talmadge, R. J. and Roy, R. R. (1993). Electrophoretic separation of rat skeletal muscle myosin heavy-chain isoforms. *Journal of Applied Physiology* **75**, 2337-2340.

Tannerstedt, J., Apro, W. and Blomstrand, E. (2009). Maximal lengthening contractions induce different signaling responses in the type I and type II fibers of human skeletal muscle. *J Appl Physiol* **106**, 1412-8.

Thomson, D., Fick, C. and Gordon, S. (2008). AMPK activation attenuates S6K1, 4EBP1 and eEF2 signlaing responses to high-frequency electrically stimulated skeletal muscle contractions. *J Appl Physiol* **104**, 625-632.

Thomson, D. and Gordon, S. (2006). Impaired overload-induced muscle growth is associated with diminished translational signalling in aged rat fast-twitch skeletal muscle. *J Physiol* **574**, 291-305.

Thomson, D. M. and Gordon, S. E. (2005). Diminished overload-induced hypertrophy in aged fast-twitch skeletal muscle is associated with AMPK hyperphosphorylation. *Journal of Applied Physiology* **98**, 557-564.

Timson, B. (1990). Evaluation of animal models for the study of exercise-induced muscle enlargement. *J Appl Physiol* **69**, 1935-1945.

Trappe, S., Williamson, D. and Godard, M. (2002). Maintenance of whole muscle strength and size following resistance training in older men. *J Gerontol A Biol Sci Med Sci* **57**, B138-B143.

Trappe, T. A., Fluckey, J. D., White, F., Lambert, C. P. and Evans, W. J. (2001). Skeletal muscle PGF(2)(alpha) and PGE(2) in response to eccentric resistance exercise: influence of ibuprofen acetaminophen. *J Clin Endocrinol Metab* **86**, 5067-70.

Walsh, B., Howlett, R. A., Stary, C. M., Kindig, C. A. and Hogan, M. C. (2006). Measurement of activation energy and oxidative phosphorylation onset kinetics in isolated muscle fibers in the absence of cross-bridge cycling. *Am J Physiol Regul Integr Comp Physiol* **290**, R1707-13.

Wang, J. G., Miyazu, M., Matsushita, E., Sokabe, M. and Naruse, K. (2001a). Uniaxial cyclic stretch induces focal adhesion kinase (FAK) tyrosine phosphorylation followed by mitogen-activated protein kinase (MAPK) activation. *Biochemical and Biophysical Research Communications* **288**, 356-61.

Wang, X., Li, W., Williams, M., Terada, N., Alessi, D. R. and Proud, C. G. (2001b). Regulation of elongation factor 2 kinase by p90(RSK1) and p70 S6 kinase. *EMBO J* **20**, 4370-9.

Wang, Z.-M., Zheng, Z., Messi, M. L. and Delbono, O. (2005). Extension and magnitude of denervation in skeletal muscle from ageing mice. *J Physiol* **565**, 757-764.

Weber, A. (1959). On the role of calcium in the activity of adenosine 5'-triphosphate hydrolysis by actomyosin. *J Biol Chem* **234**, 2764-9.

Weiss, S., Rossi, R., Pellegrino, M.-A., Bottinelli, R. and Geeves, M. A. (2001). Differing ADP Release Rates from Myosin Heavy Chain Isoforms Define the Shortening Velocity of Skeletal Muscle Fibers. *Journal of Biological Chemistry* **276**, 45902-45908.

Welle, S., Thornton, C. and Statt, M. (1995). Myofibrillar protein synthesis in young and old human subjects after three months of resistance training. *Am J Physiol Endocrinol Metab* **268**, E422-E427.

Weng, Q. P., Kozlowski, M., Belham, C., Zhang, A., Comb, M. J. and Avruch, J. (1998). Regulation of the p70 S6 kinase by phosphorylation in vivo. Analysis using site-specific anti-phosphopeptide antibodies. *J Biol Chem* **273**, 16621-16629.

Wernbom, M., Augustsson, J. and Raastad, T. (2008). Ischemic strength training: a low-load alternative to heavy resistance exercise? *Scand J Med Sci Sports* **18**, 401-16.

Wernbom, M., Augustsson, J. and Thomee, R. (2007). The influence of frequency, intensity, volume and mode of strength training on whole muscle cross-sectional area in humans. *Sports Med* **37**, 225-64.

Widegren, U., Ryder, J. and Zierath, J. (2001). Mitogen-activated protein kinase signal transduction in skeletal muscle: effects of exercise and muscle contraction. *Acta Physiol Scand* **172**, 227-238.

Williamson, D., Gallagher, P., Harber, M., Hollon, C. and Trappe, S. (2003). Mitogen-activated protein kinase (MAPK) pathway activation: effects of age and acute exercise on human skeletal muscle. *J Physiol* **547**, 977-987.

Williamson, D. L., Bolster, D. R., Kimball, S. R. and Jefferson, L. S. (2006). Time course changes in signaling pathways and protein synthesis in C2C12 myotubes following AMPK activation by AICAR. *American Journal of Physiology - Endocrinology And Metabolism* **291**, E80-E89.

Winter, J. N., Jefferson, L. S. and Kimball, S. R. (2011). ERK and Akt signaling pathways function through parallel mechanisms to promote mTORC1 signaling. *Am J Physiol Cell Physiol* **300**, C1172-80.

Witkowski, S., Lovering, R. M. and Spangenburg, E. E. (2010). High-frequency electrically stimulated skeletal muscle contractions increase p70s6k phosphorylation independent of known IGF-I sensitive signaling pathways. *FEBS Letters* **584**, 2891-5.

Wojtaszewski, J. F., MacDonald, C., Nielsen, J. N., Hellsten, Y., Hardie, D. G., Kemp, B. E., Kiens, B. and Richter, E. A. (2003). Regulation of 5'AMP-activated protein kinase activity and substrate utilization in exercising human skeletal muscle. *Am J Physiol Endocrinol Metab* **284**, E813-22.

Wolff, J. (1892). Das Gesetz der Transformation der Knochen. *Hirschwald, Berlin*.

Wong, T. and Booth, F. (1990). Protein metabolism in rat gastrocnemius muscle after stimulated chronic concentric exercise. *J Appl Physiol* **69**, 1709-1717.

Wong, T. and FW, B. (1990). Protein metabolism in rat tibialis anterior muscle after stimulated chronic eccentric exercise. *J Appl Physiol* **69**, 1718-1724.

Wretman, C., Lionikas, A., Widegren, U., Lannergren, J., Westerblad, H. and Henriksson, J. (2001). Effects of concentric and eccentric contractions on phosphorylation of MAPK(erk1/2) and MAPK(p38) in isolated rat skeletal muscle. *Journal of Physiology* **535**, 155-64.

Yan, Z., Okutsu, M., Akhtar, Y. N. and Lira, V. A. (2011). Regulation of exercise-induced fiber type transformation, mitochondrial biogenesis, and angiogenesis in skeletal muscle. *J Appl Physiol* **110**, 264-74.

Yamane, A. (2005). Embryonic and postnatal development of masticatory and tongue muscles. *Cell and Tissue Research* **322**, 183-189.

Yeung, E. W., Head, S. I. and Allen, D. G. (2003). Gadolinium reduces short-term stretch-induced muscle damage in isolated mdx mouse muscle fibres. *J Physiol* **552**, 449-58.

Yeung, E. W., Whitehead, N. P., Suchyna, T. M., Gottlieb, P. A., Sachs, F. and Allen, D. G. (2005). Effects of stretch-activated channel blockers on [Ca2+]i and muscle damage in the mdx mouse. *J Physiol* **562**, 367-80.

Yu, B. P., Masoro, E. J., Murata, I., Bertrand, H. A. and Lynd, F. T. (1982). Life span study of SPF Fischer 344 male rats fed *ad libitum* or restricted diets: Longevity, growth, lean body mass and disease. *J Gerontol* **37**, 130-141.

Zhang, H., Bethel, C., Smittkamp, S. and Standford, J. (2008). Age-related changes in orolingual motor function in F344 vs F344/BN rats. *Physiol Behav* **93**, 461-466.

Zheng, Z., Messi, M. a. L. and Delbono, O. (2001). Age-dependent IGF-1 regulation of gene transcription of Ca2+ channels in skeletal muscle. *Mechanisms of Ageing and Development* **122**, 373-384.

VITA

JILL ANNE RAHNERT

Jill is a native of Des Plaines, IL and later moved to Canton, MI where she graduated from Plymouth-Canton High School. She received a B.S. in Biology, with a minor in Chemistry from Georgia State University in 2002 where she was also a member of the GSU women's soccer team. Beginning in 2003 she spent 3 years as a research technician at the VA hospital in Decatur, GA before coming to Georgia Tech to pursue a doctorate in Applied Physiology. She enjoys playing soccer, music, nature and the outdoors. She loves her husband and her family.